National Library of Canada

Acquisitions and Bibliographic Services Branch

395 Wellington Street
Ottawa, Ontario
K1A 0N4

Bibliothèque nationale du Canada

Direction des acquisitions et des services bibliographiques

395, rue Wellington
Ottawa (Ontario)
K1A 0N4

Your file Votre référence

Our file Notre référence

NOTICE

The quality of this microform is heavily dependent upon the quality of the original thesis submitted for microfilming. Every effort has been made to ensure the highest quality of reproduction possible.

If pages are missing, contact the university which granted the degree.

Some pages may have indistinct print especially if the original pages were typed with a poor typewriter ribbon or if the university sent us an inferior photocopy.

AVIS

La qualité de cette microforme dépend grandement de la qualité de la thèse soumise au microfilmage. Nous avons tout fait pour assurer une qualité supérieure de reproduction.

S'il manque des pages, veuillez communiquer avec l'université qui a conféré le grade.

La qualité d'impression de certaines pages peut laisser à désirer, surtout si les pages originales ont été dactylographiées à l'aide d'un ruban usé ou si l'université nous a fait parvenir une photocopie de qualité inférieure.

Canada

ISBN 0-315-82551-0

Canada

UNIVERSITÉ D'OTTAWA
UNIVERSITY OF OTTAWA

Acknowledgments

With deep gratitude, I wish to thank Professor M. H. Back, my research supervisor, for her extraordinary scientific guidance and financial support throughout my graduate studies at the University of Ottawa. Her constant enthusiasm and encouragement as well as unfailing availability were especially appreciated.

I would like to thank Dr. J. C. Scaiano for allowing me to perform the laser flash photolysis experiments in his laboratory. Special thanks are given to Dr. Peter McGarry and Jeff Banks for their help in performing the flash photolysis experiments. Also, I would like to thank Dr. C. Detellier for allowing me to use his fluorescence spectrometer.

I am also thankful to my fellow graduate student Rashmi Venkateswaran for her invaluable help and companionship. I would like to extend my grateful appreciation to the members of the support and teaching faculty in the Chemistry Department at the University of Ottawa, in particular Mr. Bob Nadon.

At this point, I would also like to sincerely thank the late Dr. Robert Back who initiated this research project. His insights and enthusiasm for this project helped me enormously.

Finally, I wish to express my sincere appreciation for the support and understanding provided by my wife, Ye Wang. To her, with my love, I dedicate this thesis.

Abstract

The thermal and photochemical reactions of the dianion of rhodizonic acid (1,2-dihydroxycyclohexenetetrone) and the kinetics of the photochemical reactions of the dianion of croconic acid (1,2-dihydroxycyclopentenetrione) have been studied in aqueous solution in the presence and absence of electron acceptors. For rhodizonate dianion, both thermal and photochemical reactions are initiated by electron transfer to an acceptor which is a sufficiently strong oxidizing agent. With hydrogen peroxide and ferricyanide, a square root dependence of the rate of disappearance of rhodizonate dianion on the concentration of additive was observed, whereas with tetracyanoethylene the rate was first order with respect to the concentration of additive. This difference in behavior is explained on the basis of the rate of separation of ions from the initial charge transfer complex. For croconate dianion, the quantum yield for disappearance of croconate dianion was small ($<10^{-3}$) in neutral solution, but was substantially increased in basic solution and in the presence of electron acceptors. At pH 12 in the presence of 4-nitrobenzylbromide or biacetyl, a quantum yield of 1 was observed. The kinetics of the rate of disappearance of croconate dianion as a function of pH and concentration of acceptor showed that the excited dianion is oxidized by acceptors and reacts with hydroxyl ion. A mechanism is proposed that is shown to be consistent with the results. The main reaction product for rhodizonate dianion is croconate dianion, while for croconate dianion, the main reaction product is squarate dianion.

Photopolymerization of acrylamide was initiated by the photochemical reactions of rhodizonate dianion and croconate dianion in the presence of various acceptors. Photoinitiation was most efficient with croconate dianion where a maximum quantum yield for polymerization of acryamide of 2×10^{3} was observed in neutral solution. Kinetic studies using croconate dianion as initiator showed that the rate of polymerization was a linear

function of the concentration of monomer and proportional to the square root of the light absorbed by the croconate dianion. The rate of initiation of radicals calculated from the rate of polymerization was compared with the rate of production of radicals calculated from the steady state photolysis study of croconate dianion.

Laser-induced flash photolysis study of rhodizonate and croconate dianions has been performed both in the presence and absence of electron acceptors. The rate constant for the recovery of the ground state from the excited state (k_D) is 2.4×10^5 s^{-1} for rhodizonate dianion and 2.8×10^5 s^{-1} for croconate dianion in neutral solution. Absorption spectra of croconate monoanion radical with a maximum at 500 nm were observed in the presence of the additives 4-nitrobenzylbromide, biacetyl and methyl viologen. Rate constants for the diffusion-controlled electron transfer reactions from the excited croconate dianion to the acceptors (k_T) were measured. The values of k_T were 2.0×10^8 $M^{-1}s^{-1}$ for biacetyl, 2.8×10^9 $M^{-1}s^{-1}$ for 4-nitrobenzylbromide and 3.7×10^{10} $M^{-1}s^{-1}$ for methyl viologen. The rate constant for quenching of the excited state of croconate dianion by oxygen was 4.5×10^9 $M^{-1}s^{-1}$.

Table of Contents

List of Tables

List of Figures

Chapter 1

Introduction

"Oxocarbon" refers to compounds in which all or nearly all of the carbon atoms are bonded to carbonyl or enolic oxygens or their hydrated or deprotonated equivalents.[1, 2] The monocyclic oxocarbon acids have the general formular $H_2C_nO_n$, where the known acids are $H_2C_3O_3$, deltic acid, $H_2C_4O_4$, squaric acid, $H_2C_5O_5$, croconic acid and $H_2C_6O_6$, rhodizonic acid. The name croconic is derived from the Greek *krokos*, meaning yellow, the color of croconic acid and its salts. The name rhodizonic comes from the Greek *rhodizene*, rose red, the color of rhodizonic acid and its salts. The chemical nomenclature of 4, 5 and 6 membered monocyclic acids are: Cyclobutenedione, 1,2-dihydroxy; Cyclopentenetrione, 1,2-dihydroxyl; and Cyclohexenetetrone, 1,2-dihydroxyl; respectively.

1. 1 History

The first discovery of an oxocarbon can be dated back to 1823,[3] when Berzelius, Wöhler and Kindt observed a black powdery residue formed in the reaction of potassium hydroxide with carbon. The isolation of potassium croconate and the preparation of its acid was not reported until two years later by Gmelin, the same year in which benzene was obtained from illuminating gas oil by Michael Faraday. Gmelin's preparation of croconic acid was therefore a synthesis of an "organic" compound in the original sense---from inorganic starting materials. As such it was perhaps the first synthesis of an organic compound ever made, predating Wöhler's classic synthesis of urea by three years. Rhodizonic acid was obtained from the same residue a few years later by Heller.[4]

Although croconic and rhodizonic acids were synthesised at approximately the same

time as benezene, studies of the oxocarbons were far fewer than of benzene. The important and interesting properties of the oxocarbons were widely ignored by chemists for more than one century.

The modern era of oxocarbon chemistry started from an accidental synthesis of squaric acid by Cohen, Lacher and Park in 1959 by hydrolysis of 1,3,3-triethoxy-2-chloro-4,4-difluorocyclobutene or by the aqueous and acid hydrolysis of 1,2-diethoxy-3,3,4,4-tetraflurocyclobutene,[5]

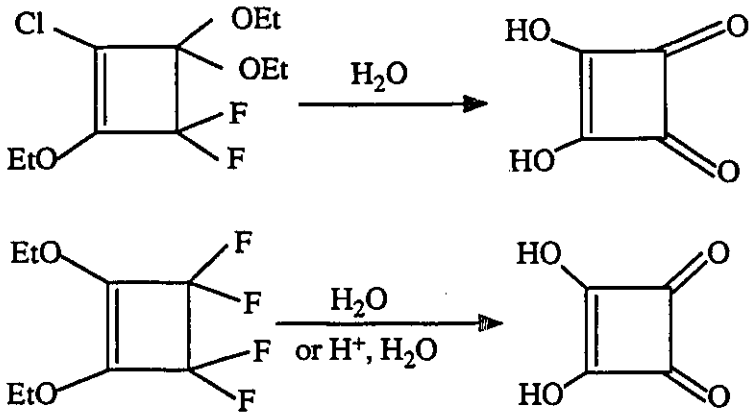

They found the solid, white dibasic squaric acid was almost as strong as sulfuric acid with pK_1=1.0 and pK_2=3.2. The infrared spectrum of the acid showed the carbonyl vibration absorption at 1818 cm^{-1} and the C=C absorption at 1640cm^{-1}. In the spectrum of its salt, both of these two absorption bands vanished and a broad band between 1480 cm^{-1} and 1540 cm^{-1} appeared, which is in the range for C-O vibration in acid salts and anions. They concluded that the anion would have much resonance stabilization, since all four atoms should become equivalent through resonance. They suggested the following electron delocalized form:

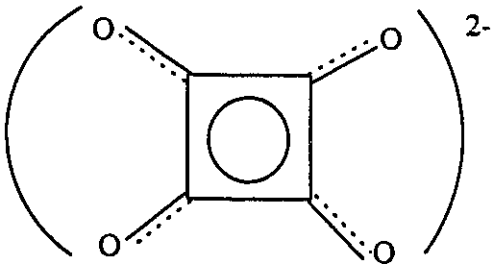

This proposed structure led to the suggestion that the squarate ion was aromatic and that the oxocarbon anions might constitute a previously unrecognised aromatic series. Although this study is gererally considered to have sparked the interests of chemists in further investigation of this series of compounds, it appears that the first suggestion of a resonance delocalized structure for croconate dianion was made by K. Yamada, an undergraduate student at Nagoga University in Japan in 1958.[6] He used the silver croconate salt to prepare the dimethyl ester of the acid. In their description of the reaction, he and his colleagues suggested a resonance structure for the croconate dianion, in which the π electrons were delocalized throughout the ring and the oxygen atoms, as follows:

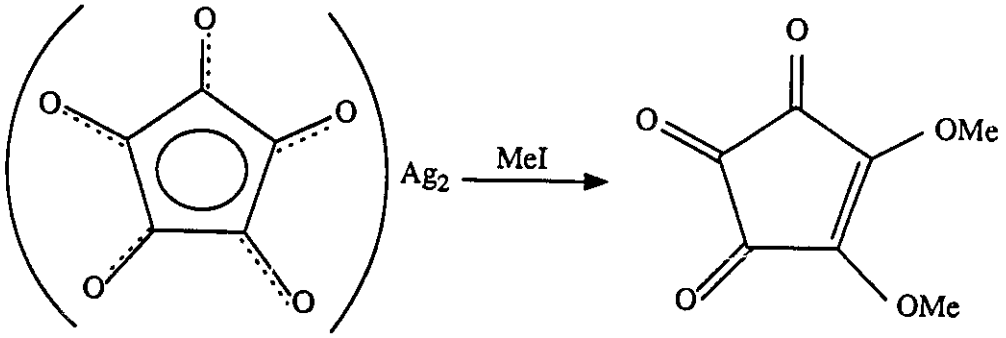

They failed, however, to justify their representation of the delocalized croconate dianion and it was overlooked by others. Nevertheless, this probably deserves to be recognized as the first resonance stabilized structure of oxocarbon anions reported in the literature.

1. 2 Properties of Oxocarbons

1. 2. 1 Aromaticity

One of the most important properties of the oxocarbon salts is their aromaticity.[1, 5-7] The resonance structure stimulated the interest of both theoretical and experimental chemists.[2, 8-10]

Infrared and Raman spectroscopies contributed much to the understanding of the structure of the oxocarbon anions.[11-13] The planar and symmetrical dianions should each have seven Raman lines, of which two (the totally symmetrical C-O stretching and ring breathing modes) should be strongly polarized. The infrared spectra for each anion should be even simpler, containing only four fundamental bands. Experimental results of the infrared and Raman spectra confirmed the assignment, demonstrating that all these anions have a planar D_{nh} symmetrical structure. There were no normal C=O vibrational bands and the C=C absorption also vanished, confirming the delocalized resonance structure. The C-C bond lengh was between the lengths of a typical C-C single bond and a C=C double bond. The C-O bond length in the anions was also shorter than the C-O single bond length, but longer than the C=O double bond length. All the C-C bond lengths in the ring were equal, as were the C-O bond lengths for a particular anion. These values are compared to normal values in Table 1. 1.

It seems that $C_6O_6^{2-}$ has less aromaticity than the corresponding four or five membered ring dianions, as seen from the longer C-C and shorter C-O distances, which indicate less π-bonding in the ring in this species. The shortest C-C distance was found for squarate dianion. The diamagnetic anisotropies suggest strongly the existence of a ring current in all oxocarbon anions.

Table 1. 1 Bond Lengths of $C_nO_n^{2-}$ and Normal C-C, C-O Bond Lengths

	Oxocarbon Dianions			Normal Bond Lengths			
	n=4	n=5	n=6	C=C	C-C	C=O	C-O
d_{cc}(Å)	1.440	1.458	1.471	1.34	1.54		
d_{co}(Å)	1.249	1.243	1.240			1.20	1.43

Oxocarbon dianions are a very interesting subject for theoretical chemists[2, 7-9]. The quantum chemical studies of the cyclic oxocarbon dianions revealed that the dianions show a delocalization of the two "extra" electrons of the double charge, thus contributing to the overall stability.[14] The interaction between neighbouring carbon atoms decreases with increasing ring size. Double-bond character for the C-C bonds exists in all members of the series, but the degree of aromaticity cannot be determined precisely.

1. 2. 2 Electronic Excited States and Absorption Spectra of Oxocarbon Dianions

The calculated electronic states of oxocarbon dianions are shown in Figure 1.1. Solid and broken lines in Figure 1.1 indicate the states allowed and forbiden, respectively, for electronic transitions from the ground state.[15, 16] It seems from the figure there is only one allowed excited state above 200 nm for each of the oxocarbon anions. These transitions are represented as $E_u(\pi,\pi^*)\leftarrow A_{1g}$, $E'(\pi,\pi^*)\leftarrow A'_1$ and $E_{1u}(\pi,\pi^*)\leftarrow A_{1g}$ for $C_4O_4^{2-}$, $C_5O_5^{2-}$ and

$C_6O_6^{2-}$, respectively.

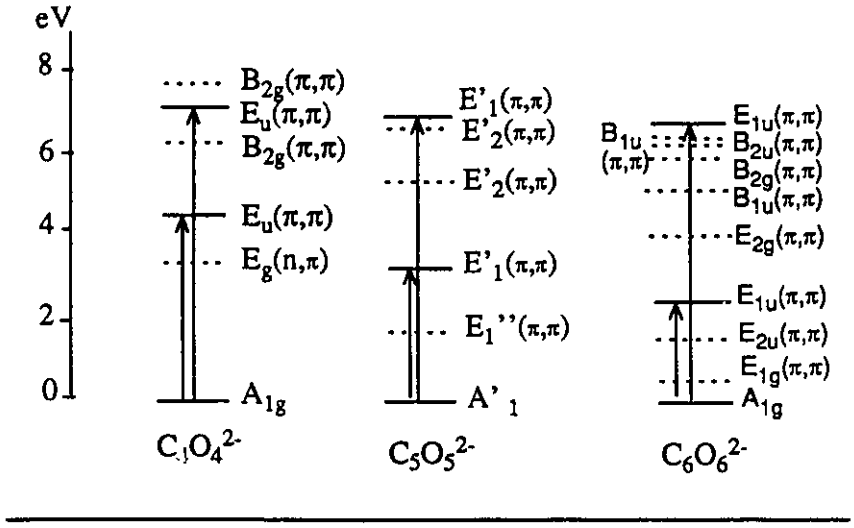

Figure 1. 1 Calculated Electronic States of Oxocarbon Dianions

The absorption spectra of the oxocarbon anions in aqueous solution are shown in Figure 1.2. The maximum wavelength of the absorption shifts progressively toward longer wavelength with increasing ring size. The shape of the absorption spectra is very similar for all three anions: the maximum absorption is accompanied by a shoulder at shorter wavelength with a separation of about 50 nm for each ion. This double maximum is due to the fact that the lowest allowed excited state is a degenerate π, π^* state for all the ions. The occurrence of a Jahn-Teller effect is expected in the very high symmetry oxocarbon dianions.[17]

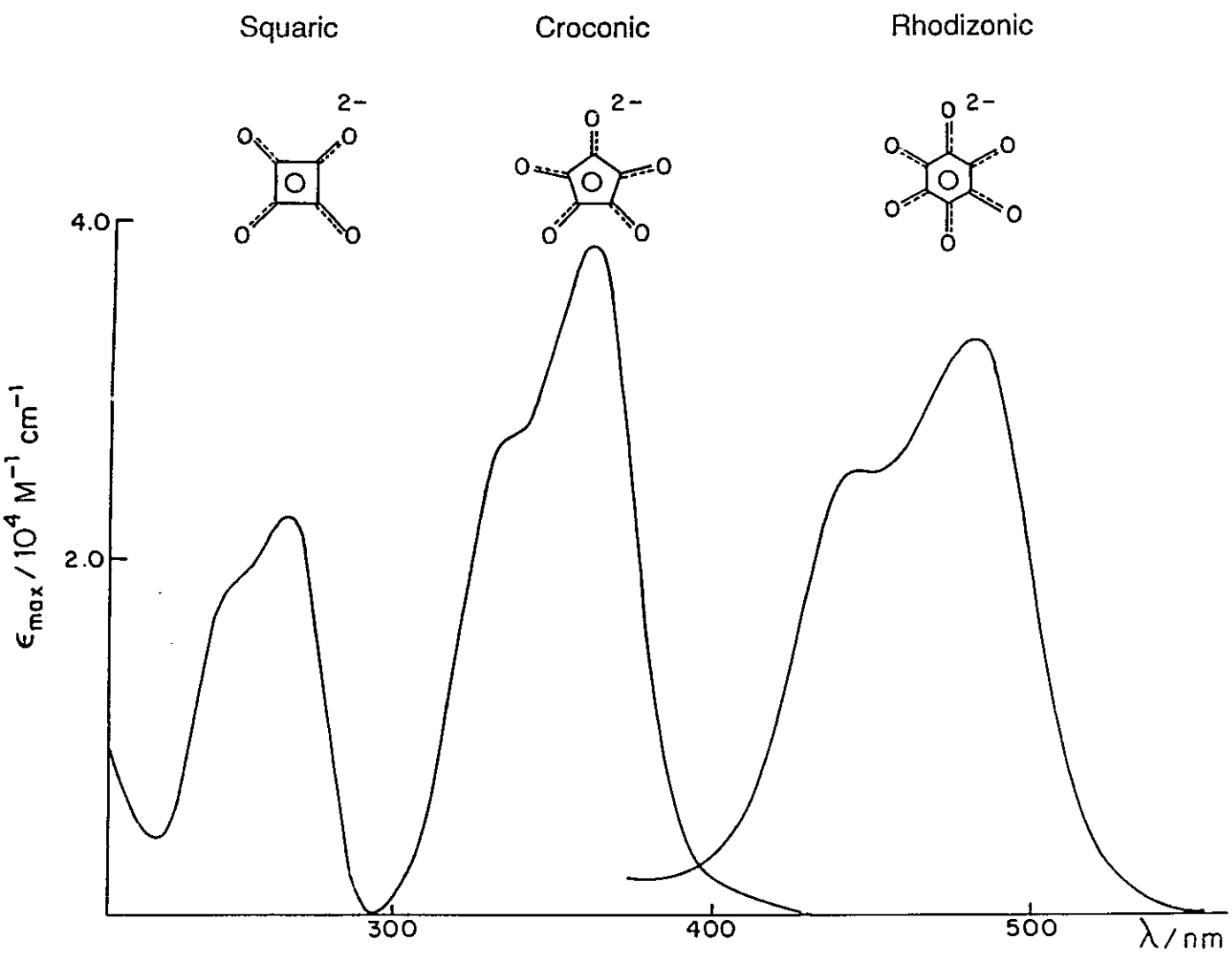

Figure 1. 2. Absoption Spectra of Dianions of Squaric, Croconic and Rhodizonic Acids

1. 2. 3 Dissociation Constants and the Structure of Oxocarbon Acids in Aqueous Solution

(a) Dissociation Constants of Oxocarbon Acids

The ionization of the diprotic oxocarbon acids may be represented by the following reactions:

$$H_2C_nO_n + H_2O \rightleftharpoons HC_nO_n^- + H_3O^+ \quad (1\text{-}1)$$

$$HC_nO_n^- + H_2O \rightleftharpoons C_nO_n^{2-} + H_3O^+ \quad (1\text{-}2)$$

Studies of the structure of oxocarbon acids in aqueous solution showed that these simple proton transfers between the parent acids or monoanion acids and water do not adequately reflect the actual structure changes that occur when oxocarbon acids deprotonate in aqueous solution[18-20]. Neverthless, the strength of the acids still can be expressed by the ionization constants in the normal sense. Table 1.2 summarizes the dissociation constants of oxocarbon acids and the methods used to measure the constants.[21, 22]

The methods used in the determination of the equilibrium constants of the oxocarbon acids are: potentiometric, conductimetric and spectrophotometric. Spectrophotometric was particularly useful with croconic acid as there is a substantial change in the UV absorption as the equilibrium composition is shifted from $H_2C_5O_5$ to $HC_5O_5^-$, and to $C_5O_5^{2-}$ with increasing pH. The potentiometric method can be used to measure K_2 accurately but is less suitable for K_1 because the determination is quite sensitive to the reagent purity and to the response of the glass electrode, and these factors introduce a relatively large uncertainty.

Table 1. 2. Dissociation Constants of Oxocarbon Acids

Oxocarbon Acids	pK_1 (Method)	pK_2 (Method)
$H_2C_4O_4$	0.51±0.02 (Cond.)	3.19±0.01 (Pot.)
	1.2±0.2 (Pot.)	3.21 (Pot.)
	0.96±0.3 (Pot.)	3.48±0.03 (Pot.)
$H_2C_5O_5$	0.50±0.05 (Spect.)	1.97 (Spect.)
	0.68 (Spect.)	2.28±0.14 (Pot.)
	0.80±0.08 (Spect.)	2.24±0.01 (Spect.)
$H_2C_6O_6$	4.02±0.05 (Spect.)	4.62±0.05 (Spect.)
	4.20±0.05 (Spect.)	4.65±0.01 (Spect.)
	4.38±0.01 (Pot.)	4.72±0.07 (Spect.)

(b) The Structure of Croconic Acid

The structures of the croconic and rhodizonic acids in aqueous solution are complicated by hydration and are not completely understood.[23-25] The thermodynamic data for the primary ionization of $H_2C_5O_5$ and $H_2C_6O_6$ are abnormal compared with other similar compounds, suggesting that the parent acids do not have the simple structure indicated by the formula.[11, 26] From the similarity of the UV spectra of related compounds, Carpentier et al[27] first deduced that the undissociated croconic acid has one

water molecule covalently attached. ^{13}C NMR spectra[28, 29] of a series of croconate solutions over a range of pH showed that when pH>> pK_1(0.7), only the dianion or the monoanion was present, and only one single peak exists, in agreement with the charge delocalized structure shown below:

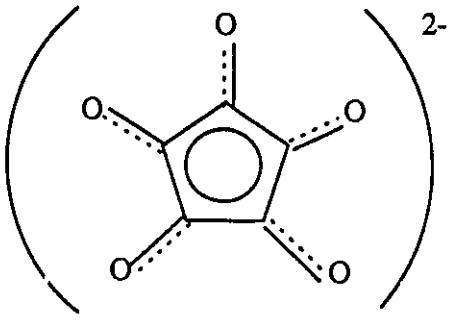

When the pH is near or less than pK_1 four peaks were observed. These three additional peaks, which appear only in the most acidic solutions, become virtually invariant with even lower pH. This implies that when $HC_5O_5^-$ and $C_5O_5^{2-}$ are present, all croconate species equilibrate rapidly relative to the NMR relaxation time, thus producing a single resonance. But at low pH, when $H_2C_5O_5$ is also present in significant amount, the equilibration time is sufficiently slow to allow the resolution of three additional widely spaced peaks. A hydrated structure of $H_2C_5O_5$ was proposed and the mechanism can be expressed as:

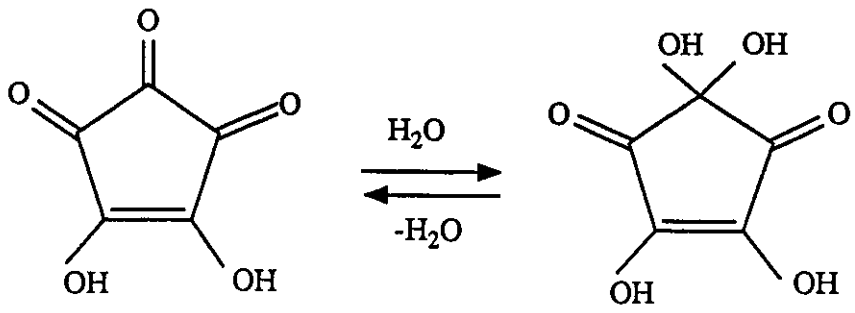

Further measurements using deuterium species led to the conclusion that 90% of the diprotonated croconate species in aqueous solution exist as the hydrated form.

The final conclusion is that the diprotonated species is hydrated, while mono- and nonprotonated croconate species are not hydrated.

(c) The Structure of Rhodizonic Acid

A similar investigation was made on the structure of rhodizonate species in aqueous solution.[30] The pH dependence of the ^{13}C NMR spectrum of rhodizonic acid was measured by changing the mole ratio of $LiOH/H_2C_6O_6$. In the absence of LiOH, the resonances observed immediately after preparation of the rhodizonic acid solution consisted of three peaks, consistent with an ortho-dihydrated structure for the undissociated acid:

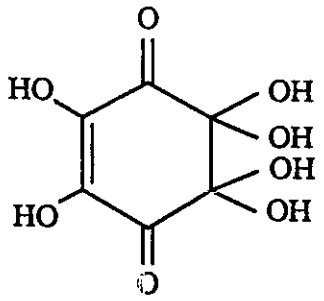

After standing for a few hours the following more stable dihydrated structure formed,

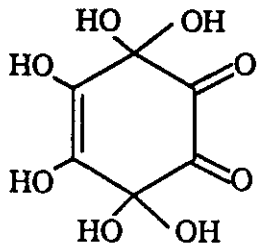

This showed only two peaks, one from the geminal diol carbons and the other from

the carbons as enols and carbonyls. The latter are equivalent because of rapid exchange of H^+. The ^{13}C NMR spectra also showed that the mono-protonated rhodizonate species is hydrated whereas the dianion is not. In the dianion only one single peak in the ^{13}C NMR spectrum was observed, showing that all carbons are equivalent.

1. 2. 4 Applications of Oxocarbon Acids and Their Salts

Oxocarbon acids and their salts are perhaps most widely used as analytical reagents.[31-45] For example, rhodizonate dianion has been used to determine the content of sulfate in Glycosaminoglycans, to detect lead from soil, drinking water and from living plant tissue. Rhodizonate dianion forms colored complexes with a variety of transition metal ions, and thus it can be used in quantitative spectrophotometric measurement of these metal ions. Examples are Yttrium, Scandium and Praseodymium. Sodium rhodizonate has been used as an indicator in the EDTA titration of Fe(II) and Cu(II).

Rhodizonic acid is also of biological importance.[46-48] It exhibits antitrypanosomal and antiviral activity. It is one of the products from the process of the respiratory chain involving simultaneous proton and electron transfer processes which occur in the mitochondrial membrane of animal cells and in the chloroplast of plant cells.[49]

Croconate anion also forms complexes with many metal ions and can be used as a quantitative analytical reagent.[50-55] For example, it has been used to determine the iron content in metallic aluminum. Derivatives of croconic acid with the following structure have been used as one of the components to make a recording medium sensitive to a (AlGa)As semiconductor laser.[56, 57]

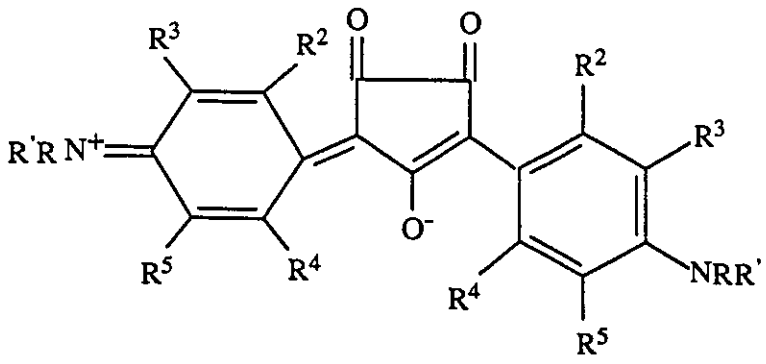

Rhodizonic and croconic acids have been used as heat stabilizers for some polymers.[58] Sodium rhodizonate has an inhibition effect on the corrosion of brass.[59]

1. 3 The Synthesis of Croconic and Rhodizonic Acids and Their Salts

1. 3. 1 Rhodizonate Dianion

(1) Cyclopolymerization of Carbon Monoxide

The earliest preparation of rhodizonic acid involved the reaction of potassium or sodium with carbon monoxide to form a polymer, $(KCO)_x$. When the temperature of the reaction mixture was increased to about 300^0 C, the product $K_6C_6O_6$ formed.[15] Oxidation of this product, hexapotassium hexahydroxybenzene, produces rhodizonate dianion. The whole process can be expressed as follows:

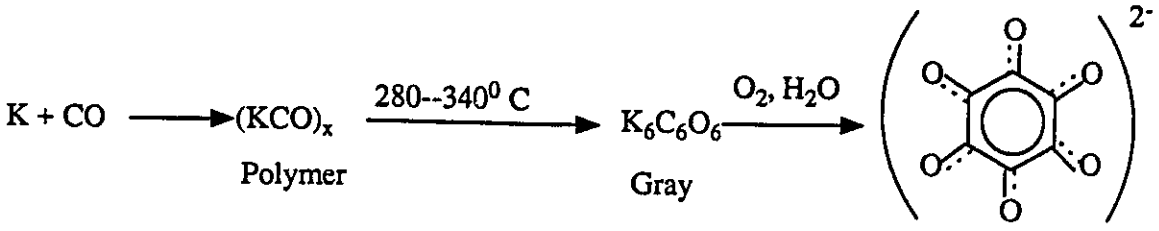

(2) Cyclotrimerization of Glyoxal

Glyoxal undergoes oxidative cyclotrimerization to form tetrahydroxyquinone salt, which on heating yields the rhodizonate salt.

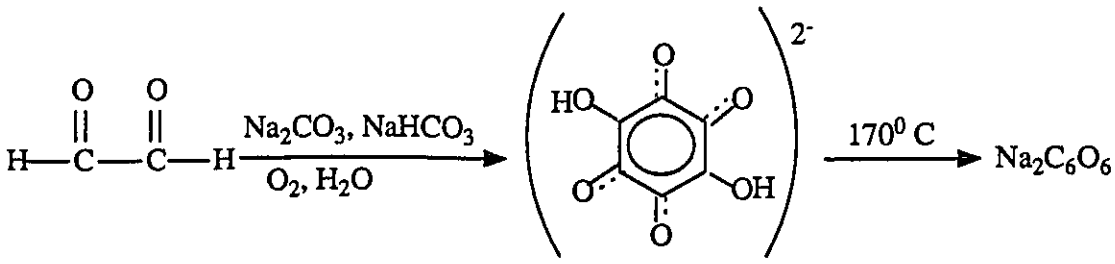

The yield of this procedure is low.

(3) Oxidation of Inositol

When inositol is oxidized with nitric acid in the presence of potassium acetate and oxygen, dipotassium rhodizonate was formed:

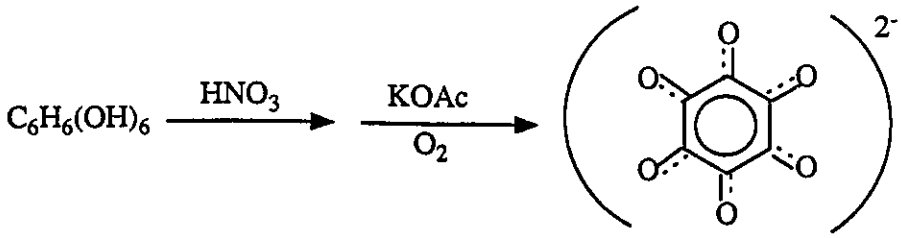

1. 3. 2 Croconate Dianion

In part **1. 1**, it was mentioned that the first oxocarbon discovered was croconate dianion, from the reaction of potassium hydroxide with carbon. Later studies showed that actually, rhodizonate dianion was the precursor of croconate dianion. The ring contraction reaction is an alpha-oxo alcohol rearrangement,[1] as shown in scheme 1.1.

This oxidative ring contraction gives quantitative conversion to croconic acid and is the usual method of preparation of croconic acid.

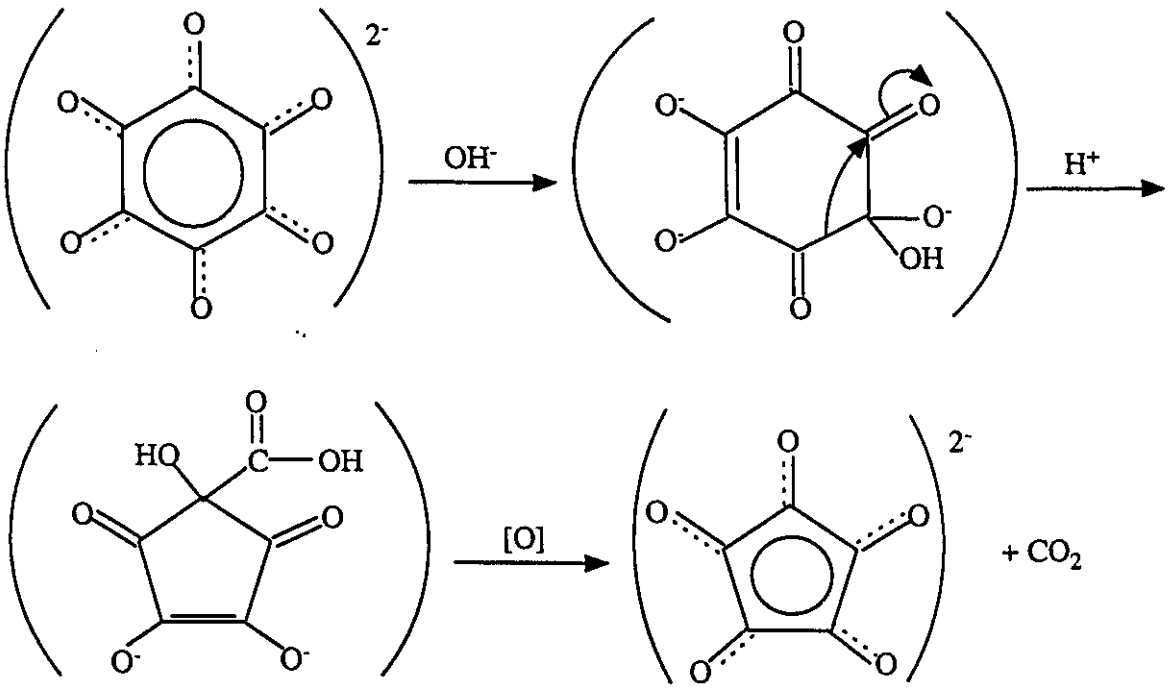

Scheme 1.1 Oxidation of rhodizonate dianion in alkaline solution

Another method of preparation of croconic acid which is not widely applied in the laboratory is the electrochemical demetallation of (η^4-tetra-t-butoxycyclopentadienone)(η^5-cyclopentadienyl) Cobalt, readily available from di-t-butoxyethyne. The reaction leads to tetra-t-butoxycyclopentadienone which can be converted into hydrocroconic acid by trifluoroacetic acid hydrolysis and then croconic acid by oxidation in basic medium.[60] The whole process can be summarized in scheme 1.2 on the following page. The reagents and reaction conditions in each step are:

Reagents: i) $(C_5H_5)Co(CO)_2$, Pentane -78^0 C

ii) Electrochemical Oxidation at +0.770mV. $(t\text{-}Bu_4N)^+ClO_4^+$/MeCN

iii) CF_3CO_2H, CH_2Cl_2, R. T.

iv) 0.1 M KOH in H_2O, R. T.

v) 0.1 M H_2SO_4 in H_2O, R. T.

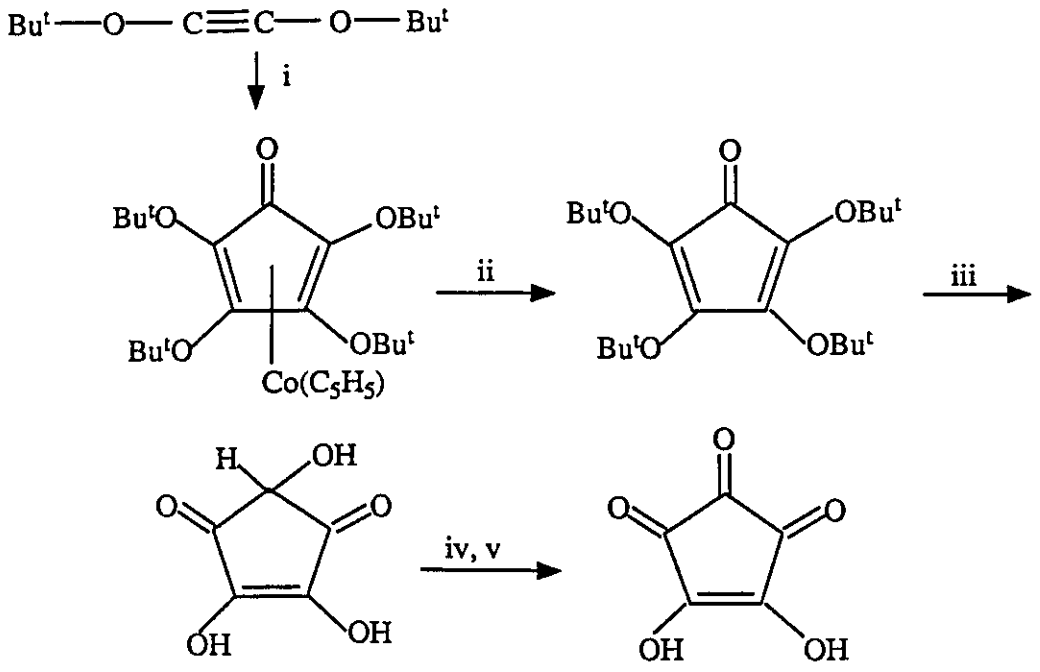

Scheme 1.2 Preparation of croconic acid using electrochemical demetallation

1. 4 Photo-induced Electron Transfer

The absorption of ultraviolet or visible light by an organic or inorganic molecule causes the excitation of an electron from a highest occupied molecular orbital (HOMO) to a lowest unoccupied molecular orbital (LUMO) and the molecule becomes electronically excited. The physical and chemical properties of the excited molecule may be greatly different from those of the ground state.[61] For example, the structure of the molecule may change and the increased energy of the excited state may facilitate chemical reactions.[62, 63]

The major processes following excitation of a molecule can be illustrated as follows:

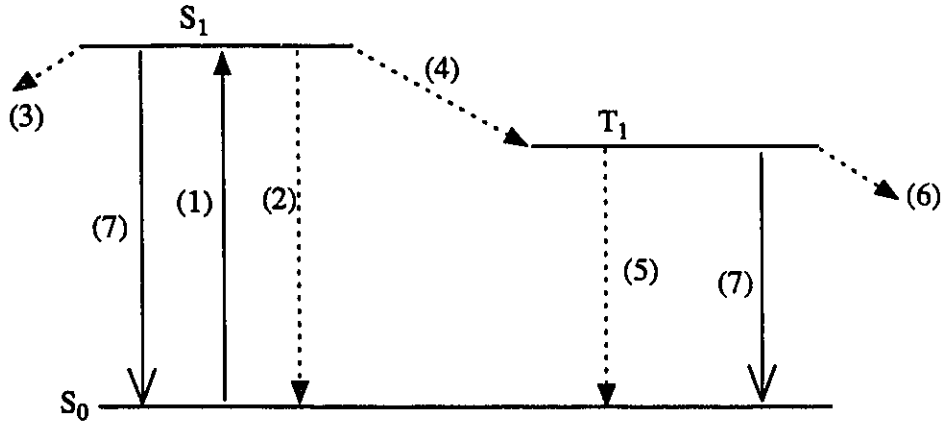

(1) Upon absorption of the light, one electron is excited to a higher energy level orbital. In an allowed process, the electron does not change its spin state during the process and the final state is a singlet.

$$^1M + h\nu \longrightarrow {}^1M^*$$

(2) The singlet excited state molecule may emit light(fluorescence) and return to the ground state.

$$^1M^* \longrightarrow {}^1M + h\nu'$$

(3) The singlet molecule may undergo energy transfer processes and return to its ground state. It may also undergo chemical reactions.

(4) The singlet excited state molecule may change its spin state and become a triplet excited state molecule with lower energy. This process is called intersystem crossing(ISC)

$$^1M^* \longrightarrow {}^3M^*$$

(5) The triplet excited molecule may emit light(phosphorescence) and return to the ground state, undergoing a spin change during the process.

$$^3M^* \longrightarrow {}^1M + h\nu''$$

(6) The triplet excited molecule may undergo energy transfer and return to its singlet ground state, or may undergo triplet chemical reactions.

(7) The excited states (both triplet and singlet) may undergo radiationless decay to the ground state.

$$M^* \longrightarrow M$$

The chemical reactions that may take place for an electronically excited molecule include:[64-67]

a) Dissociation.

b) Isomerization reaction, including structural isomerization and valence isomerization reactions.

c) Electron transfer reaction, if a suitable electron acceptor or donor is present.

An excited molecule has an increased ability either to receive an electron or to donate an electron compared to its ground state.[63] Promoting an electron from the HOMO to the LUMO leaves an electron hole in the lower energy orbital and adds an electron to the higher energy orbital. This can be schematically demonstrated as follows:

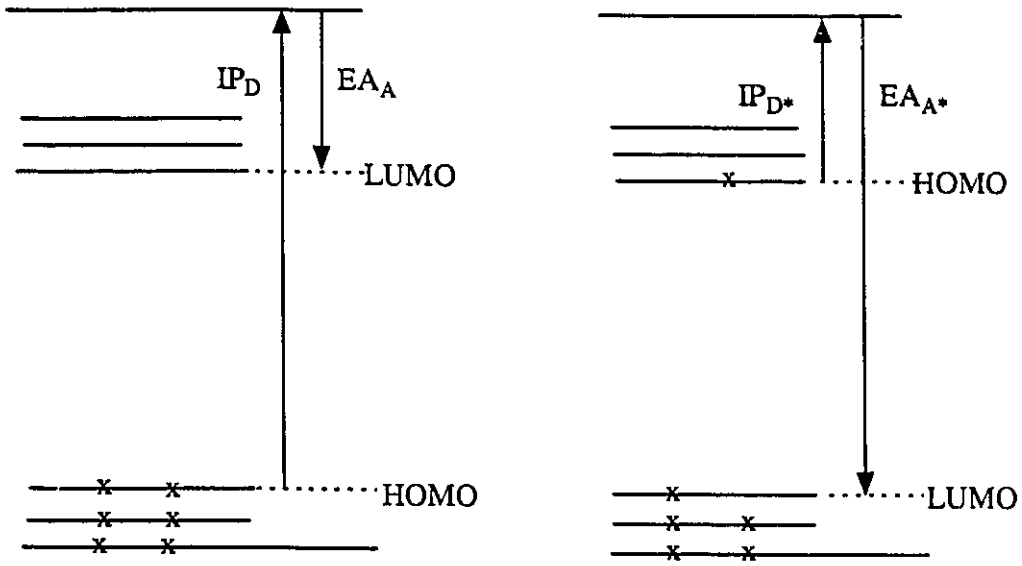

Ground State Molecule Excited State Molecule

Upon excitation, the ionization potential has been reduced and the electron affinity has been increased:

$$IP_{D*} = IP_D - E_D^* \qquad (1\text{-}3)$$

$$EA_{A*} = EA_A + E_A^* \qquad (1\text{-}4)$$

Here E_D^* or E_A^* is the excitation energy, which is equal to the energy difference between the LUMO and the HOMO.

The free energy change during the electron transfer in the ground state is:

$$\Delta G = IP_D - EA_A \qquad (1\text{-}5)$$

When the donor or acceptor is electronically excited the free energy change during the electron transfer becomes:

$$\Delta G = IP_D - EA_A - E_D^* \qquad (1\text{-}6)$$ or

$$\Delta G = IP_D - EA_A - E_A^* \qquad (1\text{-}7)$$

In general, simple rules for determining the feasibility of electron transfer can be derived from the above equations.

For $D^* + A \rightleftharpoons D^{+\cdot} + A^{-\cdot}$

when $IP_{D^*} - EA_A < 0$ allowed

$IP_{D^*} - EA_A > 0$ forbidden

For $D + A^* \rightleftharpoons D^{+\cdot} + A^{-\cdot}$

when $EA_{A^*} - IP_D < 0$ allowed

$EA_{A^*} - IP_D > 0$ forbidden

The photo-induced electron transfer reactions between donor and acceptor in solution can be expressed as in Scheme 1.3.

In solution, if the electron transfer occurs during the lifetime of the collision complex (i.e. when the reaction partners are in contact), the charge-transfer species immediately formed is a "contact ion pair". The collision complex can also separate slightly, undergo electron transfer, and generate a "solvent-separated" ion pair. Following electron transfer, solvent molecules rapidly stabilize contact ion pairs and solvent-separated ion pairs. Contact ion pairs and solvent separated ion pairs are sometimes described as "geminate" ion pairs, provided that each ionic partner is a descendant of the same parental pair. If solvent-separated ions dissociate into the bulk of the fluid medium where they become separated by a large distance, they are classified as free or solvated ions.[68]

The energy change in formation of a solvated radical ion pair from electron transfer in solution is:[62]

$$\Delta G_{SSIP}(\text{kcal/mol.}) = 23.06[E(D^{+\cdot}/D) - E(A/A^{-\cdot}) - e^2/\varepsilon d_{SSIP}] - E_D^* \qquad (1\text{-}8)$$

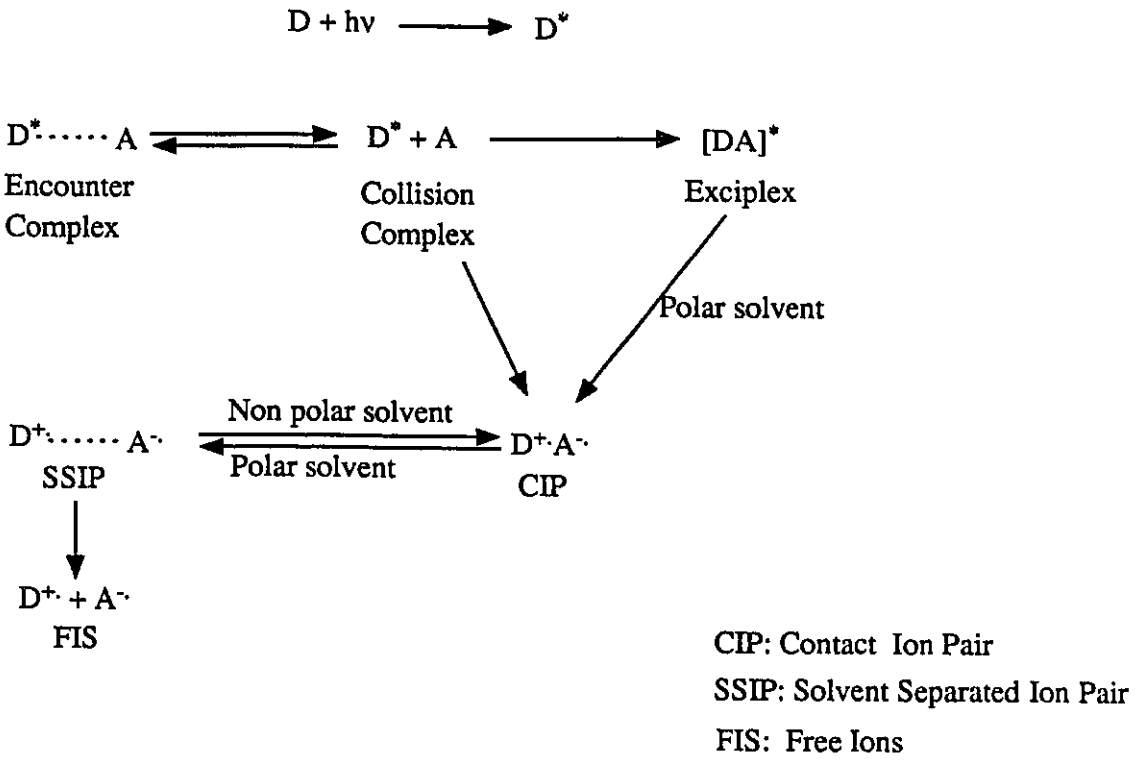

Scheme 1.3 Electron transfer reaction process in solution

where $E(D^{+\cdot}/D)$ and $E(A/A^{-\cdot})$ are redox potentials of the donor and acceptor, respectively, ε is the solvent dielectric constant, d_{SSIP} is the distance between the ions and the numerical term 23.06 involves the conversion factor to kcal mol^{-1} from volts. If the solvent-separated ion pair dissociates into free ions so that they are sufficiently separated beyond their respective Coulombic fields, or if the solvent has a large dielectric constant, the Coulombic energy term can be neglected and equation (1-8) can be simplified to:

$$\Delta G_{FIS}(Kcal/mol.)=23.06[E(D^{+\cdot}/D)-E(A/A^{-\cdot})]-E_D^* \qquad (1\text{-}9)$$

1. 5 Purpose of the Study

Both rhodizonate and croconate dianions are strong absorbers in the visible or near ultraviolet region in aqueous solution. Rhodizonate dianion has an extinction coefficient of 3.2×10^4 $cm^{-1}M^{-1}$ at its maximum absorption at 483 nm, and croconate dianion has an extinction coefficient of 3.9×10^4 $cm^{-1}M^{-1}$ at its maximum absorption at 363 nm. In spite of this favorable situation for absorption and possible utilization of visible or near UV radiation, no systematic study of the photochemical reaction of any of the oxocarbon dianions has been reported. The purpose of the present study was to explore the photochemical reactions of the oxocarbon dianions with emphasis on the kinetics of the reaction. The investigation is divided into four parts.

(1) A study of the photochemical reactions of rhodizonate and croconate dianions in aqueous solution as a function of pH, in the absence of additives.

(2) An investigation of the mechanism, kinetics and reaction products of the photo-induced electron transfer reaction between rhodizonate dianion (or croconate dianion) and electron acceptors, under various reaction conditions.

(3) Detection of radical intermediates by polymerization of acrylamide and by reaction with 2,2'-Di(4-tert-octlphenyl)-1-picrylhydrazyl (DPPH). The kinetics of the acrylamide photopolymerisation was also investigated.

(4) Detection of reaction intermediates using laser-induced flash photolysis. Radicals generated by the electron transfer reaction between the excited croconate dianion and electron acceptors were detected by absorption spectroscopy.

Chapter 2.

Photochemical Reactions of Rhodizonate Dianion

2. 1. Experimental

2. 1. 1. Technique for Degassing

Oxygen reacts thermally with rhodizonate dianion in aqueous solution, leading to the disappearance of the anion, and is also an efficient quencher of excited states. It was therefore important to remove it completely from the reaction solution. Two methods for degassing were used in these experiments.

(a) Nitrogen Gas Bubbling

By saturating the reaction solution with high purity nitrogen gas for long periods of time (depending on the volume of the solution to be degassed), it is possible to drive oxygen from the solution, leaving only traces of oxygen in the solution. In addition, deionized distilled water used to prepare the rhodizonate dianion solution was saturated with high purity nitrogen gas before preparation of the solution. The loss of rhodizonate dianion during solution preparation due to the thermal reaction was thus reduced to minimum. Solutions of other reactants were prepared and degassed separately. Mixing of these solutions with the rhodizonate dianion solution was performed under a flow of nitrogen. Finally, 3 mL of reaction solution containing both rhodizonate dianion and additives was transferred to the spectrophotometer cell, and the nitrogen flow was maintained in the solution in the cell for another 10 minutes. The cell was then capped with a rubber septum and was ready for irradiation. During all these degassing procedures, the reaction solution containing rhodizonate dianion was protected from light.

(b) Freeze-pump-thaw

A special cell was designed for freeze-pump-thaw degassing and is shown in Fig. 2. 1. Solutions of rhodizonate dianion and of additives could be degassed separately in B and then mixed under vacuum in the quartz cell before photolysis. In this way, thermal reaction prior to photolysis was greatly reduced. The degassing procedure using this device was as follows:

One of the reactant solutions was admitted to reservoir B through opening F. After degassing for five cycles with freeze-pump-thaw technique, the whole apparatus was disconnected from the vacuum line while maintaining vacuum. The sample solution was transferred to cell A, stopcock C was closed and reservoir B was cleaned and dried under vacuum. The second reactant solution was admitted to B and degassed with five freeze-pump-thaw cycles, then transferred to cell A and mixed with the previous degassed solution. Cell A was sealed by closing teflon stopcock C, disconnected at ground joint D and was ready for spectrophotometric measurements or photochemical reaction. In this way, the time required between mixing reactant solutions in cell A and the measurement of the absorption of the solution was reduced to about 15 seconds. During saturation with nitrogen a much longer time elapsed before measurement of the mixture. Particularly at high pH, the thermal reaction was significant and a noticeable drop of the reactant concentration was observed during the nitrogen bubbling process, thus reducing the accuracy of the measurement of initial rates. In the micellar solution, it was difficult to drive oxygen out completely by nitrogen bubbling and the freeze-pump-thaw method was much more efficient.

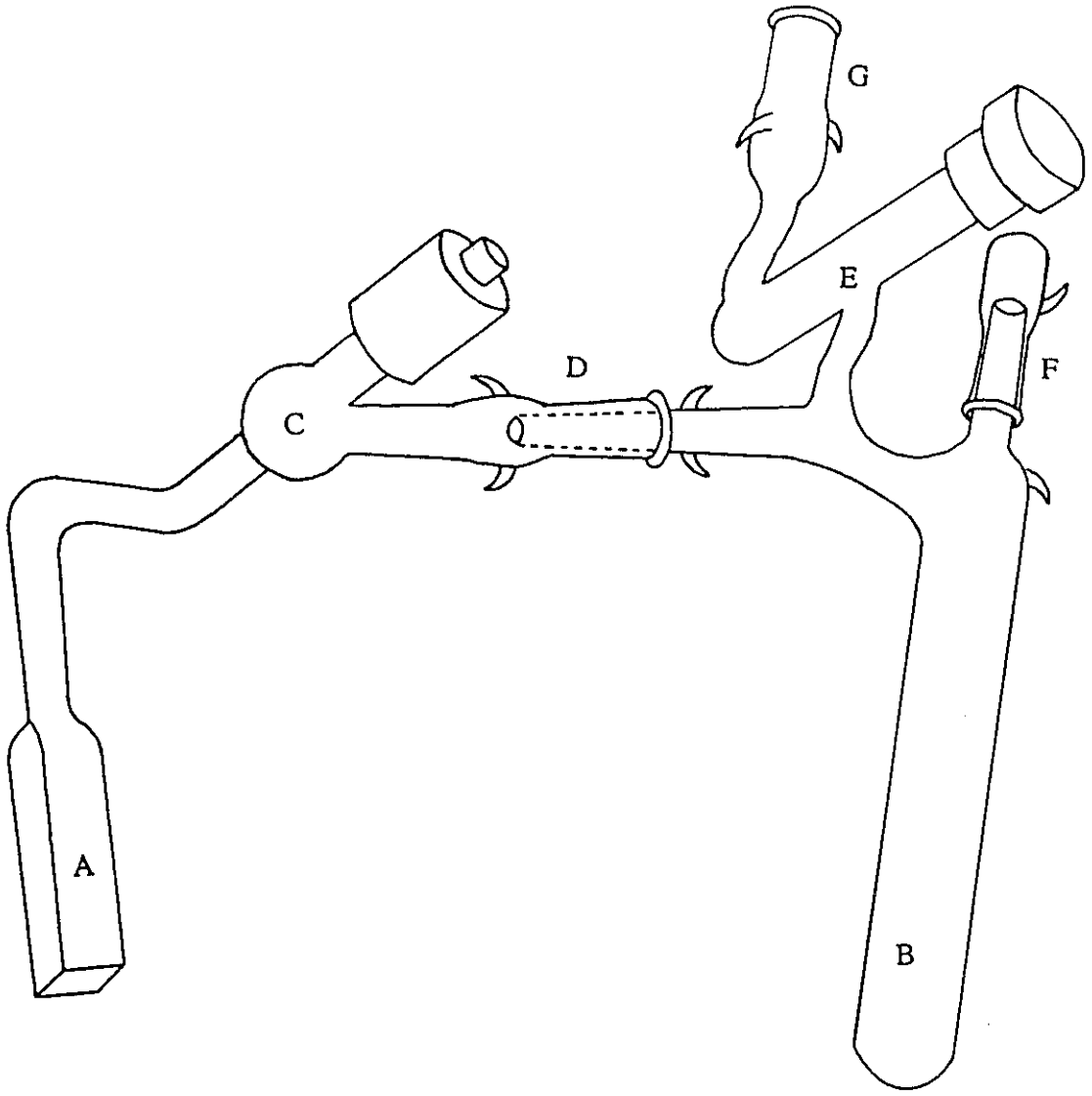

Figure 2.1 Apparatus for freeze-pump-thaw degassing

A: Quartz cell; B: Reservoir; C & E: Stopcock;

D, F & G: Ground Joint.

2. 1. 2 Light Source

The light source used for the irradiation of rhodizonate dianion solution was a fan-cooled 625 W tungsten filament lamp used in conjuction with a GM 250 high intensity quarter meter grating monochromator (Schoeffel Light and Light Measurement, New Jersey). A bandwidth of about 20 nm was used. The wavelength of 483 nm, the maximum absorption wavelength of rhodizonate dianion, was selected for the photolysis of rhodizonate dianion solution.

2. 1. 3 Measurement of Light Intensity

The intensity of light incident on the reaction cell at the wavelength of 483 nm was measured using the potassium ferrioxalate actinometer. The actinometer was prepared according to the procedures outlined by J. F. Rabek.[69]

When an acidic aqueous solution of $K_3Fe(C_2O_4)_3$ is irradiated, the ferric ions Fe^{3+} are reduced to ferrous ions Fe^{2+} and CO_2 is formed.[70, 71] The over-all reaction is the following:

$$[Fe^{(III)}(C_2O_4)_3]^{3-} + h\nu \rightarrow [Fe^{(II)}(C_2O_4)_2]^{2-} + C_2O_4^-$$

$$[Fe^{(III)}(C_2O_2)_3]^{3-} + C_2O_4^- \rightarrow [Fe^{(III)}(C_2O_4)_3]^{2-} + (C_2O_4)^{2-}$$

$$[Fe^{(III)}(C_2O_4)_3]^{2-} + h\nu \rightarrow [Fe^{(II)}(C_2O_4)_2]^{2-} + 2CO_2$$

The product $[Fe^{(II)}(C_2O_4)_2]^{2-}$ does not absorb light of λ>250 nm and the concentration of Fe^{2+} ion can be measured spectrophotometrically through formation of the red complex with 1,10-phenanthroline. The quantum yield of Fe^{2+} ion formation at 480 nm

is 0.94.[69, 70]

(a) Preparation of Potassium Ferrioxalate Actinometer

Three volumes of 1.5 M potassium oxalate $K_2C_2O_4$ solution and one volume of 1.5 M ferric chloride $FeCl_3.7H_2O$ solution were mixed while stirring. A green precipitate of potassium ferrioxalate was formed:

$$3K_2C_2O_4 + FeCl_3.7H_2O \rightarrow K_3Fe(C_2O_4)_3.3H_2O + 3KCl + 4H_2O$$

The solid potassium ferrioxalate was filtered and recrystallized twice from warm water. The final purified product was dried at 45^0 C for 20 hours and was kept in the dark.

(b) Measurement of the Extinction Coefficient of the Complex $Fe^{(II)}$-Phenanthroline at 510 nm

(1) A 0.1 M $FeSO_4.7H_2O$ solution containing 0.1 N H_2SO_4 was prepared and the concentration of the ferrous ion was standardized against $K_2Cr_2O_7$ by titration using sodium diphenylamine sulfonate as indicator.

(2) Ten standard solutions of $Fe^{(II)}$-Phenanthroline complex with Fe^{2+} concentration of from 5.0×10^{-6} M to 5.0×10^{-5} M were prepared in a buffer solution of pH 4.7. The solutions were kept in the dark for one hour for color development.

(3) The absorbance of the $Fe^{(II)}$-Phenanthroline complex solutions were measured at 510 nm using the same cell which was used for photolysis. From the plot of the absorbance of the solution against the concentration of $Fe^{(II)}$, the extinction coefficient of the $Fe^{(II)}$-Phenanthroline complex at 510 nm of 1.11×10^4 $M^{-1}cm^{-1}$ was obtained.

(c) Photolysis of Actinometer and Determination of I_0

A solution of 0.15 M in $K_3Fe(C_2O_4)_3.3H_2O$ and 0.1 N in H_2SO_4 was prepared. 3.0 mL of this solution was photolysed at 483 nm for ten minutes.

The total solution was transferred to a 25 mL volume metric flask, and to this flask was added 2.5 mL of 0.1% phenanthroline and 10 mL of 0.6 N NaAc solution. Sulfuric acid was added to make the final concentration of H_2SO_4 in the flask 0.1 N. The solution was diluted to the mark and allowed to stand in the dark for one hour for color development. The absorbance at 510 nm was measured.

The number of Fe^{2+} ions ($n_{Fe(II)}$) formed during the photolysis can be calculated according to the following equation:

$$n_{Fe(II)} = \frac{A \times V \times N}{\epsilon}$$

A: absorbance of the complex at 510 nm

V: volume of the actinometer

N: Avogadro's number

ε: Extinction coefficient of Fe(II)-phenanthroline complex at 510 nm

The incident light intensity can be calculated as:

$$I_0 = \frac{n_{Fe(II)}}{t \times \phi\,(1-10^{-A})}$$

t: time of the photolysis (second)

ϕ: quantum yield of formation of Fe^{2+} at 480 nm

A: absorbance of actinometer before photolysis at 483 nm

Following the procedure mentioned above, in one particular measurement of the light intensity at 483 nm, the absorbance of the Fe^{2+} complex was 0.115 at 510 nm. The number of ferrous ions formed during the photolysis is therefore:

$$n_{Fe(II)} = \frac{0.115 \times 0.025 \times 6.02 \times 10^{23}}{1.11 \times 10^{4}}$$

$$= 1.56 \times 10^{17}$$

The photolysis time was 10 minutes (600 sec.), the absorbance of the actinometer before photolysis was 0.20 at 483 nm and the quantum yield for the formation of Fe^{2+} is 0.94 at 480 nm, so that the light intensity reaching the photolysis cell at 483 nm is:

$$I_0 = \frac{1.56 \times 10^{17}}{600 \times 0.94\ (1-10^{-0.20})}$$

$$= 7.5 \times 10^{14} \text{ quanta } s^{-1}$$

2. 1. 4 Other Measurements

The UV-Visible absorption spectra were measured using a Unicam SP-1800 Ultraviolet Spectrophotometer coupled with a Unicam AR 25 Recorder, supplied by Pye Unicam Ltd. Cambridge, England. The scan speed of the spectrophotometer was set at 4 nm $sec.^{-1}$ and the band width at 1 nm. The spectrophotometer had provision for circulating water from a thermostat through the cell holder to maintain a constant temperature in the cell.

^{13}C NMR spectra were measured using the Varian XL-300 nuclear magnetic

resonance spectrometer. Dioxcine was used as external reference and the resonance frequency was at 75.429 MHz.

The pH value of the solution was measured using a Model 320 Expanded Scale Research pH Meter from Fisher Accumet with a Corning combination electrode.

2. 1. 5 Preparation of Reaction Solution

(a) Solutions for Irradiation

Aqueous rhodizonate dianion is unstable in the presence of oxygen and solutions were prepared daily. A stock solution, 5×10^{-3} M, was prepared by dissolving 0.102 gram of disodium rhodizonate in 100 mL of nitrogen-saturated distilled water. This solution was protected from light and nitrogen was continuously passed through the solution. The preparation of the solutions for irradiation and the degassing techniques, both by nitrogen saturation and by freeze-pump-thaw cycles, were described in section 2. 1. 1. The concentration of the rhodizonate dianion in the cell was determined from the absorbance at 483 nm provided that none of the additives absorbed light at this wavelength.

(b) Solution for ^{13}C NMR Measurement

For measurement of the ^{13}C NMR spectrum, 200 mL of reaction solution containing an electron acceptor and rhodizonate dianion with concentration of 5.0×10^{-4} M was photolysed using a 250 W incandescent lamp. A small amount of buffer solution was added to the reaction system. When oxygen gas was used as oxidant, rhodizonate dianion solution was bubbled with high grade oxygen gas. After the rhodizonate dianion was completely consumed, the reaction solution was concentrated by evaporating under vacuum at temperatures below 60^0 C to about 2.5 mL.

2. 1. 6 Reagents

Electron acceptors used in the investigation of the photo-induced electron transfer reactions of rhodizonate dianion include anionic, neutral and cationic species. Acceptors used were: potassium ferricyanide, tetracyanoethylene, hydrogen peroxide, cupric ion, methyl viologen (1,1'-Diethyl-4,4'-bipyridinium dichloride), 3-nitrobenzaldehyde, 4-nitrobenzaldehyde.

Disodium rhodizonate, anhydrous oxalate acid, 3-nitrobenzaldehyde, 4-nitrobenzaldehyde and buffers were purchased from Aldrich; potassium ferricyanide, cupric chloride were purchased from Fisher Scientific Company; potassium oxalate, methyl viologen, hydrogen peroxide, ferric chloride were purchased from BDH. Nitrogen and oxygen were high purity grade (> 99.99%), purchased from Air Products. Cupric chloride and potassium ferricyanide were recrystallized from warm water-ethanol solution. Other reagents were used without further purification.

Deionized distilled water was obtained by passing distilled water first through ion exchange columns and redistilled using a Model AG-2 Water Distillation apparatus supplied by Corning Glass Works.

2. 2. Results

2. 2. 1 Rate of Disappearance of Rhodizonate Dianion

Rhodizonate dianion is rapidly oxidized in air-saturated solutions in the dark and the rate of this reaction increased with increasing pH of the solution. Removal of oxygen stabilizes the system, but in the pH range 6--8 of the present experiments a small residual rate of disappearance of rhodizonate dianion was observed in all solutions regardless of the procedures used for degassing. Typical results are shown in Table 2.1. The loss of rhodizonate dianion in the absence of additive is probably due to traces of oxidizing impurities in the solution.

Table 2.1 Rate of Disappearance of Rhodizonate Dianion Without Additive

$[C_6O_6^{2-}] = 2.5\times10^{-5}$ M

pH	Thermal (Ms^{-1})	Photochemical (Ms^{-1})
6.0	1.3×10^{-10}	1.5×10^{-10}
7.0	1.0×10^{-10}	1.0×10^{-10}
8.0	1.5×10^{-10}	1.9×10^{-10}

At pH ≥ 9 the dark reaction initiated by the OH^-, discussed in the introduction, become too fast to allow accurate kinetic measurements. Measurements of the photochemical reaction were therefore limited to pH ≤ 8 and ≥ 6, where the acid was completely in the form of the dianion. (see values for pK_1 and pK_2 in Table 1. 2.). In the present studies, the pH of the reaction solutions containing rhodizonate dianion were maintained between pH 6 and 8 using buffers. The rates of disappearance of rhodizonate dianion in the absence of additives both in the dark and on irradiation were negligible compared to the rates in the presence of additives. Kinetic measurements were therefore

made only with rhodizonate dianion in the presence of additives.

The thermal and photochemical rates of disappearance of rhodizonate dianion were measured at 20^0C in Deaerated solutions in the presence of the following additives: potassium ferricyanide ($K_3Fe(CN)_6$), hydrogen peroxide (H_2O_2), tetracyanoethylene (TCNE), cupric ion (Cu^{2+}), methyl viologen cation (MV^{2+}), 3-nitrobenzaldehyde (3-NO_2-C_6H_4CHO) and 4-nitrobenzaldehyde (4-NO_2-C_6H_4CHO). The results showed that only the additives cupric ion, ferricyanide anion, hydrogen peroxide and tetracyanoethylene caused a thermal reaction substantially faster than the residual rate and only with the latter three additives was the rate increased on irradiation. The measurements of photochemical rates were reproducible within about 5% as were the higher thermal rates. The slower residual dark reaction had more uncertainty, but was generally consistent. The results are summarized in Table 2.2. Table 2.2(a) summarizes the rates of disappearance of rhodizonate dianion both in the dark and on irradiation from reaction with those electron acceptors which caused a faster reaction on irradiation. Table 2.2(b) summarizes the rates of disappearance of rhodizonate dianion from reaction with those additives which caused no remarkable rate increase over the rate without additive or no noticeable increase on irradiation compared with the rate in the dark. The quantum yields of the disappearance of rhodizonate dianion in Table 2.2(a) were calculated from the rate of disappearance of rhodizonate dianion under photolysis after subtracting the rate of disappearance of rhodizonate dianion in the dark. For example, when the concentration of tetracyanoethylene was 2.0×10^{-5} M and the concentration of rhodizonate dianion was 2.5×10^{-5} M, at pH 7 the rates of disappearance of rhodizonate dianion in the dark and under photolysis were 5.2×10^{-10} Ms^{-1} and 2.3×10^{-9} Ms^{-1} respectively. The net rate of loss of rhodizonate dianion due to photolysis was:

$$2.3\times10^{-9}\ Ms^{-1} - 5.2\times10^{-10}\ Ms^{-1} = 1.8\times10^{-9}\ Ms^{-1}$$

Table 2. 2 (a)

Thermal and Photochemical Oxidation of Rhodizonate Dianion at 20^0 C

Additive	pH	Conc. of Reactants		Rate		ϕ
		[A]	$[C_6O_6^{2-}]$	Thermal	Photochemical	(10^{-3})
		$(M\times10^{-5})$		$(Ms^{-1}\times10^{-9})$		
TCNE[a]	7	2.0	2.5	0.52	2.3	6.2
E^0 = +0.48v	7	5.0	2.5	1.6	4.9	12
	7	10	2.5	3.8	10.2	23
	7	15	2.5	5.3	14.5	33
	7	20	2.5	6.6	19.3	45
H_2O_2	7	2.5	2.5	1.5	2.3	3.3
E^0 = +1.33v	7	5.0	2.5	2.0	3.0	3.9
	7	10.0	2.5	2.9	4.5	6.3
	7	20.0	2.5	4.1	6.4	8.4
	7	25.0	2.5	4.6	7.0	9.6
	7	50.0	2.5	13.3	16.4	13
$Fe(CN)_6^{3-}$	7	2.5	2.5	1.1	2.3	4.4
E^0 = +0.36v	7	5.0	2.5	1.6	3.2	5.6
	7	10.0	2.5	2.1	4.3	7.6
	7	15.0	2.5	2.4	4.9	9.2
	7	20.0	2.5	2.6	5.7	11
	7	25.0	2.5	2.9	6.3	12

a) E^0 vs NHE. E^0 for TCNE was measured in CH_3CN solution, others were in H_2O

Table 2. 2(b)

Thermal and Photochemical Oxidation of Rhodizonate Dianion at 20^0 C

Additive	pH	Conc. of Reactants		Rate	
		[A]	$[C_6O_6^{2-}]$	Thermal	Photochemical
		(10^{-5} M)		(10^{-10} Ms^{-1})	
Cu^{2+}	6	5.0	5.0	3.4	3.4
E^0 = +0.153v	7	5.0	5.0	4.2	4.2
	8	5.0	5.0	9.4	11
MV^{2+}	6	25	2.5	1.2	3.1
E^0 = - 0.44v	7	25	2.5	2.0	2.0
3-NO_2-C_6H_4-CHO					
E^0 = - 0.90v	6	5.0	5.0	1.6	1.6
	7	5.0	5.0	2.0	2.0
4-NO_2-C_6H_4-CHO					
E^0 = - 0.86v	6	5.0	5.0	2.3	4.2
	7	5.0	5.0	2.0	2.1

The quantum yield was calculated as follows:

$$\phi = \frac{R \times N \times L}{I_0 \times (1 - 10^{-A})}$$

Where R: rate of disappearance of rhodizonate dianion caused by photolysis (Ms^{-1})

N: Avogadro's constant (6.02×10^{23})

L: Volume of the reaction solution used for photolysis (Liter).

I_0: light intensity reaching the photolysis cell (Quanta s^{-1}).

A: absorbance of rhodizonate dianion at 483 nm.

In the example cited, the quantum yield was therefore:

$$\phi = \frac{1.8 \times 10^{-9} \times 6.02 \times 10^{23} \times 0.0031}{6.32 \times 10^{14} \times (1 - 10^{-0.80})}$$

$$\phi = 6.2 \times 10^{-3}$$

The initial rates of disappearance of rhodizonate dianion were obtained from plots of the rhodizonate dianion concentration against the reaction time. From randomly repeated experiments, the uncertainty in the initial rates was less than 5%.

2. 2. 2 Product Detection

From the UV-visible absorption spectra, the only product detected from the reaction system of rhodizonate dianion and electron acceptors was the croconate dianion. The percentage conversion from rhodizonate dianion to croconate dianion varied with the electron acceptors used and the pH value of the reaction solution. The highest conversion

rate occurred when cupric ion was used as electron acceptor at pH 7.0 Fig 2.2 shows the appearance of the absorption of the croconate dianion and the corresponding decrease of the absorption of the rhodizonate dianion at pH 7.0 during photolysis in the presence of cupric ion.

Detection of products from the reaction of rhodizonate dianion with hydrogen peroxide, ferricyanide and oxygen was also done using ^{13}C NMR spectra. The ^{13}C NMR spectrum of the dianions of croconic and rhodizonic acids each has only one single chemical shift, at 188 ppm for croconate dianion and at 177 ppm for rhodizonate dianion. The amount of croconate dianion formed from the reaction of rhodizonate dianion with additive could be estimated by comparing the area under the resonance peak at 188 ppm of a ^{13}C NMR spectrum of the reaction solution with the area of the same peak at 188 ppm of a sample of pure croconate dianion with a known volume. Because of the uncertainty in the volume of solution from the experiment the amount obtained from the reaction may be uncertain by 10%. The acquisition time for ^{13}C NMR signal should be long enough to allow the relaxation process to be complete before next pulse was applied, so that it usually took one night for measurement of one sample.

The fractional conversions of rhodizonate dianion to croconate dianion are summarized in Table 2.3, along with the detection techniques used for each sample.

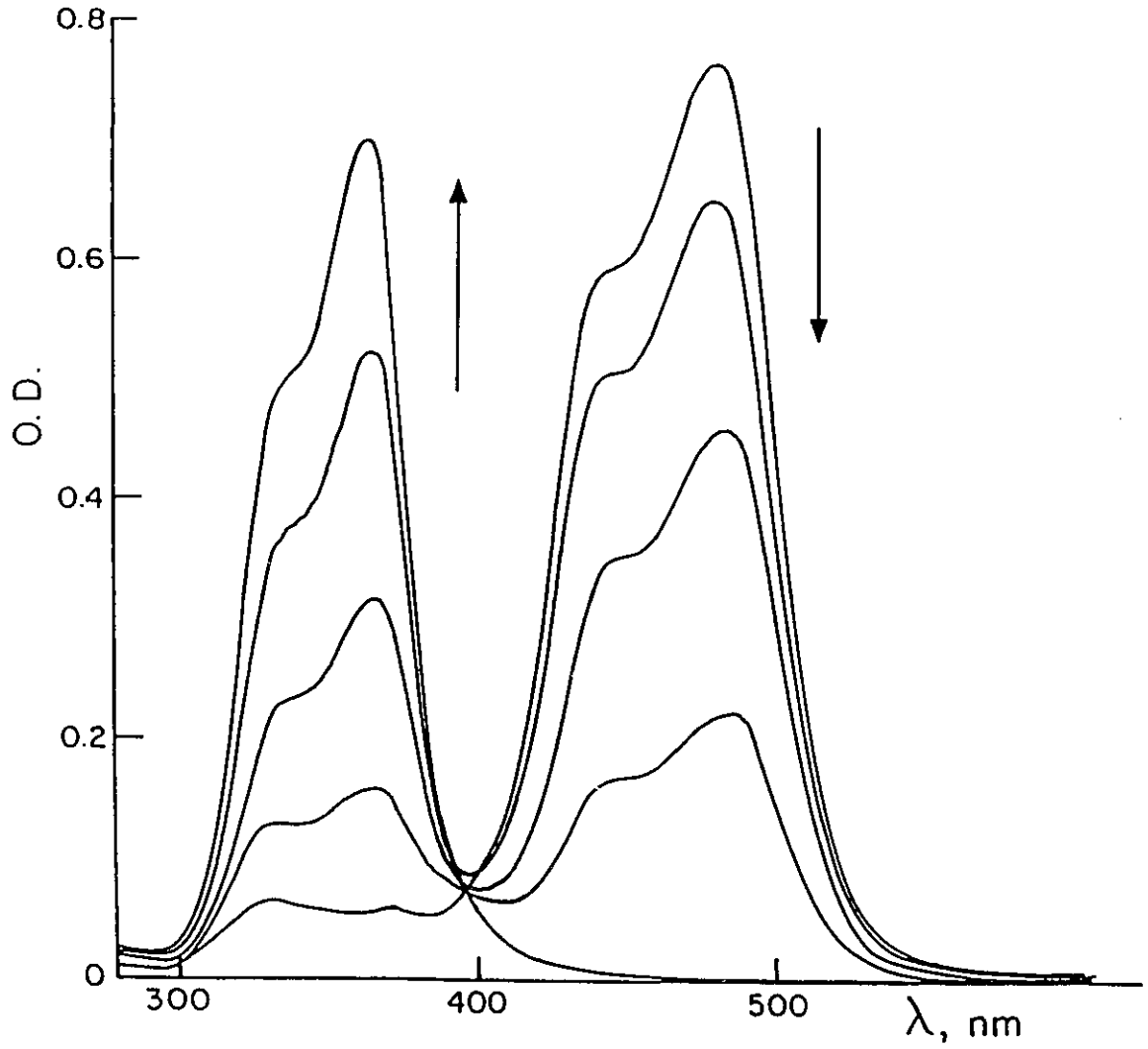

Figure 2.2 Absorption spectra of a solution of rhodizonate dianion in the presence of cupric ion, showing formation of croconate dianion. pH=7.0 Complete reaction of the rhodizonate dianion required three days.

Table 2.3

Fraction of Conversion of Rhodizonate Dianion to Croconate Dianion

Additive	pH	% Conversion to $C_5O_5^{2-}$	Detection Technique
Cu^{2+}	6.0	48	UV-Visible Spectra
	7.0	78	
	8.0	77	
H_2O_2	7.0	33	^{13}C NMR
$Fe(CN)_6^{3-}$	7.0	26	^{13}C NMR
O_2	7.0	11	^{13}C NMR

* Thermal reactions in the cases of Cu^{2+} and O_2, photochemical reactions in the cases of H_2O_2 and $Fe(CN)_6^{3-}$.

2. 3 Discussion

2. 3. 1 The Thermal Dark Reaction

Rhodizonate dianion is oxidized rapidly by oxygen or hydrogen peroxide in basic solution to give croconate dianion quantitatively. The first step in the reaction is believed to be attack by the hydroxide anion. The mechanism of the reaction was illustrated in chapter 1 (page 15). The present results show that conversion to croconate dianion and other products occurs also in neutral or slightly acidic solution and can be initiated by several oxidizing agents as well as oxygen and hydrogen peroxide.

The fact that reagents such as Cu^{2+}, $Fe(CN)_6^{3+}$ and TCNE are effective suggests that the first step is electron transfer and the first stages of the reaction may be written as:

[1] $C_6O_6^{2-} + A \rightleftharpoons (C_6O_6^{-\cdot}...A^-)$

[2] $(C_6O_6^{-\cdot}...A^-) \rightleftharpoons C_6O_6^{-\cdot} + A^-$

[3] $C_6O_6^{-\cdot} \rightarrow$ Product

Where A stands for additive and $(C_6O_6^{-\cdot}...A^-)$ represents the caged charge transfer complex before the ions separate.

Assuming a steady state concentration of the intermediate $(C_6O_6^{-\cdot}...A^-)$.

$$k_1[C_6O_6^{2-}][A] + k_{-2}[C_6O_6^{-\cdot}][A^-] = (k_{-1} + k_2)[(C_6O_6^{-\cdot}...A^-)]$$

The concentration of the caged complex may be written as:

$$[(C_6O_6^{-\cdot}...A^-)] = \frac{k_1[C_6O_6^{2-}][A] + k_{-2}[C_6O_6^{-\cdot}][A^-]}{k_{-1} + k_2}$$

Also since $[C_6O_6^{-\cdot}] = [A^-]$

$$k_2[(C_6O_6^{-\cdot}...A^-)] = k_{-2}[C_6O_6^{-\cdot}]^2 + k_3[C_6O_6^{-\cdot}]$$

Two limiting cases may be considered.

(a) Only a small fraction of the ions escape the cage before the reverse electron transfer regenerates the reactants but all those that escape react to form product. This assumes the following requirements:

$$k_2 << k_{-1}$$

$$k_{-2}[C_6O_6^{\cdot-}]^2 << k_3[C_6O_6^{\cdot-}]$$

Also, since all the monoanion radicals react to form products,

$$k_{-2}[C_6O_6^{\cdot-}]^2 << k_1[C_6O_6^{2-}][A]$$

Therefore:

$k_3[C_6O_6^{\cdot-}] = k_2[C_6O_6^{\cdot-}...A^-]$ and

$$[C_6O_6^{\cdot-}...A^-] = \frac{k_1}{k_{-1}} [C_6O_6^{2-}] [A]$$

The rate of disappearance of rhodizonate dianion therefore is:

$$\frac{-d[C_6O_6^{2-}]}{dt} = \frac{k_1k_2}{k_{-1}} [C_6O_6^{2-}][A] \qquad (2\text{-}1)$$

The rate is therefore first order with respect to the concentrations of both rhodizonate dianion and electron acceptor.

(b) If the ions escape the cage but still a major fraction undergo the reverse electron transfer and only a small fraction form products, it follows that:

$$k_3[C_6O_6^{\cdot-}] << k_{-2}[C_6O_6^{\cdot-}]^2$$

$$k_2 << k_{-1}$$

In this case, the concentration of the monoanion radical will be controlled by the equilibrium constants for reactions [1] and [2] and the rate of the disappearance of rhodizonate dianion can be derived as follows:

$$k_2[C_6O_6^{\cdot-}...A^-] = k_{-2}[C_6O_6^{\cdot-}]^2$$

$$[C_6O_6^{\cdot-}] = \left\{ \frac{k_2}{k_{-2}} [C_6O_6^{\cdot-}...A^-] \right\}^{1/2}$$

$$k_1[C_6O_6^{2-}][A] = k_{-1}[C_6O_6^{\cdot-}...A]$$

$$[C_6O_6^{\cdot-}...A^-] = \frac{k_1}{k_{-1}} [A]\,[C_6O_6^{2-}]$$

The rate of disappearance of rhodizonate dianion becomes in this case:

$$-\frac{d[C_6O_6^{2-}]}{dt} = k_3\,[C_6O_6^{\cdot-}]$$

$$= k_3 \left\{ \frac{k_1 k_2}{k_{-1} k_{-2}} [C_6O_6^{2-}]\,[A] \right\}^{1/2}$$

$$= k_3 \left\{ K_1 K_2\,[C_6O_6^{2-}]\,[A] \right\}^{1/2} \qquad (2\text{-}2)$$

In this case the rate of disappearance of rhodizonate dianion is proportional to the square root of the concentrations of both electron acceptor and rhodizonate dianion. For this case, it is not necessary that the intermediate step [1] attain equilibrium. Only an overall equilibrium involving the electron transfer is indicated and the intermediate step may not be kinetically important.

In the present experiments, case (b) was observed with the oxidizing agents hydrogen peroxide and potassium ferricyanide. The results are shown in Fig. 2.3 and Fig. 2.4, where the rate of the reaction at a fixed concentration of rhodizonate dianion is plotted as a function of the square root of the concentration of electron acceptor $[A]^{1/2}$. Measurements of the rate at 30^0 C with $Fe(CN)_6^{3-}$ are also included in Fig. 2.4. The rate of the reaction with TCNE, on the other hand, was a linear function of [A] and for this reagent therefore the mechanism corresponds to case (a). The results at both 20^0 C and 30^0 C are

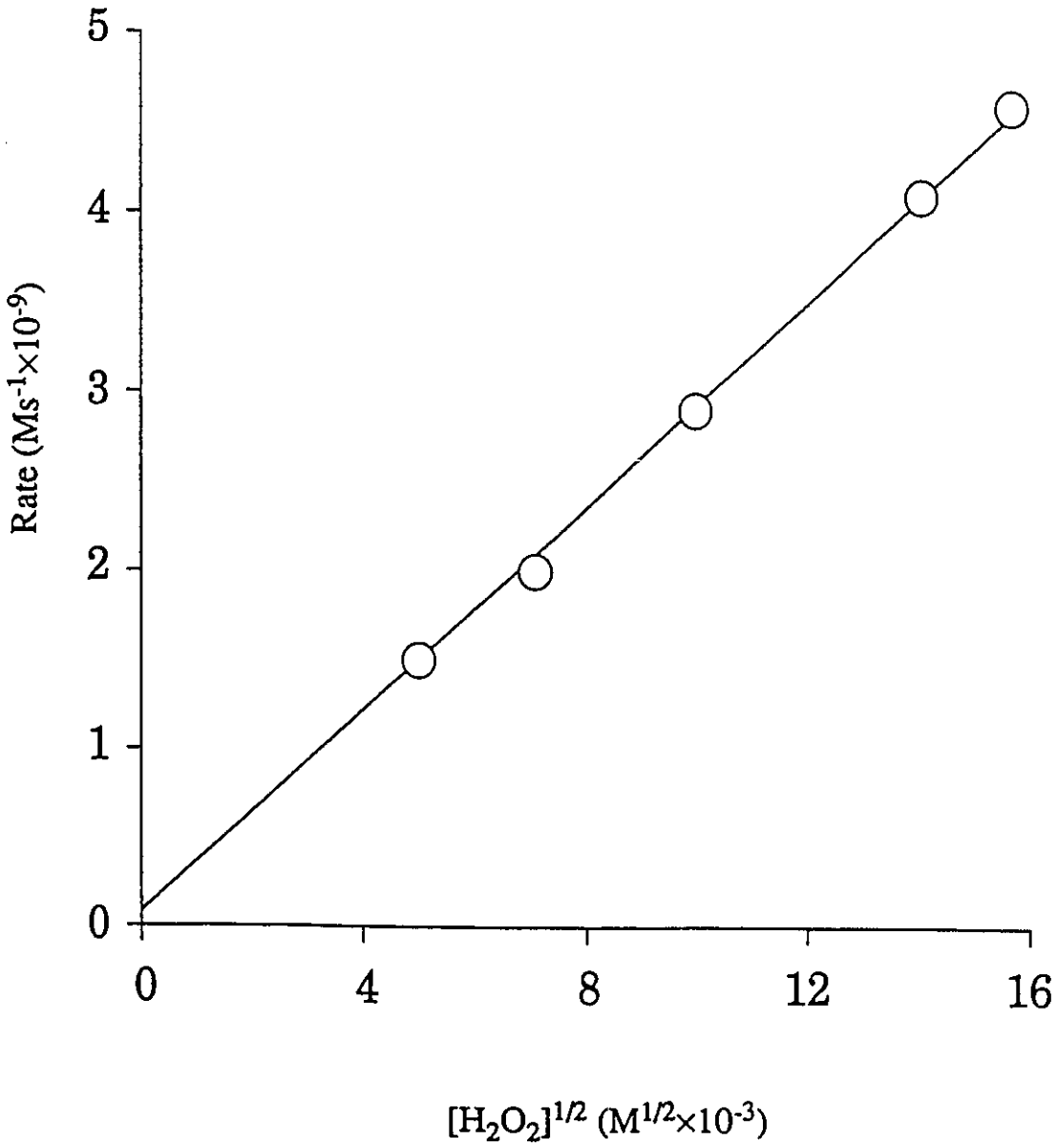

Figure 2.3 Rate of the disappearance of rhodizonate dianion as a function of square root of concentration of hydrogen peroxide.

T=293 K; pH=7.0

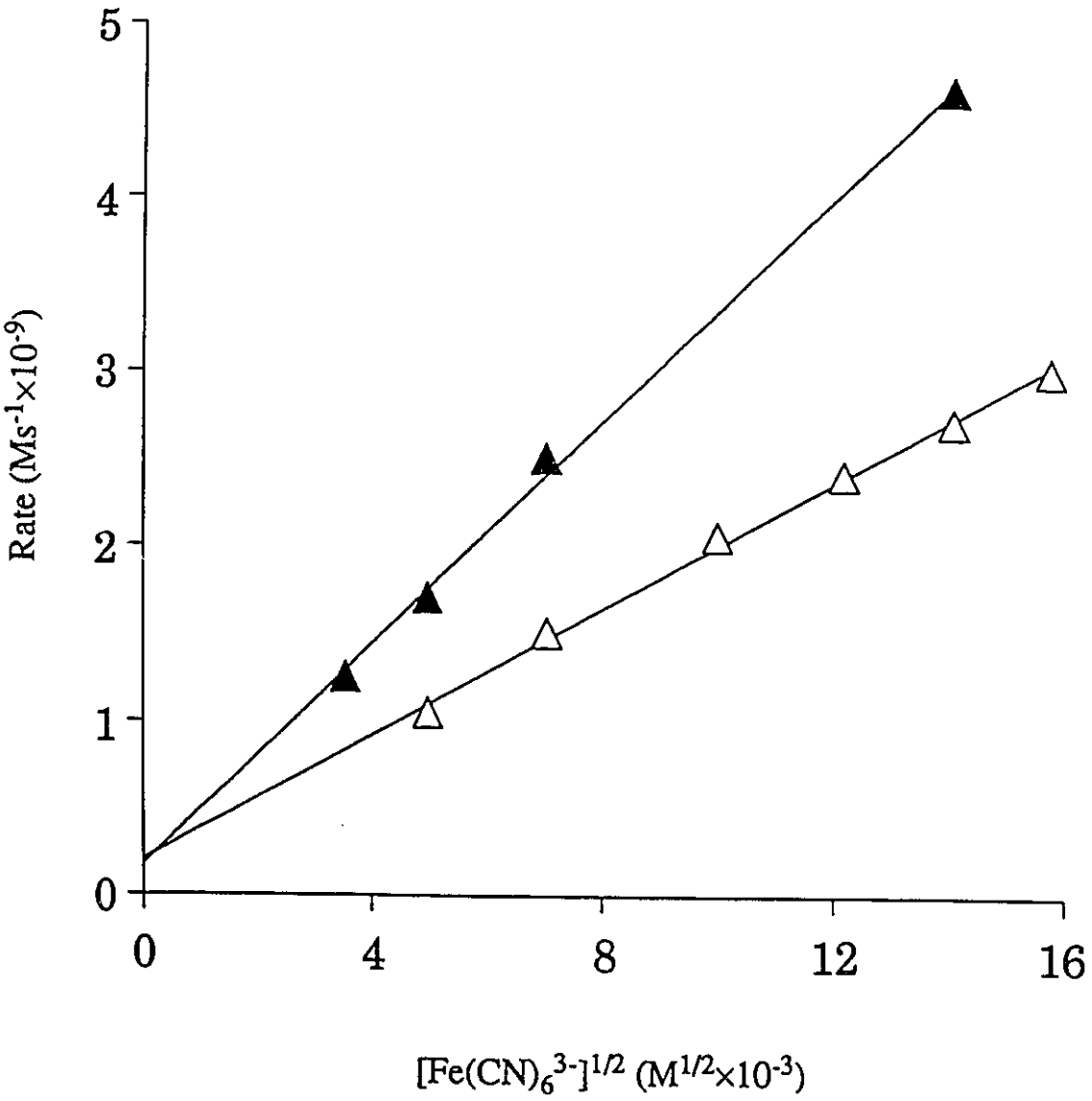

Figure 2.4 Rate of the disappearance of rhodizonate dianion as a function of square root of concentration of potassium ferricyanide.

△: T=293 K; ▲: T=303 K; pH=7.0

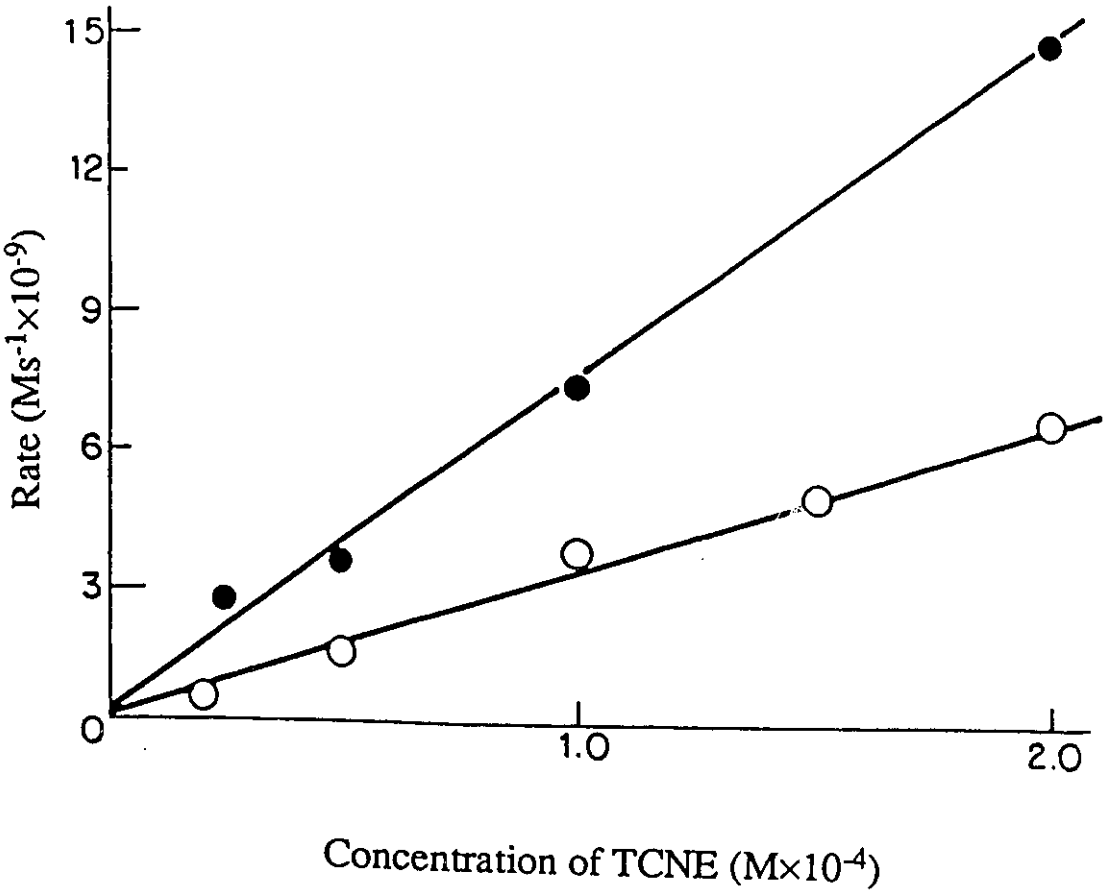

Figure 2.5 Rate of the disappearance of rhodizonate dianion as a function of concentration of tetracyanoethylene

o: T=293 K; •: T=303 K; pH=7.0

shown in Fig. 2.5. The rates of disappearance of rhodizonate dianion at 30^0 C using TCNE and $Fe(CN)_6^{3-}$ as electron acceptors are summarized in Table 2.4.

Some experimental results with constant concentration of TCNE and $Fe(CN)_6^{3-}$ and variable concentration of rhodizonate dianion are summarized in Table 2.5. With TCNE the rate was proportional to the concentration of rhodizonate dianion while with $Fe(CN)_6^{3-}$, the rate was proportional to the square root of the concentration of the dianion.

At first sight it appears improbable that different limiting cases would be observed for similar reactions, particularly when k_3 is the same, and k_{-2} is similar for each reaction. The difference in rates between $k_{-2}[C_6O_6^{-\cdot}]^2$ and $k_3[C_6O_6^{-\cdot}]$, which governs the order of the rate, arises through the difference in the concentration of rhodizonate monoanion radical in the two systems. The change-over in the order occurs when $[C_6O_6^{-\cdot}] = k_3/k_{-2}$. The concentration of the monoanion radical is largely determined by the rate of separation of the caged complex, which is a function of the structure and properties of the oxidizing agent, including the charge distribution in the complex. It is interesting that similar rates are observed for TCNE and the other two reactants and indicates the compensating effects of k_2, k_{-2} and k_3.

For TCNE, the rates of disappearance of rhodizonate dianion measured at several different temperatures are summarized in Table 2. 6 and shown in an Arrhenius plot in Fig. 2.6. This data shows the change in the rate constant for formation of product as a function of temperature. The reaction may be represented as:

$$C_6O_6^{2-} + A \rightarrow C_6O_6^{-\cdot} + A^- \qquad (T)$$

$$C_6O_6^{-\cdot} \rightarrow \text{Products}$$

If all the monoanion radicals $C_6O_6^{-\cdot}$ react to form products then reaction (T) represents the rate of loss of rhodizonate dianion and the rate may be expressed as:

$$-d[C_6O_6^{2-}]/dt = k_T[C_6O_6^{2-}][A]$$

Table 2.4

Thermal Oxidation of Rhodizonate Dianion at 30^0 C

$[C_6O_6^{2-}] = 2.5\times10^{-5}$ M, pH = 7.0

Additive	Concentration of Additive ($M\times10^{-5}$)	Rate ($Ms^{-1}\times10^{-9}$)
TCNE	2.5	2.8
	5.0	3.6
	10	7.4
	20	14.7
$Fe(CN)_6^{3-}$	1.25	1.2
	2.5	1.7
	5.0	2.5
	20	4.6

Table 2. 5

Thermal and Photochemical Oxidation of Rhodizonate Dianion at Different Concentration of Rhodizonate Dianion at 20^0 C, pH=7.0

Additive	[A] (M)	$[C_6O_6^{2-}]$ ($M\times10^{-5}$)	Rate ($Ms^{-1}\times10^{-9}$) Thermal	Photochem.	ϕ (10^{-3})
$Fe(CN)_6^{3-}$	2.0×10^{-4}	1.25	2.0	4.6	12
	2.0×10^{-4}	2.5	4.6	5.7	11
	2.0×10^{-4}	5.0	4.2	7.5	9.7
TCNE	2.0×10^{-4}	1.25	3.2	12.1	44
	2.0×10^{-4}	2.5	6.6	19.3	45
	2.0×10^{-4}	5.0	13.5	28.4	44

Table 2. 6

Thermal Oxidation of Rhodizonate Dianion

$[C_6O_6^{2-}] = 2.5\times10^{-5}$ M; [TCNE] = 5.0×10^{-5} M; pH=7.0

T (K)	1000/T	Rate($Ms^{-1}\times10^{-9}$)	lnk_T
283.2	3.53	1.0	-0.223
293.2	3.41	1.6	0.259
303.2	3.30	3.6	1.06
313.2	3.19	5.5	1.48

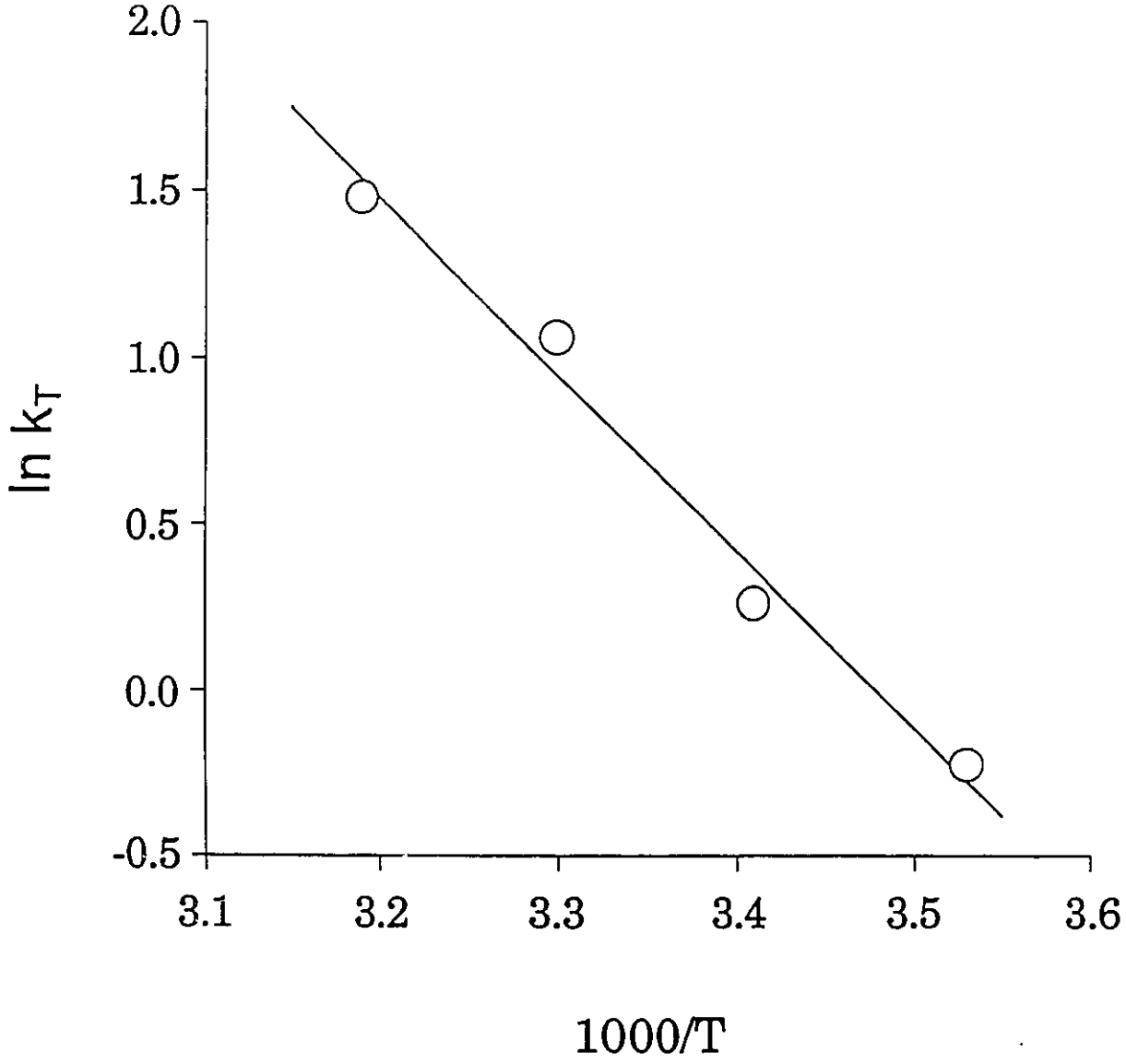

Figure 2.6 Rate constant of the disappearance of rhodizonate dianion as a function of temperature in the presence of tetracyanoethylene
[TCNE]=5.0×10^{-5} M; pH=7.0

From the slope of the plot, the over-all activation energy for the reaction of rhodizonate dianion with TCNE may be estimated as 42 kJ mol^{-1}.

The equilibrium constant for the over-all one-electron transfer process :

[T] $C_6O_6^{2-} + A \rightleftharpoons C_6O_6^{\cdot-} + A^-$

may be expressed as:

$$RT\ln K_T = nFE^0$$

where E^0 is the standard cell potential for the cell represented by reaction [T] which may be expressed as

$$E^0 = E^0(A/A^-) - E^0(C_6O_6^{\cdot-}/C_6O_6^{2-})$$

where $E^0(A/A^-)$ and $E^0(C_6O_6^{\cdot-}/C_6O_6^{2-})$ represent the standard reduction potentials for the reactions indicated. Although the experiments were not performed under standard conditions, the concentration of rhodizonate dianion and additives were in the same range, and $[C_6O_6^{\cdot-}] = [A^-]$; hence:

$$E(A/A^-) - E(C_6O_6^{\cdot-}/C_6O_6^{2-})$$

will be similar to the cell potential under standard conditions.

For a particular concentration of rhodizonate dianion, $\ln K_T$ and hence $[C_6O_6^{\cdot-}]$ will therefore be proportional to $E^0(A/A^-)$. From the results in Table 2.2 it appears that the rate of the thermal reaction correlates roughly with the strength of the oxidizing agents. No oxidation was observed with the reactants of MV^{2+}, 3-nitrobenzaldehyde and 4-nitrobenzaldehyde. It may be concluded that oxidizing agents with standard reduction potentials below approximately zero volts have not sufficient strength to oxidize rhodizonate dianion in aqueous solution. This correlation of the rate with potential supports the mechanism of electron transfer.

2. 3. 2 The Photochemical Reaction

An increase in the rate of disappearance of rhodizonate dianion on irradiation was observed with the reactants hydrogen peroxide, ferricyanide and tetracyanoethylene. The quantum yields in all cases were low (maximum 4×10^{-2}) as expected when the reverse of reaction [2] is fast. A simple extension of the mechanism for the thermal reaction may be written as follows:

[I_{abs}] $C_6O_6^{2-} + h\nu \rightarrow C_6O_6^{2-*}$

[D] $C_6O_6^{2-*} \rightarrow C_6O_6^{2-}$

[4*] $C_6O_6^{2-*} + A \rightarrow (C_6O_6^{-\cdot}...A^-)$

[-4] $(C_6O_6^{-\cdot}...A^-) \rightarrow C_6O_6^{2-} + A$

[5] $(C_6O_6^{-\cdot}...A^-) \rightleftharpoons C_6O_6^{-\cdot} + A^-$

[3] $C_6O_6^{-\cdot} \rightarrow$ Product

Kinetic analysis of the reaction mechanism assuming a steady state concentration of intermediates leads to the following expressions:

The concentration of the caged complex is:

$$[C_6O_6^{-\cdot}...A^-] = \frac{k_4^* [C_6O_6^{2-}] [A] + k_{-5} [C_6O_6^{-\cdot}]^2}{k_{-4} + k_5}$$

$$\frac{d [C_6O_6^{-\cdot}]}{dt} = 0 \qquad \text{and we have:}$$

$$k_5[C_6O_6^{-\cdot}...A^-] = k_{-5}[C_6O_6^{-\cdot}]^2 + k_3[C_6O_6^{-\cdot}]$$

Since only reaction [3] leads to the loss of rhodizonate dianion, the rate of disappearance of rhodizonate dianion is:

$$\frac{-d[C_6O_6^{2-}]}{dt} = k_3 [C_6O_6^{-\cdot}]$$

Two limiting cases similar to those described in the kinetics of the dark reaction are considered.

For case (a) the concentration of the rhodizonate monoanion radical is:

$$[C_6O_6^{\cdot-}] = \frac{k_5\, k_4^*}{k_3\, k_{-4}}\, [C_6O_6^{2-*}][A]$$

and the photochemical rate of disappearance of rhodizonate dianion is therefore:

$$\frac{-d[C_6O_6^{2-}]}{dt} = k_3[C_6O_6^{\cdot-}]$$

$$= \frac{k_5\, k_4^*}{k_{-4}}\, [C_6O_6^{2-*}][A]$$

The total rate of disappearance of rhodizonate dianion from both thermal and photochemical reactions becomes:

$$\frac{-d[C_6O_6^{2-}]}{dt} = k_2\, K_1\, [C_6O_6^{2-}]\, [A] + \frac{k_4^*\, k_5}{k_{-4}}\, [C_6O_6^{2-*}]\, [A]$$

The steady state concentration of $C_6O_6^{2-*}$ is given as

$$[C_6O_6^{2-*}] = \frac{I_{abs}}{k_D + k_4^*[A]}$$

So the expressions for the rate and quantum yield of the disappearance of rhodizonate dianion are:

$$\frac{-d[C_6O_6^{2-}]}{dt} = k_2.K_1[C_6O_6^{2-}][A] + k_4^*k_5\frac{I_{abs}[A]}{k_{-4}(k_D + k_4^*[A])} \qquad (2\text{-}3)$$

$$\phi = \frac{k_4^*k_5[A]}{k_{-4}(k_D + k_4^*[A])} \qquad (2\text{-}4)$$

In calculating the quantum yield, only the loss of rhodizonate dianion initiated by the photo-induced chemical reaction is considered, so that only the second term in the total rate expression of equation (2-3) was taken into account.

Since the rate of disappearance of rhodizonate dianion is not independent of [A], k_D must be greater than $k_4^*[A]$, and equation (2-4) can be simplified further to:

$$\phi = \frac{k_4^*\, k_5}{k_D\, k_{-4}}\, [A]$$

As in the thermal reaction, this case was observed with additive TCNE. The quantum yield for the disappearance of rhodizonate dianion was linearly dependent on the

concentration of TCNE, as shown in Fig. 2.7, where the measurements were made with constant concentration of rhodizonate dianion.

For case (b) the concentration of rhodizonate monoanion radical is,

$$[C_6O_6^{\cdot-}] = \left\{ \frac{k_5}{k_{-5}} [C_6O_6^{\cdot-}...A^-] \right\}^{1/2}$$

$$= \left\{ K_5 [C_6O_6^{\cdot-}...A^-] \right\}^{1/2}$$

and the concentration of the complex cage is:

$$[C_6O_6^{\cdot-}...A^-] = \frac{k_4^*}{k_{-4}} [C_6O_6^{2-*}][A]$$

The rate of disappearance of rhodizonate dianion by the photo-induced reaction is:

$$\frac{-d[C_6O_6^{2-}]}{dt} = k_3[C_6O_6^{\cdot-}]$$

$$= k_3 \left\{ K_5 \frac{k_4^*}{k_{-4}} [C_6O_6^{2-*}][A] \right\}^{1/2}$$

$$[C_6O_6^{2-*}] = \frac{I_{abs}}{k_D + k_4^*[A]}$$

and $$\frac{-d[C_6O_6^{2-}]}{dt} = k_3 \left\{ K_5 \frac{k_4^*}{k_{-4}} \cdot \frac{I_{abs}[A]}{(k_D + k_4^*[A])} \right\}^{1/2}$$

The total rate of disappearance of rhodizonate dianion by both thermal and photochemical reactions is:

$$\frac{-d[C_6O_6^{2-}]}{dt} = k_3 \left\{ K_1K_2[C_6O_6^{2-}][A] \right\}^{1/2} + k_3 \left\{ K_5 \frac{I_{abs}k_4^*[A]}{k_{-4}(k_D + k_4^*[A])} \right\}^{1/2} \qquad (2\text{-}5)$$

Following the previous reasoning, where it was shown that $k_D >> k_4^*[A]$, the quantum yield is given as:

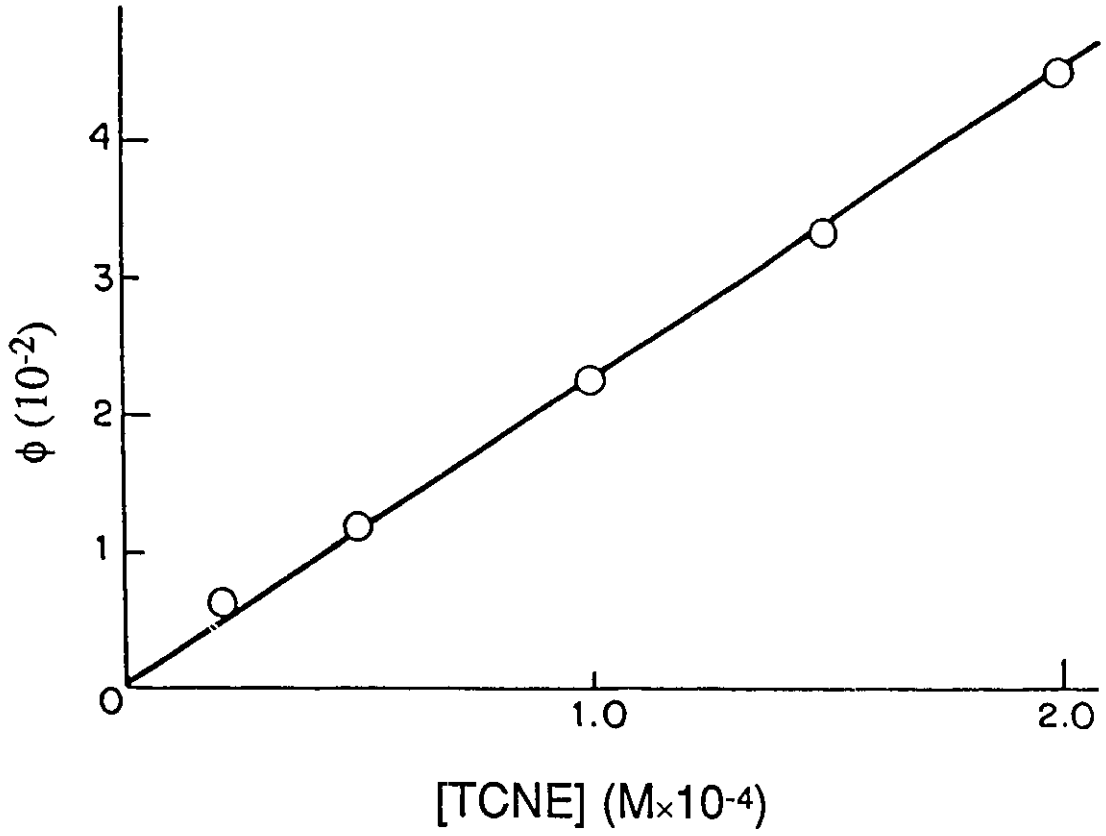

Figure 2.7 Quantum yield of the disappearance of rhodizonate dianion as a function of concentration of tetracyanoethylene.

pH=7.0; T=293 K

$$\phi = k_3\left\{\frac{k_4^* K_5 [A]}{I_{abs} k_D k_{-4}}\right\}^{1/2} \qquad (2\text{-}6)$$

As in the thermal reaction this mechanism was found when hydrogen peroxide and potassium ferricyanide were used as electron acceptors. The quantum yields for the photochemical reaction with these two additives are shown as a function of $[A]^{1/2}$ for constant concentration of rhodizonate dianion in Fig. 2.8 and Fig. 2.9, respectively.

With TCNE and at fixed concentration of additive, the thermal reaction rate is proportional to the concentration of rhodizonate dianion, while the photochemical reaction rate is proportional to the light intensity absorbed by rhodizonate dianion. For example, when the concentration of rhodizonate dianion increased from 1.25×10^{-5} M (I_{abs}=0.60 I_0) to 2.5×10^{-5} M (I_{abs}=0.84 I_0) and then to 5.0×10^{-5} M (I_{abs}=0.975 I_0), the thermal rate for the disappearance of rhodizonate dianion increased in the ratio of 1.0:2.1:4.2. The light intensity absorbed by rhodizonate dianion increased in the ratio of 1.0:1.4:1.6 and the corresponding net photochemical reaction rates increased in the ratio of 1.0:1.4:1.7. These changes in the concentration of rhodizonate dianion and the light intensity absorbed by rhodizonate dianion as well as the rates of both thermal and photochemical reactions are presented in Table 2.7. The quantum yield was unchanged with the change of rhodizonate dianion concentration as shown in Table 2.5. All these results showed that the mechanism of the reaction between TCNE and rhodizonate dianion corresponds to the limiting case (a)

On the other hand, the mechanism of the reaction between ferricyanide and rhodizonate dianion is consistent with the limiting case (b). The relative thermal and photochemical rates at different rhodizonate dianion concentrations and fixed ferricyanide concentration are summarized in Table 2.7. These results show that the rate of thermal reaction between rhodizonate dianion and ferricyanide is proportional to the square root of the concentration of rhodizonate and the rate of the photochemical reaction is proportional

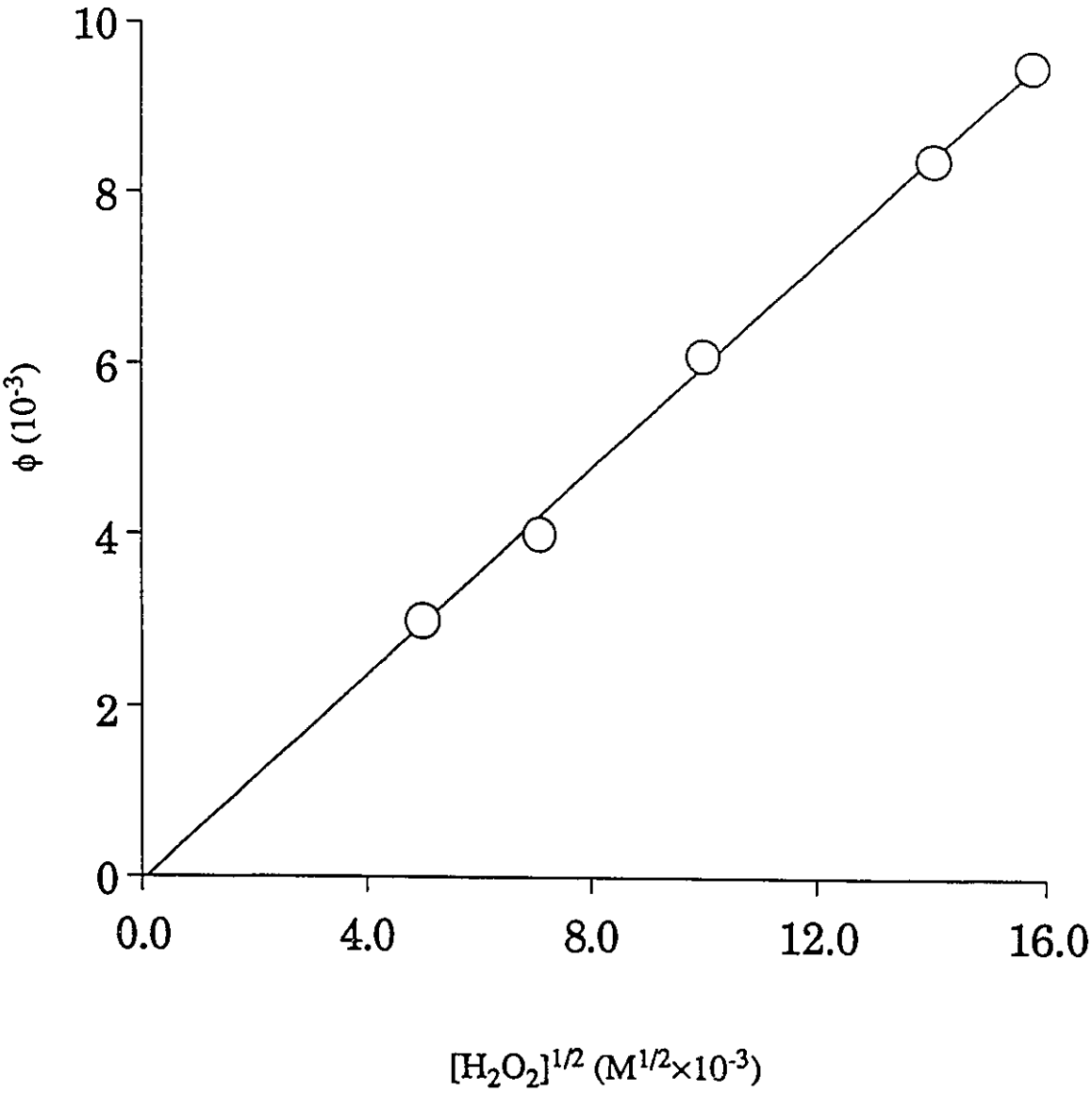

Figure 2.8 Quantum yield of the disappearance of rhodizonate dianion as function of square root of concentration of hydrogen peroxide

pH=7.0; T=293 K

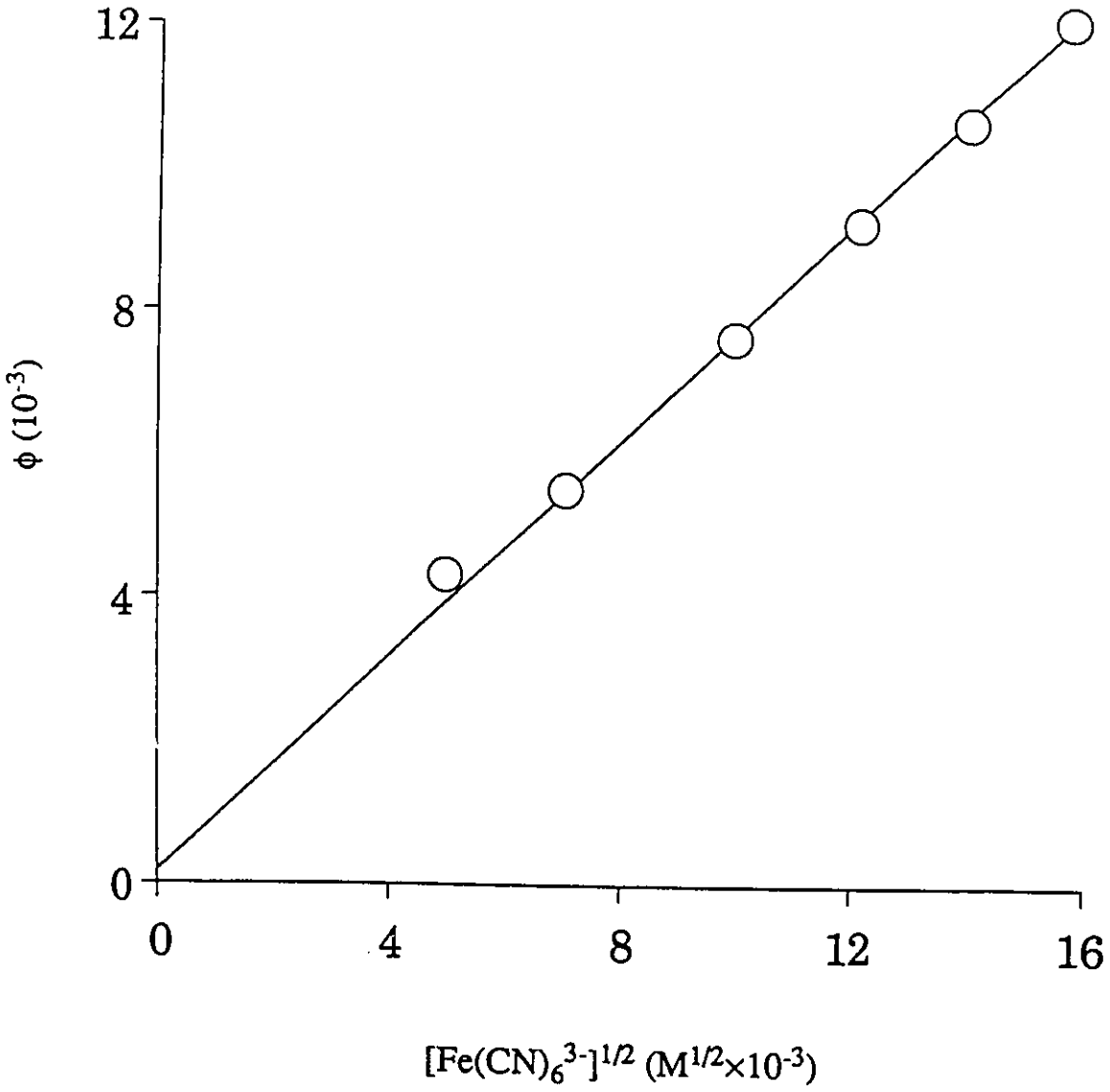

Figure 2.9 Quantum yield of the disappearance of rhodizonate dianion as a function of square root of concentration of potassium ferricyanide

pH=7.0; T=293 K

Table 2.7

Relative Thermal and Photochemical Reaction Rate

pH = 7.0

[TCNE] = 2.0×10^{-4} M:

$[C_6O_6^{2-}]$ [M]	Relative $[C_6O_6^{2-}]$	Relative Therm. Rate	Relative $[I_{abs}]$	Relative Photochem. Rate
1.25×10^{-5}	1.0	1.0	1.0	1.0
2.5×10^{-5}	2.0	2.1	1.4	1.4
5.0×10^{-5}	4.0	4.2	1.6	1.7

$[Fe(CN)_6^{3-}] = 2.0\times10^{-4}$ M:

$[C_6O_6^{2-}]$ [M]	Relative $[C_6O_6^{2-}]^{1/2}$	Relative Therm. Rate	Relative $[I_{abs}]^{1/2}$	Relative Photochem. Rate
1.25×10^{-5}	1.0	1.0	1.0	1.0
2.5×10^{-5}	1.4	1.3	1.2	1.2
5.0×10^{-5}	2.0	2.1	1.3	1.3

to the square root of the light intensity absorbed by the rhodizonate dianion.

Thus the mechanism of the oxidation of rhodizonate dianion with each oxidizing agent is the same under both thermal and photochemical reactions. Irradiation of the dianion simply increases the rate of the initial electron transfer.

2. 3. 3 Products of the Reaction

Detection and analysis of products in the dilute solutions used in the present experiment presented some difficulty. In an aqueous solution of ions absorption in the visible or ultraviolet often provides a basis for identification. The only product detected and quantitatively measured by its absorption spectrum was croconate dianion. When Cu^{2+} was present in the reaction system the majority of the product was croconate dianion. With other additives the fraction of rhodizonate dianion converted to croconate dianion was smaller and detection of croconate dianion by absorption spectra was difficult. For these cases, ^{13}C NMR detection was used. The fraction of conversion of rhodizonate dianion to croconate dianion under different reaction conditions is listed in Table 2.3.

In basic solution rhodizonate dianion is quantitatively converted to croconate dianion with the oxidizing agents hydrogen peroxide or oxygen. In neutral solution the fraction converted was much less, 33% with hydrogen peroxide and only 10% with oxygen. The most efficient conversion occurred with Cu^{2+} at pH 7, and the experimental results showed that changing the ratio of additive to rhodizonate dianion in the reaction system had no noticeable effect on the fraction of conversion. The fact that each oxidizing agent produced a different rate of conversion to croconate dianion indicates that additional steps after the initial electron transfer are required for this conversion, and these steps may involve the oxidizing agent. It should be noted that secondary photolysis of croconate dianion is not important because the wavelength of maximum absorption of the croconate

dianion (363 nm) is far outside the narrow band width of the incident radiation. In basic solution the ring contraction is believed to occur by an α-oxo alcohol rearrangement following attack by hydroxyl ion. The present results show that the ring contraction giving croconate dianion may be initiated in neutral solution with several oxidizing agents. No evidence for absorption in the visible and near ultra-violet due to other products was obtained with any of the additives. Weak absorbers would, of course, escape detection.

The ^{13}C NMR spectra of the reaction products formed during the reactions of rhodizonate dianion with ferricyanide, hydrogen peroxide and oxygen are summarized in Table 2.8, including the single resonance at 177 ppm observed in the neutral solution of rhodizonate dianion. With all the reactants rhodizonate dianion was completely consumed. The resonance at 188.8 ppm shows the presence of croconate dianion formed in all three reactants. Other carbonyl resonances are present in the products formed from all three reactants. Carbonyl resonance due to oxalic or formic acid are, however, absent, as there were no resonances at 162.9 ppm and 166.5 ppm, as observed for pure oxalic and pure formic acid respectively. Oxalic acid and formic acid were observed by Isbell[72] as products of the reaction of rhodizonate dianion and H_2O_2 in aqueous solution. In these experiments H_2O_2 was in large excess and probably secondary oxidation occurred. No evidence for products containing C-H bonds was obtained with the additives ferricyanide and hydrogen peroxide and except for the resonance at 76 ppm, the products appear similar from both reactants.

With oxygen the products are diverse and may include secondary oxidation. The proton decoupled spectra showed the resonances at 91.5 ppm with coupling constant of 163.3 HZ and at 76.1 ppm with coupling constant of 149.9 HZ represent carbon atoms bonded to a single hydrogen atom. Fig 2. 10 shows a Heteronuclear Chemical Shift Correlation spectrum showing both ^{13}C and ^{1}H chemical shifts. The ^{1}H-NMR chemical

Table 2. 8

^{13}C NMR Spectra of the Products of the Photochemical Reaction of Rhodizonate Dianion

Additives			
$C_6O_6^{2-}$	$Fe(CN)_6^{3-}$	H_2O_2	O_2
	^{13}C Chemical Shift		
177.0	188.6	188.9	188.8
	176.4	177.2	177.3
	172.6	173.7	176.5
		76.0	170.5
			93.7
			91.5
			76.1

shift of the proton attached to the carbon which has ^{13}C-NMR chemical shift of 91.5 ppm is about 4.8 ppm, while the ^{1}H-NMR chemical shift of the proton attached to the carbon which has ^{13}C-NMR chemical shift of 76.1 ppm is about 4.4 ppm. Using the DEPT technique, the results showed that both carbons which have ^{13}C-NMR chemical shifts of 91.5 ppm and 76.1 ppm had either one or three protons. Because it seems unlikely that three protons would be attached to a carbon derived from the rhodizonate dianion, the structure most probably involves a C-H bond. The resonance at 93.7 ppm which did not involve a C-H bond may indicate a geminol diol carbon, as suggested by Gelb, Schwargz and Laufer[30] in their interpretation of the NMR spectra of aqueous solutions of rhodizonate dianion. It seems clear that in the oxygen system reduction at a carbon atom has occurred and there is strong indication, particularly from the resonance at 91.5 ppm that an oxygen atom has been incorporated into the ring in an ether linkage. Possible products are ring compounds of the type:

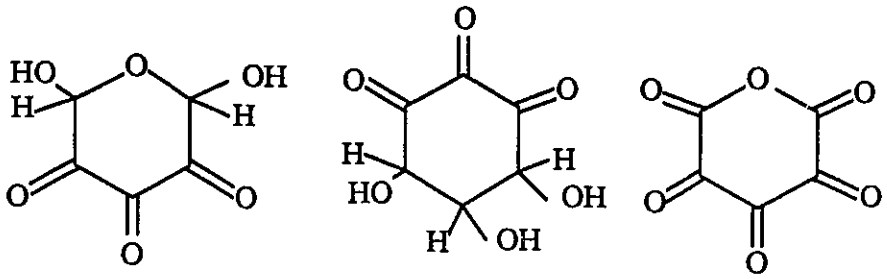

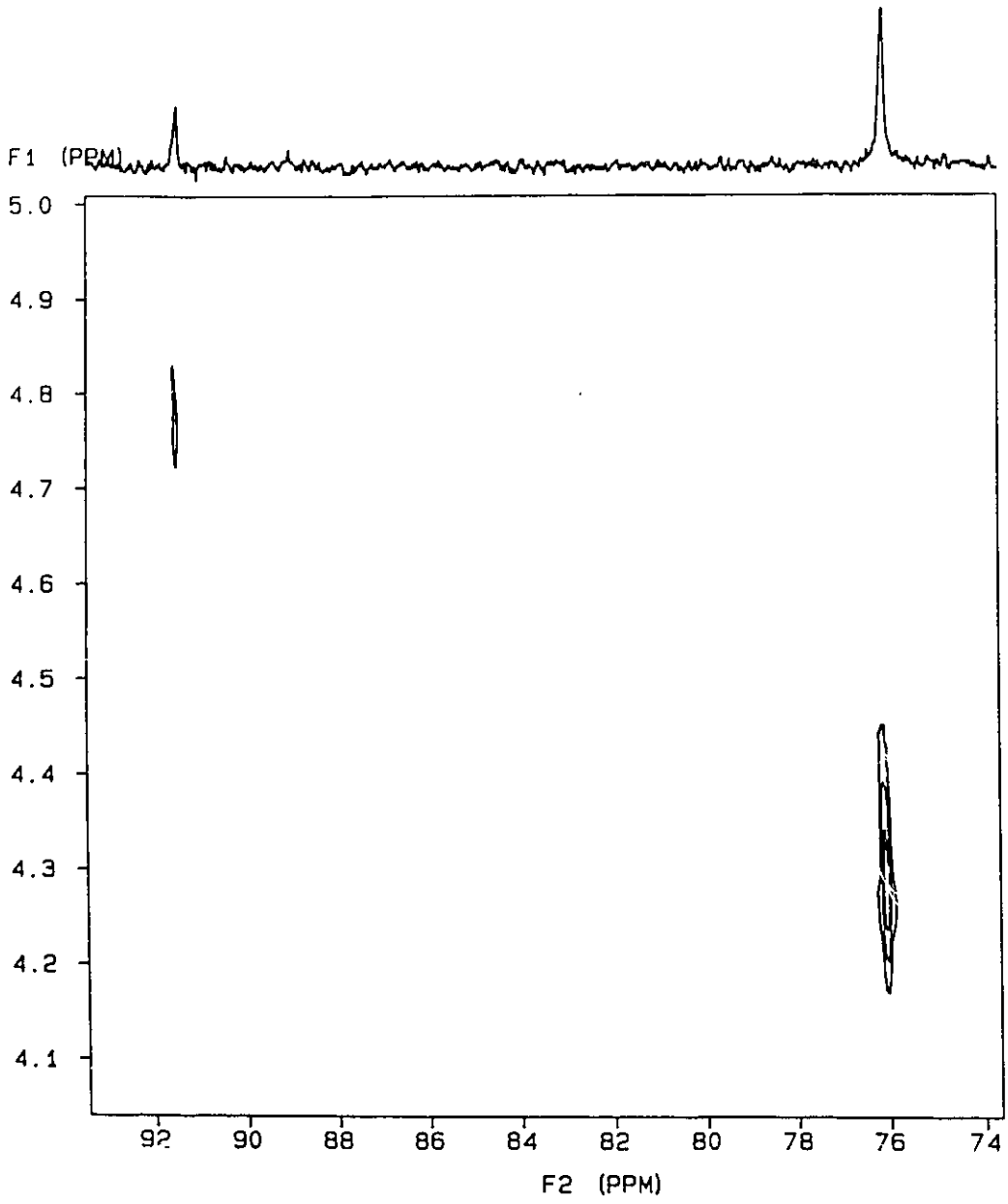

Figure 2.10 HETCOR spectrum of the photolysis product of rhodizonate dianion in the presence of oxygen. pH=7.0

2. 4 Conclusions

The most important conclusion obtained from the present study is that the thermal and photochemical conversion of rhodizonate dianion to croconate dianion and other products in aqueous solution are initiated by electron transfer to an acceptor which is a sufficiently strong oxidizing agent. This conclusion is based on several observations.

(a) The rate of the thermal reaction in the absence of oxygen is increased in the presence of oxidizing agents with positive standard reduction potentials.

(b) Photolysis of the rhodizonate dianion in the presence of additives increased its rate of disappearance only with those additives which noticeably increased its thermal rate of reaction.

(c) For any one oxidizing agent, the rates of the thermal and photochemical reactions have the same order with respect to the concentration of additive (either square root or linear).

Details of the subsequent reactions of the monoanion radical following the initial electron transfer step cannot be established at this stage. Because the fraction of the product appearing as croconate dianion is not the same with each additive, several competing reactions must occur, which will be dependent on the pH of the solution as well as the reduction potential of the additive. The other products suggest that hydration of the monoanion is important and that oxygen may be incorporated into the ring through a ring -contraction mechanism. This type of mechanism does not invalidate the mechanism involving an α-oxo alcohol rearrangement following attack by hydroxide ion suggested for the conversion of rhodizonate dianion to croconate dianion in an oxygenated alkaline solution. The present results simply show that this conversion is a more general reaction and can occur in neutral solution and with other oxidizing agents.

Chapter 3

Photochemical Reactions of Croconate Dianion

3. 1 Experimental

3. 1. 1 Preparation of Disodium Croconate

Neither croconate acid nor its salts are commercially available. Sodium croconate used in this study was prepared by the oxidation of sodium rhodizonate. Rhodizonate salts can be quantitatively converted to croconate salts in basic solution in the presence of an oxidizing agent. The mechanism of this ring contraction reaction has been suggested to be an alpha-oxo alcohol rearrangement, as described in the introduction (p.10). Several oxidants have been used for the reaction. For the present experiments the procedure developed by Schwartz, Gelb and Yardley was followed, using hydrogen peroxide as oxidant.[20] The procedure was as follows: 6.42 grams of disodium rhodizonate $Na_2C_6O_6$ (0.03 mole) and 3.0 grams of sodium hydroxide NaOH (0.075 mole) were dissolved in 15 mL of hot water in a 125 mL Erlermeyer flask. The solution was stirred for an extended period of time to dissolve the sodium rhodizonate and allowed to cool. When the solution had reached room temperature 34 mL of 3% hydrogen peroxide solution was added. After adding the hydrogen peroxide, the solution quickly became clear and turned yellow.

The Erlermeyer flask was cooled in an ice bath and a yellow precipitate appeared. The precipitate was filtered using a glass filter, washed a few times with 1:1 ethanol-water solution, and recrystallized from a warm ethanol-water solution. The final product was dried at 120^0 C for ninety minutes. According to Schwartz et. al., sodium croconate prepared in this way is monohydrated, $Na_2C_5O_5.H_2O$. (M. W. 204.0g/mol). The yield of sodium croconate was 48%. The ^{13}C NMR spectrum of this product showed only one

single peak at 188 ppm in agreement with the chemical shift reported by Gelb, Schwartz, Laufer and Yardley.[28] The UV-visible absorption spectrum of the aqueous solution of this sodium croconate gave an extinction coefficient of 3.9×10^4 $M^{-1}cm^{-1}$ at its maximum π-π^* absorption at 363 nm. The absorption spectrum showed the characteristic double maximum as reported previously.[20]

3. 1. 2 Light Source

The light source for the photolysis of croconate dianion solution was a medium-pressure mercury arc (Hanovia 673 A10) with a water-cooled housing. The lamp was operated at 250 V and 2.9 amp. A Pyrex plate was attached to the housing at the exit of the beam to cut off light of wavelength shorter than 300 nm and hence reduce the formation of ozone. A round bottomed flask filled with water was placed between the lamp and the photolysis cell to absorb heat from the lamp as well as to focus the light. A Corning filter #7-37 was used to allow only the light of wavelength 366 nm to reach the photolysis cell. The arrangement of the photolysis apparatus and the transmission of Corning filter #7-37 are shown in Figure 3.1.

3. 1. 3 Measurement of Light Intensity

The incident light intensity at 366 nm was measured using the uranyl oxalate actinometer,[69, 70] and the measurement was performed periodically. The quantum yield for oxalate ion loss from the photolysis of uranyl of oxalate at 366 nm is 0.492 at 25^0 C[73].

(1) Preparation of Uranyl Oxalate

Concentrated uranyl nitrate solution (0.047 mole) was mixed with an excess of hot oxalic acid (0.13 mole) solution. Uranyl oxalate precipitated from the solution.

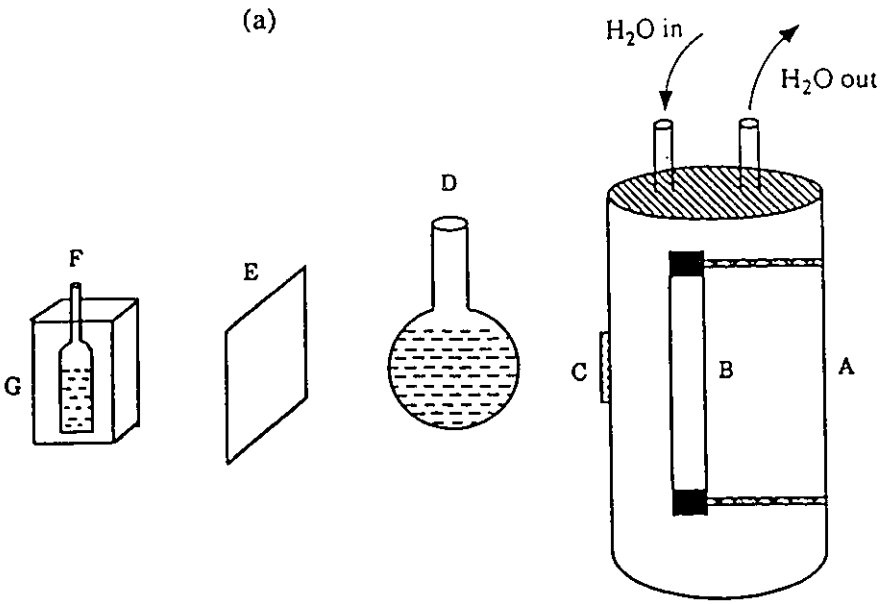

A: Housing Holder (water cooled) B: Mercury Lamp C: Pyrex Plate

D: Pyrex Flask E: Corning Filter #7-37 F: Quartz Cell G: Cell Holder

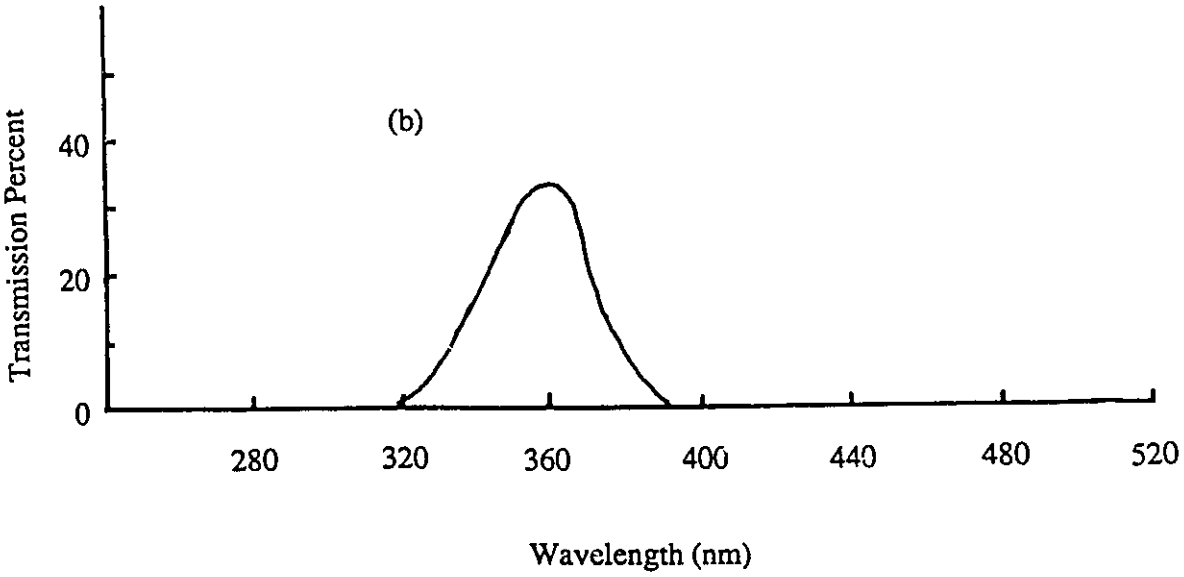

Figure 3.1 (a) Arrangement of the photolysis apparatus

(b) Transmission pattern of Corning filter #7-37

$$UO_2(NO_3)_2 + H_2C_2O_4 \rightarrow UO_2C_2O_4 + 2HNO_3$$

The precipitate was recrystallized three times from warm water and dried at 110^0 C for 2 hours. It was kept in the dark.

(2) Preparation and Photolysis of Uranyl Oxalate Solution

The actinometer was an aqueous solution, 0.01M in $UO_2C_2O_4$ and 0.05 M in $H_2C_2O_4$. 3 mL of the actinometer was photolysed in the spectrophotometer cell at 366 nm for 12 hours.

(3) Calculation of Incident Light Intensity

3 mL of uranyl oxalate actinometer were titrated before and after photolysis using potassium permangnate, previously standardized against sodium oxalate. The difference in the number of oxalate ions before and after photolysis is equal to the number of oxalate ions lost during the photolysis.

The incident light intensity reaching the photolysis cell may be expressed as:

$$I_0 = \frac{\Delta n \times N_0}{\phi . t\,(1-10^{-A})}$$

ϕ: quantum yield of loss of oxalate ion at 366 nm at 25^0 C.

t: photolysis time (second)

A: absorbance of actinometer at 366 nm before photolysis.

Δn: moles of oxalate ions lost during the photolysis.

N_0: Avogadro's number.

As an example, when the loss of $C_2O_4^{2-}$ was 2.99×10^{-5} moles after twelve hours of photolysis, and the absorbance of the actinometer at 366 nm before photolysis was 0.215, the incident light intensity reaching the photolysis cell therefore is:

$$I_0 = \frac{2.99\times10^{-5} \times 6.02\times10^{23}}{0.492\times3600\times12\,(1-10^{-0.215})}$$

$I_0 = 2.97 \times 10^{15}$ quanta s^{-1}

In all the manipulations the uranyl oxalate solutions were protected from visible light.

3. 1. 4 Fluorescence Measurement

Fluorescence spectra of croconate dianion were measured using a Perkin Elmer Luminescence Spectrometer LS50. A personal computer from IBM was used to receive, analyze and store the signal. An Epson Ex-800 printer was used as chart recorder. A special Xenon flash tube was the excitation source, operating at 50 Hz. The optical system consisted of two reflection grating monochromators (emission and excitation), a series of mirrors and the reference and sample photomultiplier detectors. For the croconate dianion fluorescence measurement, the excitation monochromator was set at 360 nm with band width of 5 nm. The emission was measured in the range from 440 nm to 640 nm, with the emission monochromator band width of 5 nm, and scan speed of 240 nm/minute. The solution was degassed by nitrogen bubbling for ten minutes and sealed using a rubber septum.

For the measurement of the lifetime of fluorescence, a flash photolysis apparatus in the laboratory of Dr. Konigstein at Carleton University was used. The excitation source was an excimer laser with emission wavelength of 308 nm, and the duration of the flash was 8 ns. The decay of the fluorescence at 490 nm was monitored and an estimation of the life time of fluorescence was derived from the decay trace.

3. 1. 5 Critical Micellar Concentration Measurement

Surfactants aggregate spontaneously when the concentration is raised beyond a certain specific, rather sharply defined value which is called the critical micellar

concentration (cmc).[74-76] The appearance of micellar aggregates manifests itself by a change of solution properties such as conductivity and light absorption and scattering around the cmc. Thus the value of cmc of micellar solution can be determined by measuring these property changes as a function of micelle concentration. The critical micellar concentration (cmc) of sodium dodecyl sulfate (SDS) was determined by conductivity measurements. A platinum electrode was used as the cell and a Barnstead Conductivity Bridge Model PM-70B was applied to measure the solution conductivity. The cell constant, 0.8944 cm^{-1}, was measured using a 0.1000 N potassium chloride solution. All the solutions to be measured were thermally equilibrated at 25^0 C.

The conductivities of a series of solutions with different SDS micellar concentration and micellar solutions containing croconate dianion were measured. The equivalent conductivities of the solutions were calculated according to the equation:

$$\text{Equivalent Conductivity} = \frac{\text{Conductivity}}{C} \qquad (\text{MHO cm}^{-1}\ \text{N}^{-1})$$

C is the concentration of the micelle in equivalents L^{-1}. In all calculations of the conductivity of the solution, a correction was made for the conductivity of pure water.

The critical micellar concentration (cmc) was obtained from the inflection point in the plot of equivalent conductivity against the square root of the micellar concentration. Figure 3.2 is an example showing the equivalent conductivity of the solution as function of the square root of the micellar concentration. From the inflection point, the cmc of the SDS solution is 4.0×10^{-3} M.

3. 1. 6 Reaction Solution preparation and Degassing

Aqueous croconate dianion solution is stable when it is kept in the dark, even in the presence of oxygen, for several months. Degassing procedures were basically the same as

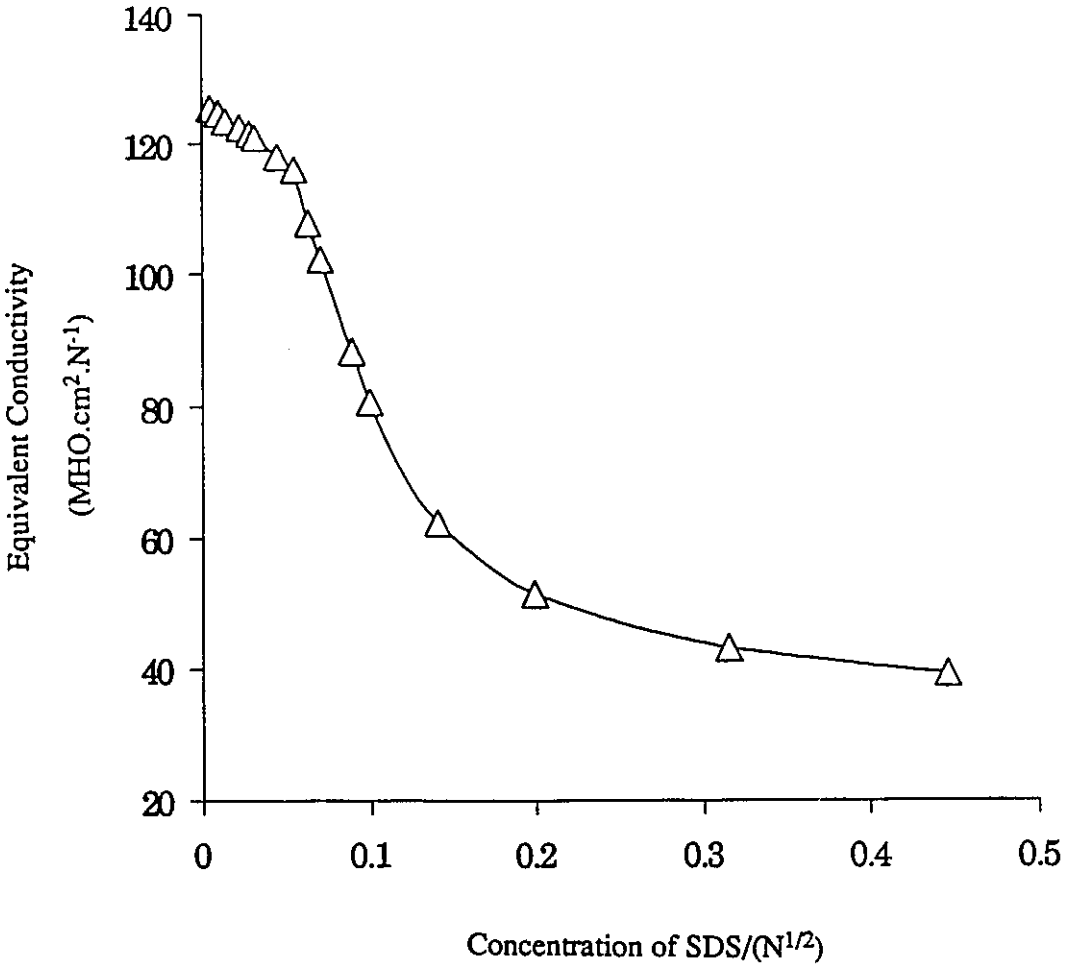

Figure 3.2 Equivalent conductivity as a function of square root of concentration of SDS (equivalent). pH=7.0; 25^0 C.

those used in the experiments with rhodizonate dianion solution. Solutions with croconate dianion and with additive were separately degassed with five freeze-pump-thaw cycles and mixed in the cell under vacuum. With the micellar solutions, only the freeze-pump-thaw degassing technique was used.

3. 1. 7 Reagents

Electron acceptors used in the investigation of the photochemical reactions of croconate dianion were: potassium ferricyanide, methyl viologen, 4-nitrobenzylbromide and biacetyl. Methyl viologen was purchased from BDH, 4-nitrobenzylbromide was purchased from Aldrich, biacetyl and potassium ferricyanide were purchased from Fisher Scientific Company, and quinine bisulfate was purchased from Plaltz & Bauer Inc. 4-nitrobenzylbromide was recrystallized from water-methanol solution and potassium ferricyanide was recrystallized from water-ethanol solution. Other reagents were used without further purification.

3. 2 Results

3. 2. 1 Products of the Photolysis

Under all conditions croconate dianion was more stable thermally than rhodizonate dianion. The rhodizonate dianion was oxidized in the dark in aerated solutions, the rate increasing with increasing pH of the solution. Croconate dianion was stable in aerated neutral solutions for several months and in basic solutions (pH>10), its concentration decreased only slightly (< 1%) after several hours in the dark. In strongly basic solution (pH=12), however, in the presence of oxygen, photolysis caused conversion to squarate dianion with a yield of 90%. Figure 3. 3 shows the disappearance of croconate dianion and at the same time the generation of squarate dianion when the croconate dianion aqueous solution was photolysed at pH 12 while oxygen gas was passing through the solution. At the beginning of the photolysis the absorption shows the presence of croconate dianion only, and at the end of the reaction, the spectrum shows only absorption from squarate dianion. All the croconate dianion has been consumed completely. Formation of squarate dianion from croconate dianion has not previously been reported and it appears that photolysis of croconate dianion under these conditions provides a useful method for preparation of squaric acid. Squarate dianion was also formed in the presence of 4-nitrobenzylbromide although absorption due to the additive at 270 nm masked to some extent the absorption by the product squarate dianion. Nevertheless some indication of the formation of squarate dianion may be observed by assuming that one molecule of the additive reacted for each dianion of croconate consumed. Thus the formation of squarate dianion may be estimated in the presence of 4-nitrobenzylbromide. The following experiments illustrate the effect of pH and of oxygen on the rate of this conversion.

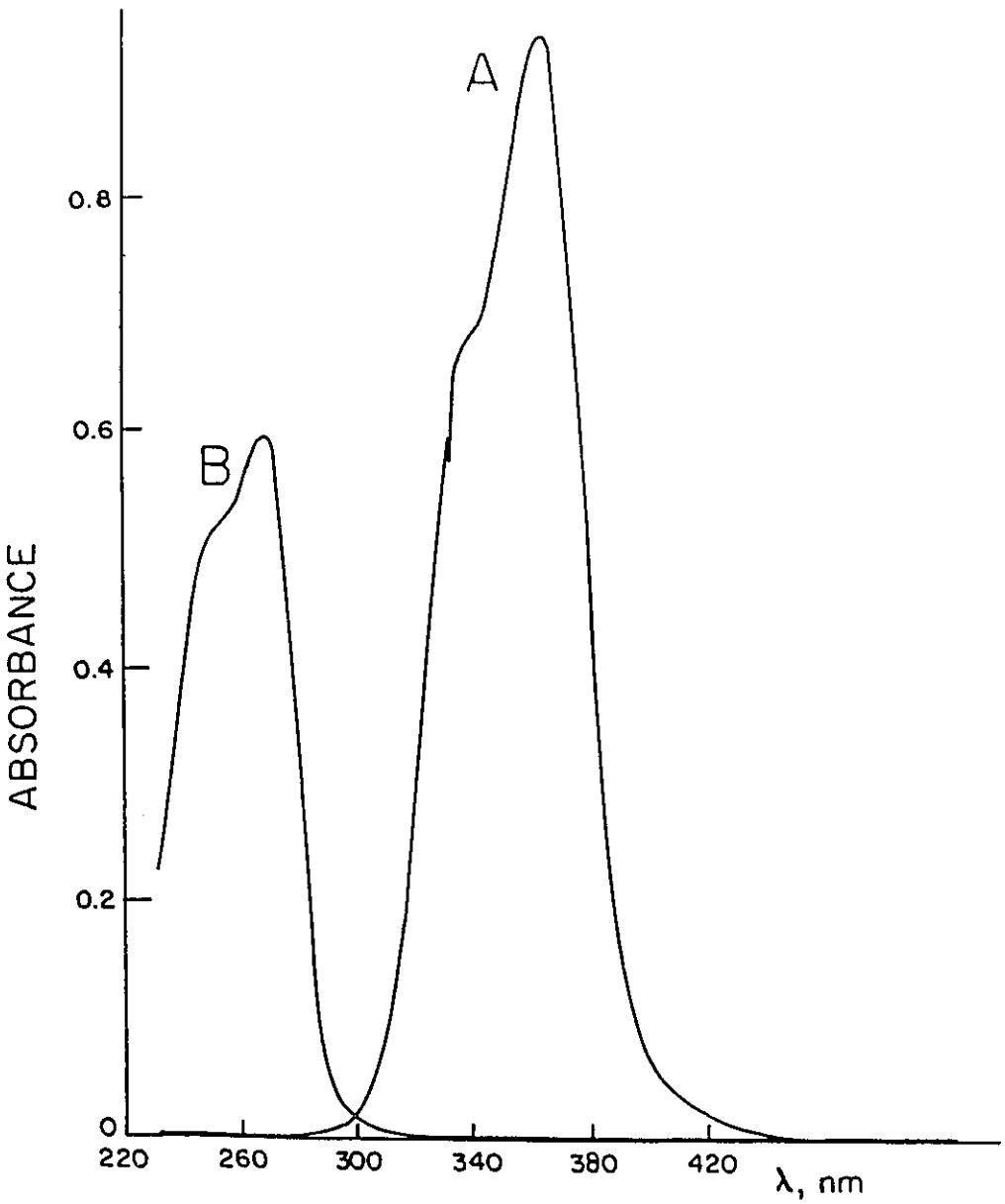

Figure 3.3 Absorption spectra of a solution of $C_5O_5^{2-}$ before and after irradiation in the presence of oxygen. Showing formation of $C_4O_4^{2-}$.

A: 2.4×10^{-5} M croconate dianion in solution before irradiation, pH=12.

B: Same solution after complete consumption of croconate dianion.

(a) De-oxygenated croconate dianion solution was photolysed at pH 7 in the presence of 4-nitrobenzylbromide. The absorbance of croconate dianion at 363 nm decreased from 0.96 to 0.17, while the absorbance of the solution at 278 nm decreased from 0.93 to 0.81. The absorbance change at 278 nm is caused by the combination of the formation of squarate dianion and the loss of 4-nitrobenzylbromide and may be expressed as follows:

$$\Delta A = \Delta n_S(\varepsilon_s) - \Delta n_B(\varepsilon_B)$$

where ΔA: absorbance change at 278 nm

Δn_s: number of moles of squarate dianion formed

Δn_B: number of moles of 4-nitrobenzylbromide reacted during the photolysis

ϵ_S: extinction coefficient for squarate dianion

ϵ_B: extinction coefficient for 4-nitrobenzylbromide.

Δn_B is equal to the number of moles of croconate dianion disappeared during the photolysis. Taking the extinction coefficient for 4-nitrobenzylbromide at 278 nm as 1.03×10^4 $M^{-1}cm^{-1}$ and for squarate dianion as 2.4×10^4 M^{-1} cm^{-1}, the fraction of croconate dianion converted to squarate dianion during the reaction is therefore 18%. In the calculation, we did not consider the absorbance from the reaction product from 4-nitrobenzylbromide which is most probably a dimer of 4-nitrobenzyl radical, as the absorbance of the dimer at 278 nm is expected to be small. This calculation probably will bring some uncertainty at the a low fraction of conversion from croconate dianion to squarate dianion, but at higher fractional conversion, the error will be small.

(b) Croconate dianion solution was photolysed at pH 12 in the presence of 4-nitrobenzylbromide. Oxygen was removed by saturation with nitrogen. The absorbance at 363 nm changed from 0.725 to 0.085, while at 278 nm the change was very small, from 0.80 to 0.806. A calculation similar to that made in case (a) showed that about 60% of

croconate dianion converted to squarate dianion in the reaction.

(c) Photolysis of croconate dianion solution at pH 12 in the presence of 4-nitrobenzylbromide with continuous bubbling with oxygen during the photolysis, gave a much slower reaction than in cases (a) and (b). The absorbance at 363 nm decreased from 0.74 to 0.065, and the absorbance at 278 nm increased from 0.785 to 0.990. Similar calculations showed that nearly 97% of the croconate dianion was converted to squarate dianion during the reaction. Another interesting point is that the maximum absorption shifted from 278 nm to 274 nm after photolysis.

Analysis of the three cases showed clearly that even in the presence of the additive, an increase in the pH of the solution and the presence of oxygen both increased the rate of conversion of croconate dianion to squarate dianion. Squarate dianion was the only product of the photolysis of croconate dianion observed by absorption over the wavelength range 200--700 nm. Products which have lost the psedo-aromatic structure of oxocarbons would be too weakly absorbing to be detected at the concentrations used in the present experiments and the quantities produced were too small to be easily measured by other methods. Attempts to use ^{13}C NMR analysis to detect reaction products were unsuccessful.

3. 2. 2 Measurement of Quantum Yield in the Presence or Absence of Electron Acceptors

Deaerated croconate dianion solutions were photolysed in the range of pH 6 to 12 in the presence and absence of the following additives: biacetyl, methyl viologen, potassium ferricyanide and 4-nitrobenzylbromide. Potassium ferricyanide absorbs about 5% of the total light at 366 nm at the concentration of 1.0×10^{-4} M. Other acceptors do not absorb light at 366 nm significantly. The quantum yield for the disappearance of croconate dianion in the absence of additives was low (<0.001) in acid solution but increased as the solution was

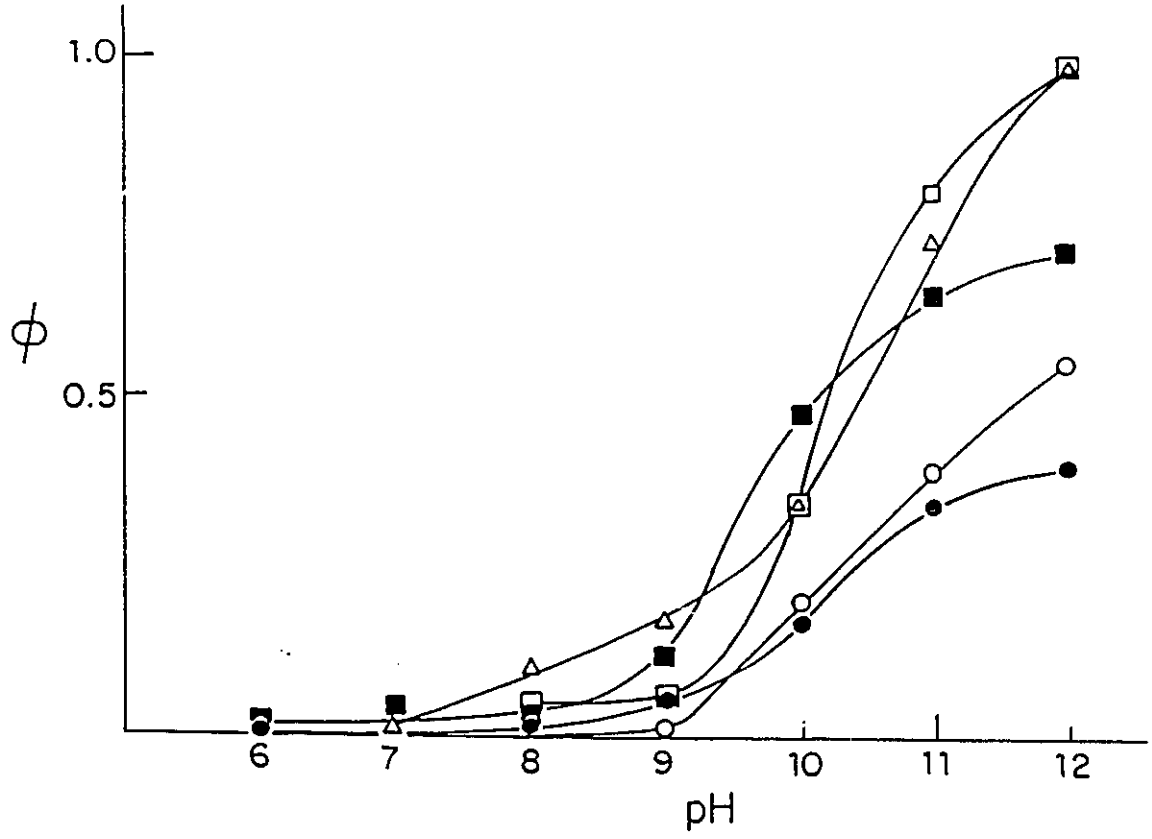

Figure 3.4 The quantum yield for loss of croconate dianion as a function of pH.
●: No additive; o: $[Fe(CN)_6^{3-}]=5.0\times10^{-4}$ M; ■: $[MV^{2+}]=1.0\times10^{-4}$ M;
△: $[BrCH_2C_6H_4NO_2]=1.0\times10^{-4}$ M; □: [Biacetyl]$=1.0\times10^{-4}$ M.

Table 3. 1

Quantum Yield for Disappearance of Croconate Dianion as a Function of pH

$[C_5O_5^{2-}] = 2.3\times10^{-5}$ M

pH	Without Additive	$Fe(CN)_6^{3-}$ (5×10^{-4} M)	MV^{2+} (1×10^{-4} M)	$BrCH_2C_6H_4NO_2$ (1×10^{-4} M)	Biacetyl (1×10^{-4} M)
6.0	0.009		0.018	0.004	
7.0	0.012	0.0014	0.042	0.005	
8.0	0.012	0.0057	0.028	0.10	0.052
9.0	0.05	0.011	0.12	0.17	0.059
10.0	0.17	0.20	0.48	0.34	0.34
11.0	0.34	0.49	0.65	0.73	0.81
12.0	0.40	0.55	0.71	0.98	0.98

made basic reaching a value of 0.4 at pH 12. The presence of additives increased the quantum yield, particularly in basic solution and approached unity at pH 12 in the presence of biacetyl and 4-nitrobenzylbromide. The quantum yield for the disappearance of croconate dianion as a function of pH in the presence and absence of additives is shown in Figure 3.4 and the data are summarized in Table 3.1.

The quantum yield was calculated using the equation on page 36, and the rate of disappearance of croconate dianion was obtained by monitoring the rate of absorbance change of the sample at 365 nm

As an example, in an experiment at pH 12 in the presence of 1.5×10^{-4} M biacetyl, the rate of disappearance of croconate dianion was 1.06×10^{-6} $M^{-1}s^{-1}$, the absorbance of croconate dianion at 366 nm before photolysis was 0.90, the volume of the solution was 3.0 mL and the light intensity reaching the photolysis cell was 2.17×10^{15} quanta s^{-1}. The quantum yield therefore is:

$$\phi = \frac{1.06\times10^{-6}\times 0.0030\times 6.02\times10^{23}}{2.17\times10^{15}\,(1-10^{-0.90})} = 1.0$$

In the presence of oxygen, the rate of disappearance of croconate dianion under photolysis decreased dramatically, and was undetectable in the pH range of 6--8. The rate was about two orders of magnitude slower than that in the deaerated system at pH >9. It may be concluded that oxygen molecules effectively quenched the excited croconate dianion.

The presence of an electron acceptor had a considerable effect on the quantum yield of disappearance of croconate dianion. As an illustration the quantum yield for disappearance of croconate dianion is shown as a function of concentration of 4-nitrobenzylbromide at pH 9 and pH 12 in Figure 3.5. The quantum yield as a function of concentration of additives of $BrCH_2$-C_6H_4-NO_2, Biacetyl and $Fe(CN)_6^{3-}$ are summarized in Table 3.2. Some measurements of the quantum yield of the disappearance of croconate

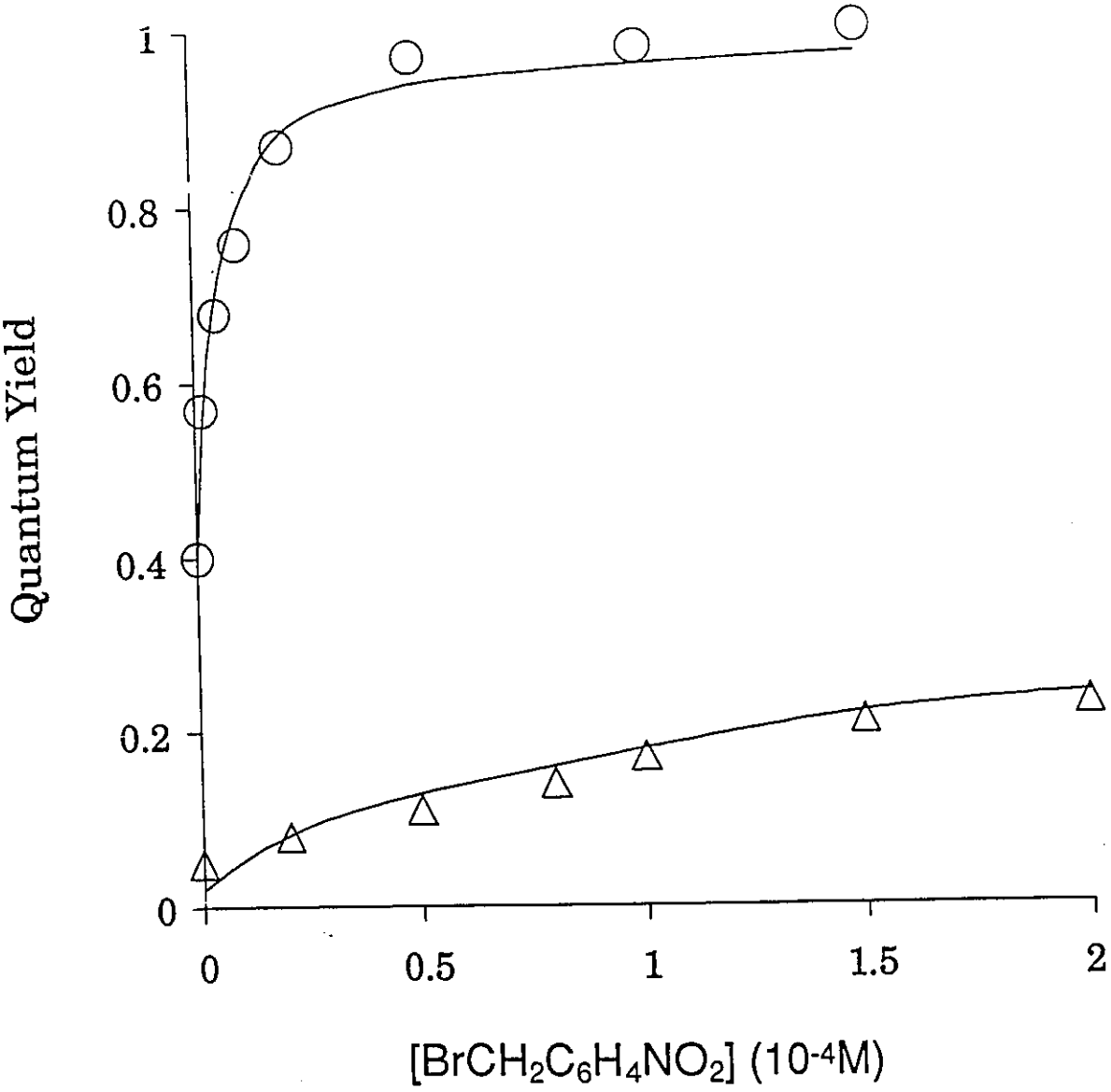

Figure 3.5 The quantum yield for loss of croconate dianion as a function of concentration of 4-nitrobenzylbromide.

Δ: pH 9, experimental results; o: pH 12, experimental results.

Solid lines are calculated values according to equation (3-9) and rate constants in Table 3.7.

Table 3. 2

Quantum Yield for Disappearance of $C_5O_5^{2-}$ at Different Concentration of Additives

$[C_5O_5^{2-}] = 2.3\times10^{-5}$ M

Additive	$Fe(CN)_6^{3-}$	$BrCH_2C_6H_4NO_2$		Biacetyl
Concent.(M)	pH=12.0	pH=9.0	pH=12.0	pH=12.0
1.5×10^{-6}			0.57	
5.0×10^{-6}			0.68	
1.0×10^{-5}			0.76	0.50
2.0×10^{-5}	0.44	0.08	0.87	0.60
3.8×10^{-5}				0.73
5.0×10^{-5}	0.57	0.11	0.97	0.81
8.0×10^{-5}		0.14		0.95
1.0×10^{-4}	0.54	0.17	0.98	0.98
1.5×10^{-4}		0.21	1.0	1.0
2.0×10^{-4}	0.53	0.23		
5.0×10^{-4}	0.52	0.33		

dianion at pH 12 in a micellar solution in the presence of methyl viologen were performed. These results are summarized in Table 3.3. It is interesting to note that the quantum yield of the disappearance of croconate dianion reached a limit at very low concentration of methyl viologen both in aqueous and micellar solutions, but the limits are different in the two systems, 0.7 in aqueous solution and unity in micellar solution.

The dependence of the quantum yield of the disappearance of croconate dianion on the concentration of croconate dianion was investigated with croconate dianion alone at pH 12 and in the presence of 4-nitrobenzylbromide at pH 9. The results are summarized in Table 3.4. These results show that in both cases the quantum yield for disappearance of croconate dianion is independent of the concentration of croconate dianion in the range of concentration 1.3×10^{-5}--3.3×10^{-5} M.

3. 2. 3 Photolysis in the Presence of Radical Traps

2,2-Di(4-tert-octylphenyl)-1-picrylhydrazyl (DPPH) is widely used as a free radical trap to detect newly-formed radicals in solution. It contains one free electron and has strong absorption in the visible and near UV wavelength range with two maxima at 360 nm and 540 nm. The concentration of DPPH can be monitored by its absorption at 540 nm. Once DPPH captures another free radical its visible absorption disappears.[77] In the present experiment, DPPH was used to detect the presence of radicals generated from the electron transfer between excited croconate dianion and additives. Because DPPH is more soluble in methanol than in water, photolysis in the presence of DPPH were performed in methanol solution degassed under vacuum in the usual way. The spectrum and absorption maximum of croconate dianion were not changed in methanol solution. Photolysis of croconate dianion in the presence of DPPH caused a loss of DPPH as measured by the absorbance at 540 nm. Although DPPH has a strong absorption at 366 nm no measurable loss of DPPH

Table 3. 3

Quantum Yield for Disappearance of Croconate Dianion in the Presence of MV^{2+}

pH=12.0

$[MV^{2+}]$ (M)	Aqueous Solution	Micellar Solution
6.0×10^{-7}	0.62	
5.0×10^{-6}	0.71	0.99
5.0×10^{-5}	0.73	1.00
6.0×10^{-5}	0.70	
1.5×10^{-4}	0.71	1.00
3.0×10^{-4}	0.67	

Table 3. 4

Dependence of Quantum Yield on the Concentration of Croconate Dianion

$[C_5O_5^{2-}]$ (M)	pH	$BrCH_2C_6H_4NO_2$ (M)	ϕ
1.28×10^{-5}	12.0	0	0.40
2.49×10^{-5}	12.0	0	0.40
3.33×10^{-5}	12.0	0	0.39
1.28×10^{-5}	9.0	5.0×10^{-5}	0.12
2.49×10^{-5}	9.0	5.0×10^{-5}	0.11
3.33×10^{-5}	9.0	5.0×10^{-5}	0.11

occurred on photolysis in the absence of croconate dianion. The rate of loss of DPPH was increased when biacetyl, 4-nitrobenzylbromide and methyl viologen were added to the system but was not affected by the presence of potassium ferricyanide. The relative loss of DPPH as a function of time in the presence and absence of additives is shown in Figure 3.6. The quantum yield for loss of DPPH, with respect to photons absorbed by croconate dianion only at 366 nm, is given in Table 3.5. The results showed that the quantum yield for loss of DPPH was independent of the concentrations of croconate dianion and of DPPH.

Polymerization of acrylamide was observed on photolysis of croconate dianion in the presence or absence of additives. This polymerization is a very sensitive method for detection of radicals. A very slow photopolymerisation of acrylamide was observed on photolysis of croconate dianion alone in aqueous solution and the rate was greatly increased in the presence of 4-nitrobenzylbromide, 4-nitrobenzylchloride and biacetyl. The results of a systematic investigation of the photopolymerisation of acrylamide will be presented in the next chapter.

3. 2. 4 Fluorescence of Croconate Dianion

Croconate dianion exhibits a weak luminescence emission. The spectrum is shown in Figure 3.7. The emission maximum is at 480 nm when excitation was at 360 nm. The quantum yield of the fluorescence of croconate dianion can be calculated according to the formula:[78]

$$\phi_u = \frac{(I_{abs})_s \times F_u}{(I_{abs})_u \times F_s} \phi_s$$

where u and s stand for unknown and standard respectively. F is the area under the emission spectra. I_{abs} is the light intensity absorbed by the standard or unknown at the excitation wavelength. Since both standard and unknown were in aqueous solution, correction for refractive index was not necessary. In the present measurement, quinine

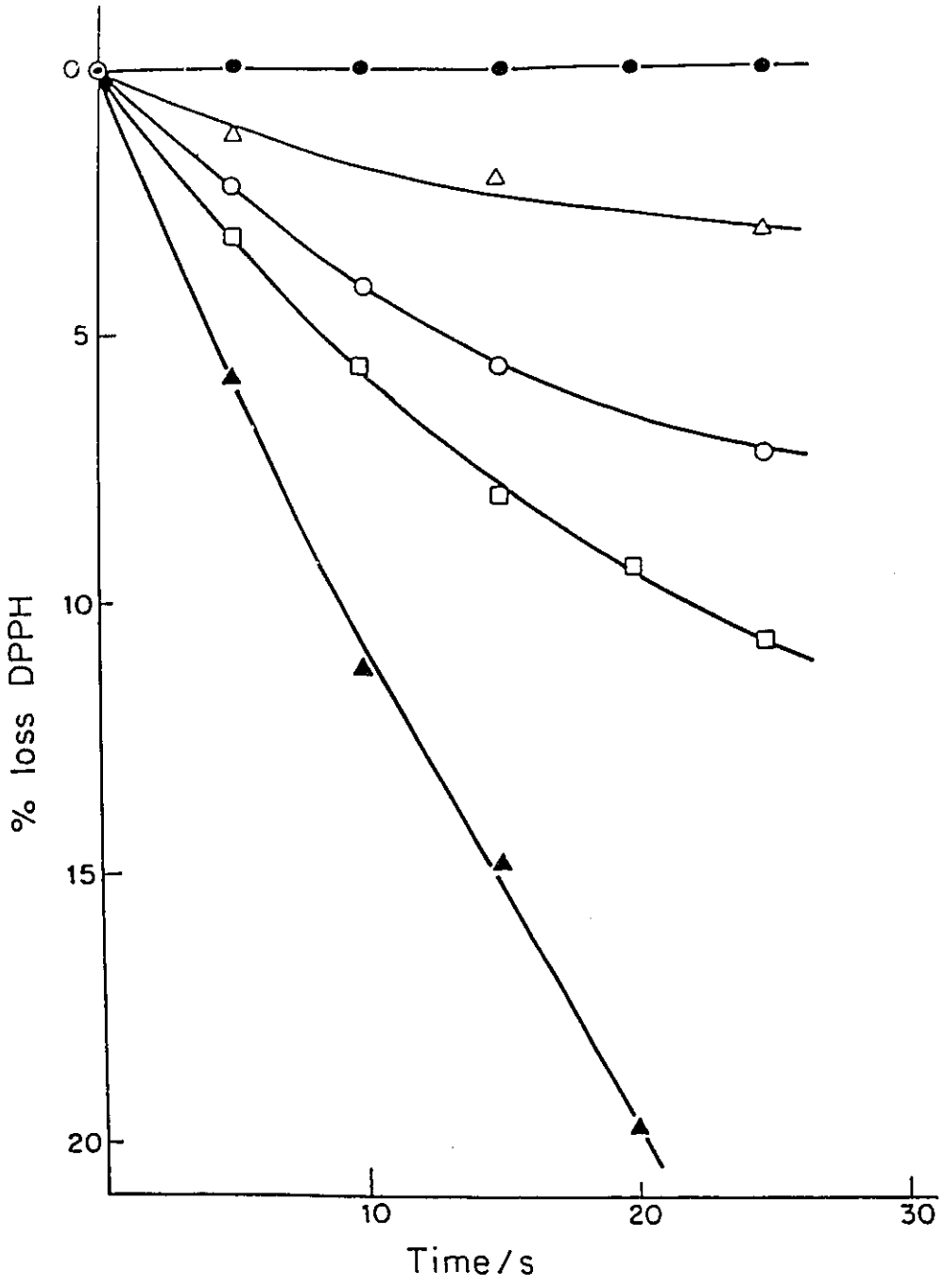

Figure 3.6 Relative loss of DPPH as a function of time, [DPPH]=3.1×10^{-5} M.

●: biacetyl+DPPH, [BA]=3.2×10^{-5} M; △: DPPH+$C_5O_5^{2-}$;

o: DPPH+$C_5O_5^{2-}$+MV^{2+}, [MV^{2+}]=6.4×10^{-4} M;

□:DPPH+$C_5O_5^{2-}$+4-nitrobenzylbromide, [$BrCH_2C_6H_4NO_2$]=6.4×10^{-5} M;

▲: DPPH+$C_5O_5^{2-}$+Biacetyl, [BA]=3.2×10^{-5} M.

Table 3. 5

Quantum Yield for Disappearance of DPPH in Methanol

Additive	[Additive] ($M\times10^{-5}$)	[DPPH] ($M\times10^{-5}$)	$[C_5O_5^{2-}]$ ($M\times10^{-5}$)	ϕ
No Additive	0	3.1	2.3	0.055
Biacetyl	3.2	3.1	0	0
Biacetyl	3.2	1.5	2.3	0.52
Biacetyl	3.2	3.1	2.3	0.53
Biacetyl	3.2	4.7	2.3	0.52
Biacetyl	3.2	6.2	2.3	0.52
Biacetyl	6.4	3.1	2.3	0.52
$BrCH_2C_6H_4NO_2$	6.4	3.1	2.3	0.28
MV^{2+}	6.4	3.1	2.3	0.20

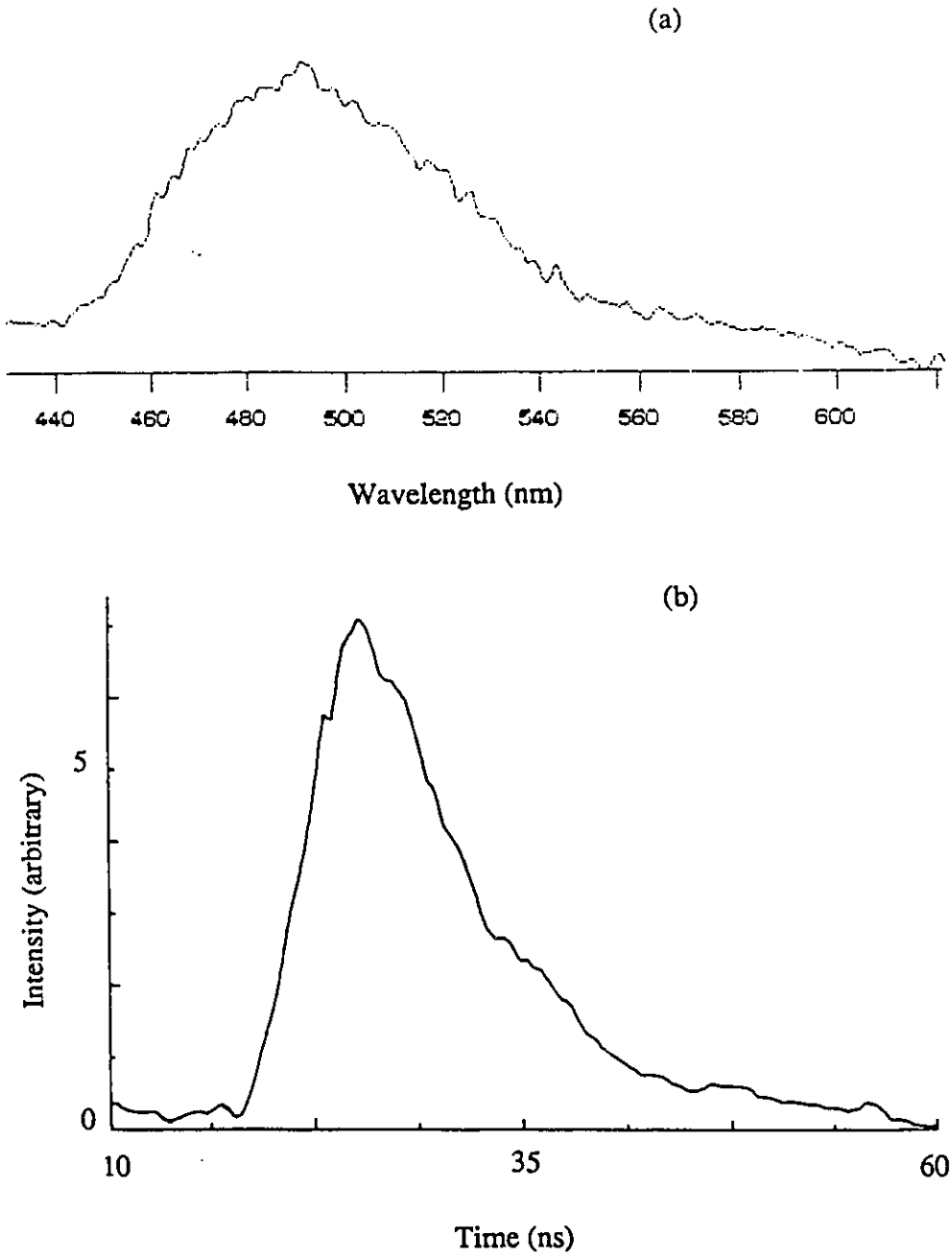

Figure 3.7 (a) Fluorescence spectrum of croconate dianion in water.

(b) Emission of croconate dianion at 490 nm as a function of time.

bisulfate was used as standard. Its emission spectrum covers a range of wavelength close to that covered by the emission from croconate dianion. Correction for the sensitivity of the detector was not necessary in the measurement. Quinine bisulfate has a quantum yield of 0.546[78] in 1.0 N H_2SO_4 solution. The area under the emission spectrum for quinine bisulfate was 19055 (arbitrary units) and the absorbance at 360 nm was 0.092, while the area under the emission spectrum for croconate dianion was only 291 with an absorbance of 0.47 at 360 nm. These areas were obtained by integration over the range of wavelength, as shown in Fig. 3.7(a). Stictly, these areas should be calculated as total energy of emission, in other words, integrated over wavelength in units of $1/\lambda$. The ratio F_u/F_s will be very similar for the two methods of calculation. The quantum yield for croconate dianion emission can be calculated as follows:

$$\phi = \frac{0.092 \times 291}{0.47 \times 19055} \times 0.546 = 1.6 \times 10^{-3}$$

This low value of the quantum yield for emission shows that it is not an important deactivation process of the excited state of the croconate dianion.

The lifetime of the fluorescence was measured in an aqueous solution of croconate dianion, without additive, degassing by saturation with nitrogen. The decay trace of the emission at 490 nm is shown in Figure 3.7. assuming the decay is first order, the lifetime of the decay curve at 490 nm is 10 ns. The lifetime of the laser pulse from the excimer laser is 8 ns, the lifetime of the laser pulse from the excimer laser is 8 ns, without attempting deconvolution of these two decays, it is clearly that the lifetime of the fluorescence is less than the lifetime of laser pulse. Clearly this lifetime is close to the limit of measurement with this light source. The main conclusion from the measurement is that this short lifetime must be associated with the singlet state of the croconate dianion, and that fluorescence is a minor role in the decay of the excited singlet state.

3. 3 Discussion

3. 3. 1 Conversion of Croconate Dianion to Squarate Dianion

The measurements of the rate of formation of squarate dianion in the photolysis of croconate dianion clearly showed that conversion is strongly favoured in basic solution and that oxygen has a remarkable effect on the rate. Thus both OH^- and O_2 must be involved in the reactions leading to the conversion of croconate dianion to squarate dianion. The mechanism of the conversion may be similar to that suggested for the conversion of rhodizonate dianion to croconate dianion in basic solution in the presence of oxidant.[1] With croconate, however, the dianion must first be excited by absorbing light before further reactions leading to the formation of squarate dianion may take place. The proposed mechanism of the conversion reaction of croconate dianion to squarate dianion is shown in scheme 3.1

The role of 4-nitrobenzylbromide in this mechanism is not clear at present. It is possible that the OH^- may react with the monoanion radical as well as the excited state.

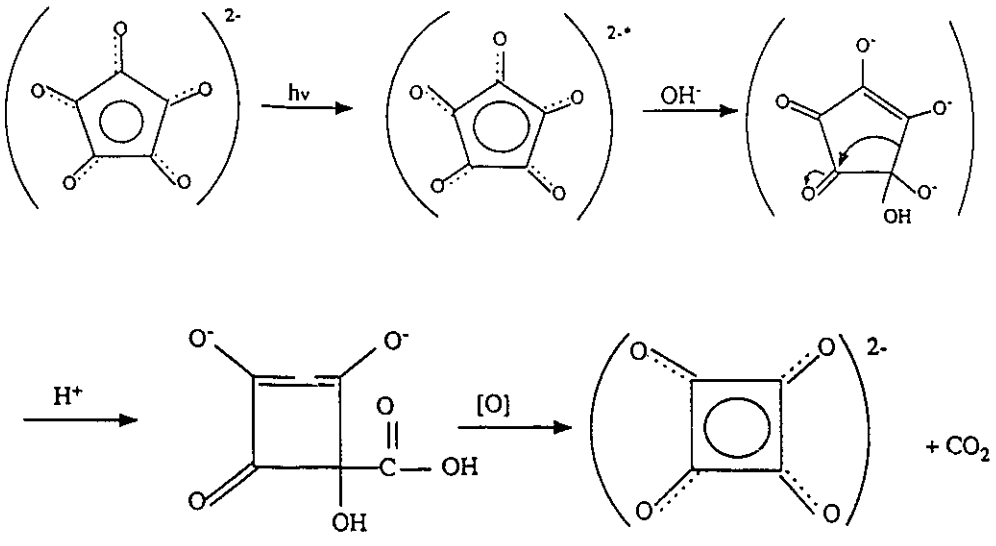

Sceheme 3.1 Photochemical conversion of croconate dianion to squarate dianion

3. 3. 2 Kinetics of Disappearance of Croconate Dianion

The effect of all four additives on the quantum yield for the disappearance of croconate dianion is convincing evidence that an electron transfer occurs from the excited dianion.

The increase in quantum yield of the disappearance of croconate dianion observed in basic solution (in the presence or absence of additive) suggests a further reaction of the excited dianion, a direct reaction with the hydroxyl ion. The two processes, electron transfer between the excited croconate dianion and additive and the addition of hydroxyl ion to the excited croconate dianion may be regarded as oxidation and reduction, respectively. Both processes are facilitated by photoexcitation. Without photolysis, reaction of croconate dianion was not observed with any additive, even at high pH. By comparison, reaction of hydroxyl ion with rhodizonate dianion was observed in basic solution without photo excitation. The effect of both concentration of additive and pH of the solution on the quantum yield of disappearance of croconate dianion can be seen clearly from Tables 3.1 and 3.2 and from Figures 3.4 and 3.5.

The reaction of DPPH indicates that the radical or radicals, formed as a result of the electron transfer have sufficient lifetime to undergo reactions in the bulk solution. This result is consistent with direct measurements of the lifetime of croconate monoanion radical formed from the electron transfer between the excited croconate dianion and 4-nitrobenzylbromide in neutral solution, which will be described in chapter 5. A value of 190 μsec. was measured, which is sufficient to allow the reaction with DPPH to take place in solution. A further interesting observation is an apparently synergistic effect of the additive and hydroxyl ions. For example, the increase in quantum yield observed on

increase of concentration of 4-nitrobenzylbromide depends greatly on the pH of the solution. This is illustrated in Figure 3.5 where the change in quantum yield is shown as a function of concentration of 4-nitrobenzylbromide at pH 9 and 12. If the effects of both reactants, hydroxyl ion and additive, were additive, the rate of change of quantum yield with concentration of additive would not change with pH of the solution. Only the quantum yield without additive would change. From Figure 3.5, we can see that the rate of increase in quantum yield with increase in concentration of 4-nitrobenzylbromide at pH 12 is much faster than that at pH 9. The limiting quantum yield at high concentration of additive is also quite different at pH 9 and at pH 12. Such an effect requires an interaction of one of the reactants with an intermediate formed by the other reactant.

A mechanism for the reaction incorporating these features and allowing for deactivation of the excited state by both acceptor and hydroxyl ion is summarized below.

$[I_{abs}]$	$C_5O_5^{2-} + h\nu \rightarrow C_5O_5^{2-*}$
[D]	$C_5O_5^{2-*} \rightarrow C_5O_5^{2-}$
[1]	$C_5O_5^{2-*} + A \rightarrow (C_5O_5^{-\cdot}...A^-)$
[2]	$(C_5O_5^{-\cdot}...A^-) \rightarrow C_5O_5^{2-} + A$
[3]	$(C_5O_5^{-\cdot}...A^-) \rightarrow C_5O_5^{-\cdot} + A^-$
[4]	$(C_5O_5^{-\cdot}...A^-) + OH^- \rightarrow$ Products
[5]	$C_5O_5^{-\cdot} \rightarrow$ Products
[6]	$C_5O_5^{2-*} + OH^- \rightarrow (C_5O_5^{2-}...OH^-)^*$
[7]	$(C_5O_5^{2-}...OH^-)^* \rightarrow C_5O_5^{2-} + OH^-$
[8]	$(C_5O_5^{2-}...OH^-)^* \rightarrow$ Products
[9]	$(C_5O_5^{2-}...OH^-)^* + A \rightarrow$ Products

where A stands for an acceptor molecule and $(C_5O_5^{\cdot-}...A^-)$ and $(C_5O_5^{2-}...OH^-)^*$ represent the transient intermediates formed between the excited state of the croconate dianion and the reactants, which in each case may reform the ground state reactants, proceed to products or react with the other reactant.

Assuming a steady-state concentration of all intermediates, their concentrations may be expressed as follows.

$$I_{abs} = k_D[C_5O_5^{2-}]^* + k_1[A][C_5O_5^{2-}]^* + k_6[OH^-][C_5O_5^{2-}]^*$$

$$[C_5O_5^{2-}]^* = \frac{I_{abs}}{k_D + k_1[A] + k_6[OH^-]} \qquad (3\text{-}1)$$

$$k_1[C_5O_5^{2-}]^*[A] = k_2[C_5O_5^{\cdot-}...A^-] + k_3[C_5O_5^{\cdot-}...A^-] + k_4[OH^-][C_5O_5^{\cdot-}...A^-]$$

$$[C_5O_5^{\cdot-}...A^-] = \frac{k_1[C_5O_5^{2-}]^*[A]}{k_2 + k_3 + k_4[OH^-]} \qquad (3\text{-}2)$$

$$k_3[C_5O_5^{\cdot-}...A^-] = k_5[C_5O_5^{\cdot-}]$$

$$[C_5O_5^{\cdot-}] = \frac{k_3}{k_5}[C_5O_5^{\cdot-}...A^-] \qquad (3\text{-}3)$$

$$k_6[OH^-][C_5O_5^{2-}]^* = k_7[C_5O_5^{2-}...OH^-]^* + k_8[C_5O_5^{2-}...OH^-]^* + k_9[A][C_5O_5^{2-}...OH^-]^*$$

$$[C_5O_5^{2-}...OH^-]^* = \frac{k_6[OH^-][C_5O_5^{2-}]^*}{k_7 + k_8 + k_9[A]} \qquad (3\text{-}4)$$

Substituting equation (3-1) into equation (3-4)

$$[C_5O_5^{2-}...OH^-]^* = \frac{k_6[OH^-]}{k_7 + k_8 + k_9[A]} \cdot \frac{I_{abs}}{k_D + k_1[A] + k_6[OH^-]} \qquad (3\text{-}5)$$

Substituting equation (3-1) into equation (3-2)

$$[C_5O_5^{\cdot-}...A^-] = \frac{k_1[A]}{k_2 + k_3 + k_4[OH^-]} \cdot \frac{I_{abs}}{k_D + k_1[A] + k_6[OH^-]} \qquad (3\text{-}6)$$

Substituting equation (3-6) into equation (3-3)

$$[C_5O_5^{\cdot-}] = \frac{k_1 k_3 [A] I_{abs}}{k_5 (k_2 + k_3 + k_4 [OH^-]) (k_D + k_1 [A] + k_6 [OH^-])} \qquad (3\text{-}7)$$

The rate of disappearance of croconate dianion is

$$\text{Rate} = k_4[OH^-][C_5O_5^{\cdot-}...A^-] + k_5[C_5O_5^{\cdot-}] + k_8[C_5O_5^{2-}...OH^-]^* + k_9[A][C_5O_5^{2-}...OH^-]^* \qquad (3\text{-}8)$$

Therefore the rate of disappearance of croconate dianion can be expressed as

$$\text{Rate} = \frac{I_{abs}\, k_1\, k_4\, [A]\ [OH^-]}{(k_2 + k_3 + k_4[OH^-])(k_D + k_1[A] + k_6[OH^-])} + \frac{I_{abs}\, k_1\, k_3\, [A]}{(k_2 + k_3 + k_4[OH^-])(k_D + k_1[A] + k_6[OH^-])}$$

$$+ \frac{I_{abs}\, k_6\, k_8\, [OH^-]}{(k_7 + k_8 + k_9[A])(k_D + k_1[A] + k_6\,[OH^-])} + \frac{I_{abs}\, k_6\, k_9\, [A]\, [OH^-]}{(k_7 + k_8 + k_9\,[A])(k_D + k_1[A] + k_6\,[OH^-])}$$

The quantum yield therefore is:

$$\phi = \frac{k_1\,[A]}{k_D + k_1\,[A] + k_6\,[OH^-]} \left[\frac{k_3 + k_4\,[OH^-]}{k_2 + k_3 + k_4\,[OH^-]} \right] + \frac{k_6\,[OH^-]}{k_D + k_1[A] + k_6[OH^-]} \left[\frac{k_8 + k_9[A]}{k_7 + k_8 + k_9[A]} \right] \qquad (3\text{-}9)$$

Quantum yields under different reaction conditions will now be examined in relation to this expression.

(a) Photolysis in the Absence of Additive

In the absence of additive, equation (3-9) may be simplified as follows

$$\phi = \frac{k_6\,[OH^-]}{k_D + k_6\,[OH^-]} \left[\frac{k_8}{k_7 + k_8} \right]$$

Rearranging this equation, gives the following expression:

$$\phi^{-1} = \frac{k_D}{k_6} \frac{k_7 + k_8}{k_8} ([OH^-])^{-1} + \frac{k_7 + k_8}{k_8} \qquad (3\text{-}10)$$

According to this mechanism a plot of ϕ^{-1} against $([OH^-])^{-1}$ should show a linear relationship with a slope equal to:

$$\frac{k_D}{k_6} \cdot \frac{k_7 + k_8}{k_8}$$

and the intercept equal to $(k_7 + k_8)/k_8$. The results are shown in Figure 3.8 and the ratios k_D/k_6 and $k_8/(k_7 + k_8)$ are given in Table 3.6. From the slope and intercept of Figure 3.8, a value of 1.4×10^{-4} M was obtained for k_D/k_6. The measurement of the lifetime of the excited croconate dianion (described in chapter 5) demonstrates that the triplet lifetime is about 3.2 μs, and the rate constant for deactivation to the ground state is about 3×10^5 s^{-1}. Taking this value for k_D, the value of k_6 is:

$$k_6 = k_D/1.4\times10^{-4} = 2.1\times10^9\ M^{-1}s^{-1}$$

This value of k_6 is close to a diffusion-controlled rate constant, showing that the addition of hydroxyl ion to the excited croconate dianion is a very fast process. On the other hand, the fact that the ratio $k_8/(k_7+k_8)=0.4$ indicates that deactivation by hydroxyl ion occurs concurrently with reaction and more than half of the intermediate $(C_5O_5^{2-}...OH^-)^*$ is deactivated to regenerate the ground state reactants.

(b) Photolysis in the Presence of Additives

The quantum yield of disappearance of croconate dianion was increased by addition of the additives $Fe(CN)_6^{3-}$, MV^{2+}, biacetyl and $BrCH_2$-C_6H_4-NO_2 into the reaction system. No indication of quenching of the excited croconate dianion through energy transfer process was observed with any of the additives. With the additives biacetyl and 4-nitrobenzylbromide a quantum yield of one was obtained at pH 12 in aqueous solution with a concentration of additives in the neighborhood of 10^{-4} M. With the additive $Fe(CN)_6^{3-}$, a maximum quantum yield of 0.57 occurred at a concentration of 5.0×10^{-5} M and then decreased with increasing concentration of additive. This apparent decrease was due to absorption of light by $Fe(CN)_6^{3-}$. If the light absorbed by the croconate dianion is corrected for the fraction absorbed by the additive, the quantum yield reached a plateau value with increasing concentration of $Fe(CN)_6^{3-}$.

The kinetics of the reaction of croconate dianion in the presence of additives will be analyzed in relation to equation (3-9). At lower pH where the reaction of excited croconate dianion with hydroxyl ion (reaction [6]) is negligible, equation (3-9) may be written as:

$$\phi = \frac{k_1[A]}{k_D + k_1[A] + k_6[OH^-]} \left(\frac{k_3 + k_4[OH^-]}{k_2 + k_3 + k_4[OH^-]} \right)$$

Assuming that k_1 and k_6 have similar values and the concentration of A is not too low, then at low pH, $k_6[OH^-]$ must be much smaller than $(k_D + k_1[A])$. This equation can be rearranged as:

$$\phi^{-1} = (1 + [A]^{-1} k_D/k_1) \frac{k_2 + k_3 + k_4[OH^-]}{k_3 + k_4[OH^-]}$$

A plot of ϕ^{-1} against $[A]^{-1}$ should yield a straight line with the intercept equal to the ratio:

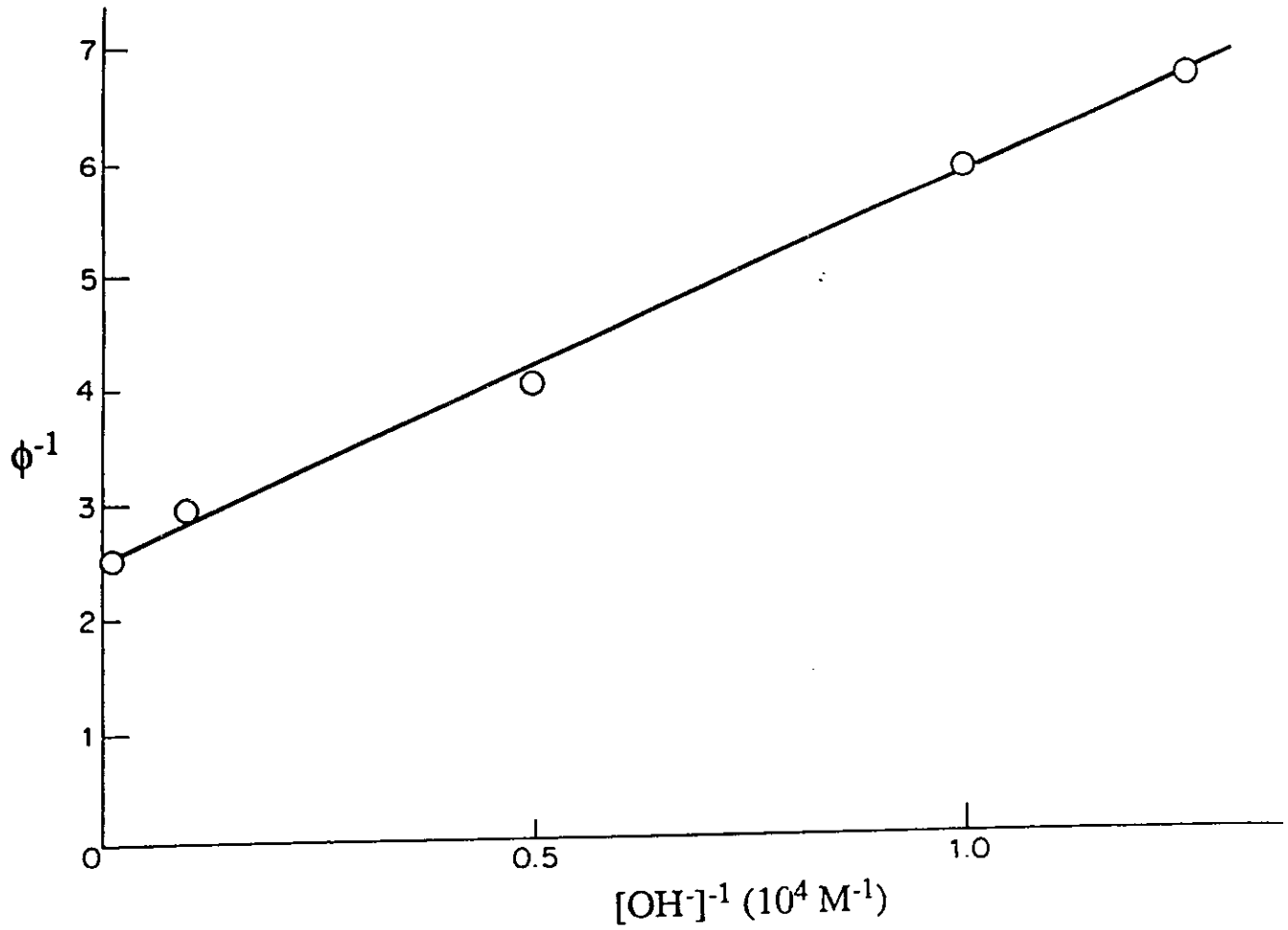

Figure 3.8 ϕ^{-1} for loss of croconate dianion as a function of $[OH^-]^{-1}$ in the absence of acceptors.

Table 3. 6

Ratios of Rate Constants Obtained from Figures 3. 7 and 3. 8

$k_D = 3.0\times10^5\ s^{-1}$

	$\frac{k_8}{k_7 + k_8}$	$\frac{k_D}{k_6}$	k_6
	0.4	1.4×10^{-4} M	$2.1\times10^9\ M^{-1}s^{-1}$
	$\frac{k_3 + k_4[OH^-]}{k_2+k_3+k_4[OH^-]}$	$\frac{k_D}{k_1}$	k_1
pH=8	2.5	1.44×10^{-4} M	$2.1\times10^9\ M^{-1}s^{-1}$
pH=9	4.1	1.36×10^{-4} M	$2.2\times10^9\ M^{-1}s^{-1}$

$$\frac{k_2 + k_3 + k_4 [OH^-]}{k_3 + k_4 [OH^-]}$$

and the slope equal to:

$$\frac{k_2 + k_3 + k_4 [OH^-]}{k_3 + k_4 [OH^-]} \cdot \frac{k_D}{k_1}$$

The plots of ϕ^{-1} against $[A]^{-1}$ for the additive 4-nitrobenzylbromide at pH 8 and pH 9 are shown in Figure 3.9. From the slopes and intercepts the value of the ratios of k_D/k_1 at pH 8 and pH 9 were 1.44×10^{-4} M and 1.36×10^{-4} M respectively. Taking an average value of 1.4×10^{-4} M for k_D/k_1 and 3.0×10^{5} s^{-1} for k_D (obtained from laser flash photolysis measurements), the value of k_1 is 2.1×10^{9} $M^{-1}s^{-1}$. These results are summarized in Table 3.6. If reaction [4] is assumed to be a diffusion-controlled reaction and an upper limit for k_4 of 5×10^{9} $M^{-1}s^{-1}$ is taken, values for k_2 and k_3 may be obtained from the intercepts of the plots in Figure 3.9, representing data at pH 8 and pH 9. The values of k_2 and k_3 are 1.3×10^{5} s^{-1} and 3.8×10^{4} s^{-1}, respectively. The ratio of $k_3/(k_2+k_3)$ is 0.22, which reflects the efficiency of separation of the charge transfer complex into the free ion pairs in solution.

(c) Evaluation of Equation (3-9)

With these estimates of the rate constants the quantum yield may be calculated from equation (3-9) as a function of the concentrations of additives and hydroxyl ion. At pH 12 the concentration of hydroxyl ion is 0.01 M, and with an additive concentration of $[A]=10^{-4}$ M, $k_1[A]<<k_6[OH^-]$. Therefore the ratio of $k_1[A]/(k_D+k_1[A]+k_6[OH^-])$ is very small and the ratio of $k_6[OH^-]/(k_D+k_1[A]+k_6[OH^-])$ is close to one. Since both ratios

$$\frac{k_8 + k_9 [A]}{k_7 + k_8 + k_9 [A]} \quad \text{and} \quad \frac{k_3 + k_4[OH^-]}{k_2 + k_3 + k_4[OH^-]}$$

have values less than 1, the first term in equation (3-9) is negligible compared with the

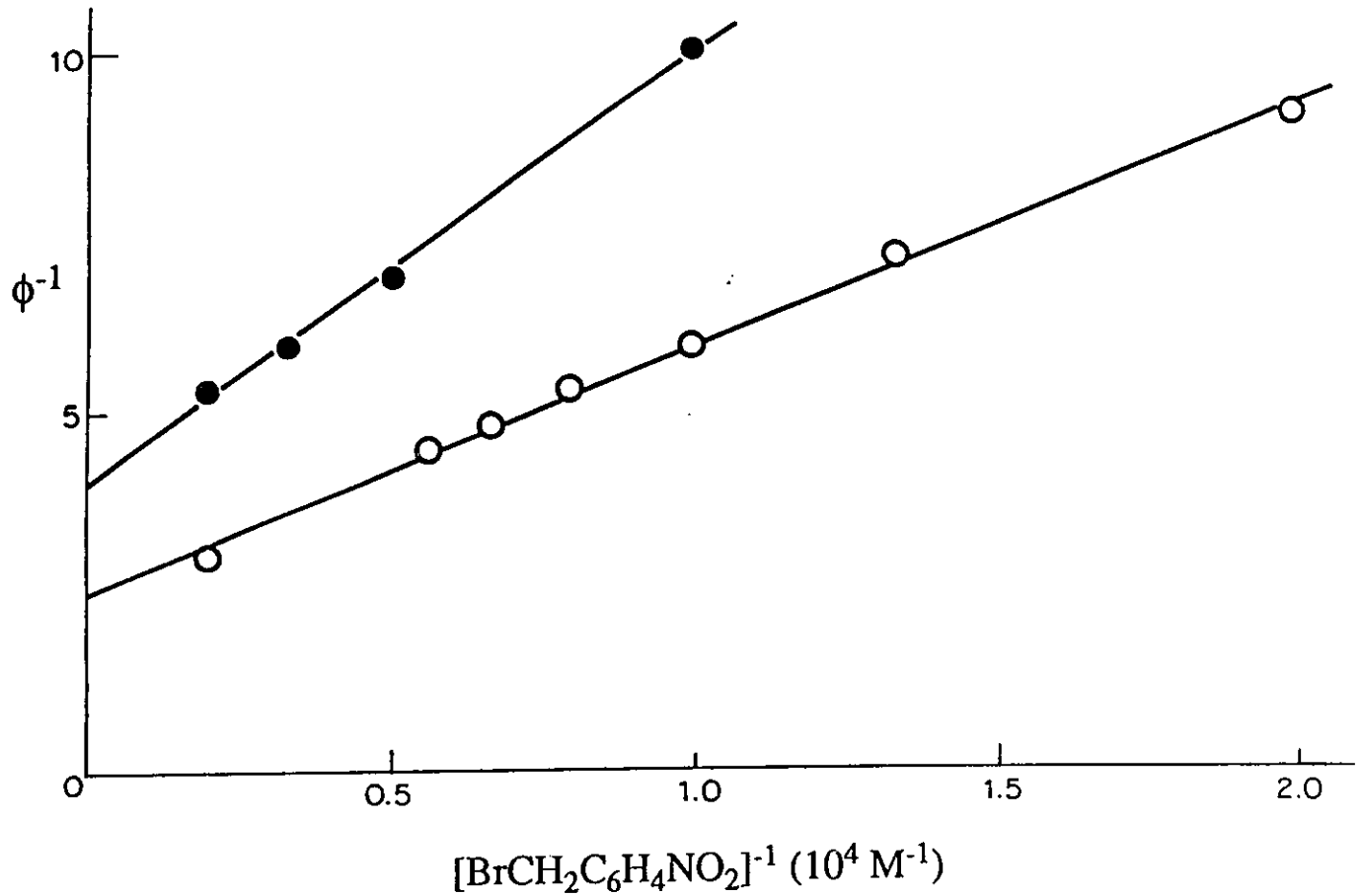

Figure 3.9 ϕ^{-1} for loss of croconate dianion as a function of $[BrCH_2C_6H_4NO_2]^{-1}$.

●: pH 8.0; o: pH 9.0.

second term. The increase in quantum yield as the concentration of additive increases to 10^{-4} M must be caused by the increasing contribution of reaction (9) through the fraction $(k_8+k_9[A])/(k_7+k_8+k_9[A])$.

Both reaction (4) and (9) are probably diffusion-controlled with rate constants of the order of 10^9 $M^{-1}s^{-1}$. At the concentration of 4-nitrobenzylbromide of 1.0×10^{-4} M, $k_9[A]$ must be much greater than (k_7+k_8) so that the ratio $(k_8+k_9[A])/(k_7+k_8+k_9[A])$ will be close to unity. Also the values of k_7 and k_8 will not differ greatly, since the ratio of $k_8/(k_7+k_8)$ (Table 3.7) is 0.4. Assuming a value for k_9 and k_4 of 5.0×10^9 $M^{-1}s^{-1}$, the maximum value for (k_7+k_8) will be 5.0×10^4 s^{-1} with k_7 equal to 3.0×10^4 s^{-1} and k_8 equal to 2.0×10^4 s^{-1}.

Minor modifications to these rate constants were made to maximize the agreement of the calculated quantum yield with the experimental measurements for the additive 4-nitrobenzylbromide at both pH 9 and pH 12. The final value for the rate constants are given in Table 3.7 and the calculated values for the quantum yield are shown as the solid lines in Figure 3.5. The calculated values of the fractions in equation(3-9) are shown in Table 3.8. At pH 12, as predicted, the first term in equation (3-9) contributes a maximum of 1.5% to the quantum yield even at highest concentration of 4-nitrobenzylbromide. At pH 9, both terms contribute to the reaction at low concentration of additive but at high concentrations of additive the first term predominates.

The value of k_3 deduced from these results is smaller than the usual values of rate constants for the separation of contact ion pairs in solution. It must be concluded that the ion pair, $(C_5O_5^{\cdot-}...A^-)$ is sufficiently stable to five a lifetime long enough to react with OH^-, reaction (4), at pH 8 and 9. That reaction (4) occurs at both pH 8 and 9 is clear from the results shown in Fig. 3.9.

With the additive biacetyl the approach of the quantum yield to the limiting value of one at pH 12 was slower over a comparable range of concentration, suggesting that reaction

[9] was substantially slower than the corresponding reaction with 4-nitrobenzylbromide. The best agreement was obtained with $k_1=4\times10^8$ $M^{-1}s^{-1}$, $k_2=5\times10^4$ s^{-1}, $k_3=8\times10^4$ s^{-1} and $k_9=7\times10^8$ $M^{-1}s^{-1}$ with the other constants remaining the same. It is understandable that the rate constants for k_6, k_7 and k_8 should be the same with both biacetyl and 4-nitrobenzylbromide if the reactions follow the same mechanism. The result for the measurement at pH 12 is shown in Figure 3. 10. Agreement is only qualitative, suggesting that additional reactions with biacetyl may be important, but the general pattern of the reaction and the change of quantum yield with pH are consistent with the mechanism.

The quantum yield in the presence of potassium ferricyanide and methyl viologen reached a limiting value less than one at pH 12, which suggests deactivation by the additive. In order to be effective at pH 12 deactivation must take place at the $(C_5O_5^{2-}...OH^-)^*$ complex rather than at the excited croconate dianion.

[10] $\quad (C_5O_5^{2-}...OH^-)^* + A \rightarrow C_5O_5^{2-} + OH^- + A$

The fraction in the second term of equation (3-9) in this case changed from

$$\frac{k_8 + k_9\,[A]}{k_7 + k_8 + k_9\,[A]} \quad \text{to} \quad \frac{k_8 + k_9\,[A]}{k_7 + k_8 + k_9\,[A] + k_{10}\,[A]}$$

This fraction approaches the limit $k_9/(k_9+k_{10})$ as the concentration of additive increases. The limit for potassium ferricyanide was 0.56 and was obtained at a concentration of 5.0×10^{-5} M. For this additive the rate of reaction [9] is therefore slightly greater than that for 4-nitrobenzylbromide. With methyl viologen the limiting quantum yield was observed at a concentration of 2.0×10^{-5} M and the rate constant for reaction [9] would therefore be of the order of 10^{10} $M^{-1}s^{-1}$. Reaction [1] would likely be very fast as well but still would not make a significant contribution at pH 12. Such a large value for k_9 (or for k_1) is reasonable considering the attraction of the positive ion towards the excited $(C_5O_5^{2-}...OH^-)^*$ complex. These estimates will be verified by direct measurements described in Chapter 5.

Table 3. 7

Values for the Rate Constants in Equation (3-9)

	$BrCH_2C_6H_4NO_2$	Biacetyl
k_1	$2.0(\pm0.1)\times10^9$ $M^{-1}s^{-1}$	$4.0(\pm0.2)\times10^8$ $M^{-1}s^{-1}$
k_2	$1.8(\pm0.1)\times10^5$ s^{-1}	$5.0(\pm0.3)\times10^4$ s^{-1}
k_3	$5.0(\pm0.3)\times10^4$ s^{-1}	$8.0(\pm0.5)\times10^4$ s^{-1}
k_4	$7.0(\pm0.4)\times10^9$ $M^{-1}s^{-1}$	$7.0(\pm0.4)\times10^9$ $M^{-1}s^{-1}$
k_6	$1.8(\pm0.1)\times10^9$ $M^{-1}s^{-1}$	$1.8(\pm0.1)\times10^9$ $M^{-1}s^{-1}$
k_7	$1.1(\pm0.05)\times10^4$ s^{-1}	$1.1(\pm0.05)\times10^4$ s^{-1}
k_8	$7.2(\pm0.4)\times10^3$ s^{-1}	$7.2(\pm0.4)\times10^3$ s^{-1}
k_9	$5.0(\pm0.3)\times10^9$ $M^{-1}s^{-1}$	$7.0(\pm0.4)\times10^8$ $M^{-1}s^{-1}$
k_D	$3.2(\pm0.2)\times10^5$ s^{-1}	$3.2(\pm0.2)\times10^5$ s^{-1}

* The error for rate constants obtained from fitting may be larger than the values given here.

Table 3. 8 (a)

Calculation of Quantum Yield for Disappearance of Croconate Dianion According to Equation (3-9) in the Presence of $BrCH_2$-C_6H_4-NO_2

$[BrCH_2C_6H_4NO_2]$ (M)	Experimental (ϕ)	Calculated (ϕ)	First Term	Second Term
pH=12.0				
0	0.40	0.39	0	0.389
1.5×10^{-6}	0.57	0.56	0	0.562
5.0×10^{-6}	0.68	0.73	0	0.732
1.0×10^{-5}	0.76	0.82	0.001	0.823
2.0×10^{-5}	0.87	0.89	0.002	0.889
5.0×10^{-5}	0.97	0.94	0.005	0.937
1.0×10^{-4}	0.98	0.96	0.011	0.951
1.5×10^{-4}	1.0	0.97	0.016	0.953
pH=9.0				
0	0.05	0.02	0	0.021
2.0×10^{-5}	0.08	0.086	0.042	0.043
5.0×10^{-5}	0.11	0.13	0.091	0.039
8.0×10^{-5}	0.14	0.16	0.129	0.035
1.0×10^{-4}	0.17	0.18	0.149	0.033
1.5×10^{-4}	0.21	0.22	0.188	0.028
2.0×10^{-4}	0.23	0.24	0.217	0.024
5.0×10^{-4}	0.33	0.31	0.300	0.013

Table 3. 8 (b)

Calculation of Quantum Yield for Disappearance of Croconate Dianion According to Equation (3-9) in the Presence of Biacetyl

pH = 12.0

[Biacetyl] (M)	Experimental (ϕ)	Calculated (ϕ)	First Term	Second Term
0	0.40	0.39	0	0.389
1.0×10^{-5}	0.50	0.59	0	0.585
2.0×10^{-5}	0.60	0.68	0	0.684
3.8×10^{-5}	0.73	0.78	0	0.775
5.0×10^{-5}	0.81	0.81	0.001	0.811
8.0×10^{-5}	0.95	0.86	0.002	0.861
1.0×10^{-4}	0.98	0.88	0.002	0.880
1.5×10^{-4}	1.0	0.91	0.003	0.909

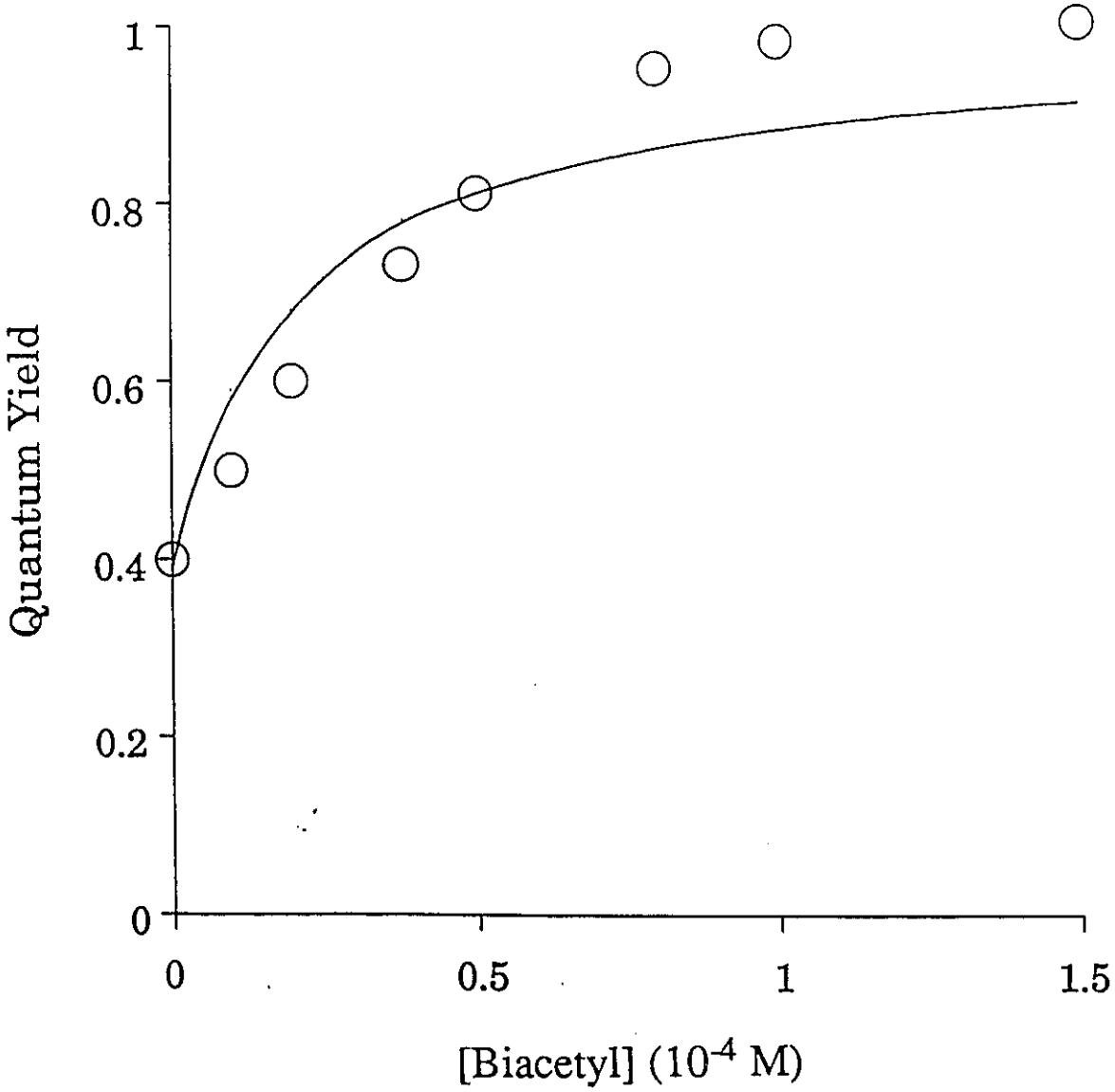

Figure 3.10 The quantum yield for the loss of croconate dianion as a function of the concentration of biacetyl. The solid line is calculated values according to equation (3-9) and rate constants in Table 3.7.

(D) Quantum Yield in Micellar Solution

It is interesting to note that the limiting quantum yield of disappearance of croconate dianion in the presence of methyl viologen was increased in micellar solution and at pH 12 approached one at very low concentration of additive (see Table 3.3). Photochemical reactions in micellar solution may be affected by local concentration changes in reactants on the surface of the surfactant, by charge transfer cage effects exerted by the presence of micelles, or by changes in the solution structure.[79-93] SDS is an anionic surfactant and it aggregates spontaneously when the concentration is raised beyond a certain specific, rather sharply defined critical surfactant concentration, called the critical micelle concentration (cmc). SDS micelle is spherical with a homogeneous surface charge at low surfactant concentration as shown in Figure 3.11. From conductivity measurements the cmc of SDS under the present experimental conditions is 4×10^{-3}M. This value is close to the value of 4.6×10^{-3} M reported by C. David, but is somewhat lower than value of $6\text{--}9\times10^{-3}$ M reported by others[94-96]. The value of cmc changes with the condition of experiment. The concentration of micelle aggregate can be calculated as:

$$C_m = \frac{C_s - C_1}{S}$$

where C_m: concentration of micelle aggregate

C_s: concentration of surfactant in solution

C_1: critical micelle concentration (cmc)

S: average number of surfactant molecules per micelle

If we take S as 60 as reported previously[95], then the concentration of micelle aggregate can be calculated as :

$$C_m = \frac{0.01 - 0.004}{60} = 1.0\times10^{-4}\ \text{M}$$

With this concentration of micelle in solution, we expect that a significant portion of methyl viologen cations will be attached to the anionic surface of the micelle aggregates and the local concentration of MV^{2+} on the micelle surface will be greater than the concentration in a homogeneous solution. This is shown schematically in Figure 3.11(b). This increase in local MV^{2+} concentration may increase the rate of the reaction with the excited state of croconate dianion and hence increase the quantum yield as the photochemical reaction takes place.

Another possible mechanism for the increased quantum yield in the micellar solution is due to the charge transfer cage effect. After the methyl viologen cation has received one electron from the excited croconate dianion, its affinity to the anionic micelle surface is weakened and would be replaced by another free methyl viologen cation from the solution phase, as illustrated in Figure 3.11(b). On the other hand, due to the negative charge carried on the surface of the micelle aggregate, the monoanion $C_5O_5^{-\cdot}$ will be repelled away from the surface of the micelle and thus inhibit the electron back reaction. These effects will increase the quantum yield of disappearance of croconate dianion.

As the limit of the quantum yield for the disappearance of croconate dianion reached unit in the micellar solution, it appears that the reaction mechanism is different from that in homogeneous solution. the reduction in the concentration of MV^{2+} in the presence of the micelles may also affect the deactivation of the excited state complex as expressed in reaction (10):

[10] $(C_5O_5^{2-}...OH^-)^* + A \rightarrow C_5O_5^{2-} + OH^- + A$

A reduction of the deactivation would also lead to an increase in the quantum yield. Because of the limited data these mechanisms are suggested without further proof.

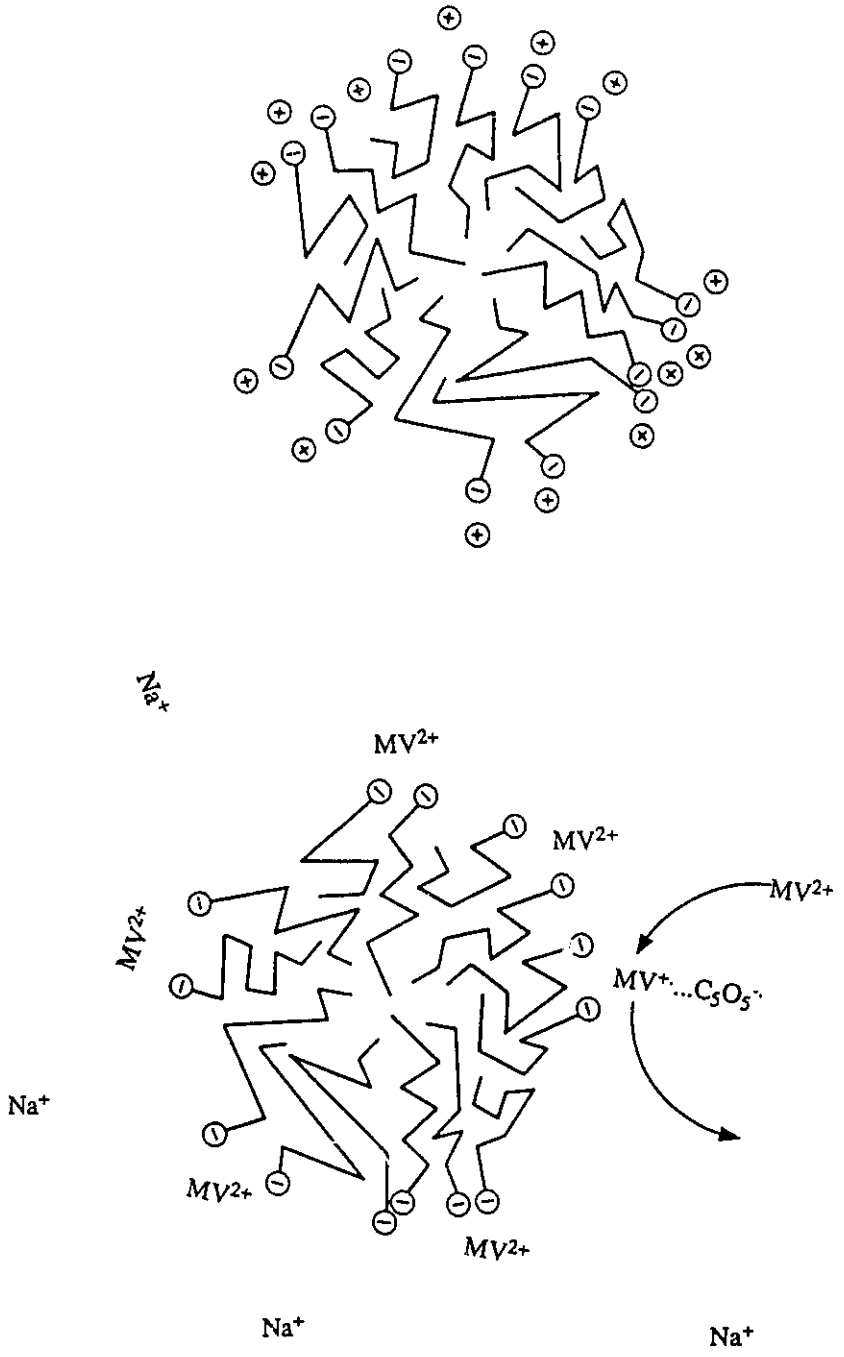

Figure 3.11 (a) Structure of SDS micelle in water.

(b) Interaction of cations on the surface of SDS micelle.

3. 3. 3 Comparison with the Photochemical reaction of Rhodizonate Dianion

Several similarities and differences are evident in the photochemical behavior of rhodizonate and croconate dianions.[97-99] Both excited dianions undergo oxidation by electron transfer to a suitable acceptor. The efficiency of the process appears much larger for croconate dianion, where a primary quantum yield of one for disappearance of the dianion was obtained for certain additives, whereas the quantum yield for disappearance of rhodizonate dianion in the presence of additives did not exceed 4×10^{-2}. The large quantum yield for loss of croconate, however, was observed only in basic solution and was the result of the synergistic effect of the additive and the hydroxyl ion. The photochemical reaction of rhodizonate dianion was measured only in neutral solution because the thermal reaction in basic solution was too fast to allow concurrent photochemical measurements. The similarity in these observations is the loss of the dianion through reactions with hydroxyl ion. In the case of rhodizonate dianion the reaction occurs in the dark, whereas with croconate dianion photochemical excitation of the dianion is required to induce the reaction.

The product of the thermal reaction of rhodizonate dianion in basic solution in the presence of oxidants is croconate dianion. Conversion of croconate dianion to squarate dianion occurred photochemically in strongly basic solution in the presence of oxygen. This reaction is an easy route to the formation of squaric acid.

Chapter 4

Acrylamide Polymerization Initiated by the Photolysis of Dianions of Rhodizonic and Croconic Acids

4. 1 Introduction

Polymerization processes can be divided into three categories: step-reaction polymerization, ionic chain reaction polymerization and radical chain reaction polymerization.[100-102] Step-reaction polymerization refers to polymerizations in which the molecular weight increases in a slow, step-like manner as reaction time increases. Polyesterification in a bulk polymerization process is one example of this kind of polymerization. Condensation reactions between dialcohol and diacid molecules lead to a slow increase of polymer molecular weight. Ionic chain reaction polymerization refers to polymerization processes initiated by ionic species produced by a heterolytic cleavage of chemical bonds. This in turn can be divided into two categories on the basis of the nature of the charge on the tip of the growing polymer chain: cationic polymerization and anionic polymerization. Carbonium ions are one example of a cationic initiator. Sulfuric acid, tin(IV) chloride, boron trifluoride and iodine have also been used as cationic initiators in polymerization processes. Base catalyzed polymerization of ethylene oxide involving a ring-opening chain reaction is one of the earliest examples of anionic polymerization. The mechanism is shown in scheme 4.1

Polymerization catalyzed by a transition metal complex is another type of ionic chain reaction polymerization process. The well known Ziegler-Natta catalyst is a typical example of this kind of catalyst. In the process of polymerization, the polymer chain grows through an active center of the transition metal complex. Many vinyl and conjugated dienes

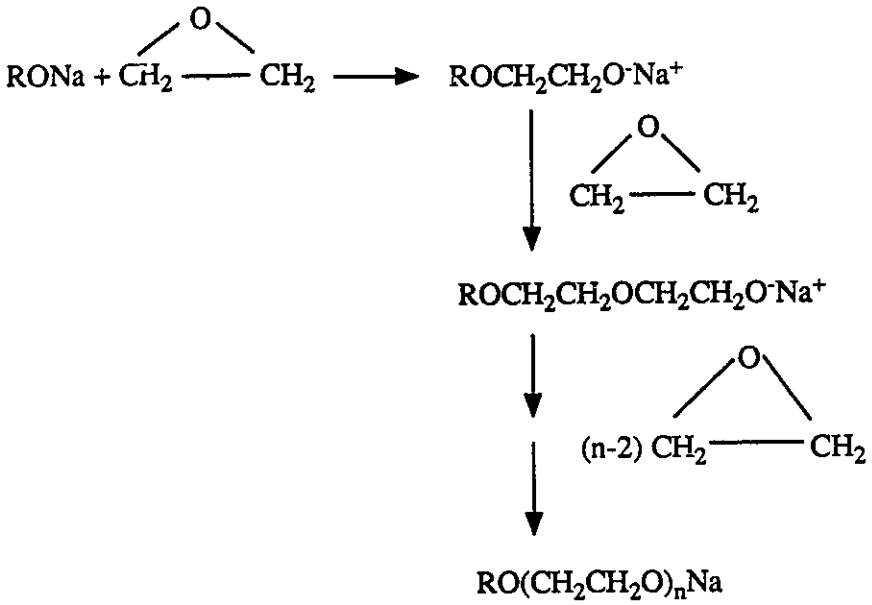

Scheme 4.1 Propagation of Polyethylene Oxide Chain

have been polymerized using Ziegler-Natta catalysts.

Radical polymerization refers to the polymerization initiated by a radical which in turn can be generated by homolytic cleavage of a chemical bond.[101] This is an easy, convenient polymerization process and has wide application in the polymer industry. In some polymerization processes, radical and ionic chain reaction polymerization mechanisms coexist.[103]

Photopolymerization is a general description of a variety of processes which result in the conversion of small molecules into large ones involving some photoactivated process.[104-107] In the conventional photopolymerization concept light is involved only in the initiating step to generate either free radicals or ions, which then propagate by a chain mechanism to give high molecular weight products. New types of photopolymerization have been described in which photochemically excited states are involved in each step of

the polymerization reaction. In this process a macromolecule is obtained from a low molecular weight material by stepwise condensation reactions in which, for each of these chain-extending steps, the absorption of a quantum of light is necessary.

Polymerization processes initiated by photoinduced electron transfer are important in the polymer industry. In this system, reactive species which are capable of inducing the spontaneous polymerization of corresponding monomers are formed through photoinduced electron transfer. These active species may be neutral or ion radicals. The production of the radicals can be expressed in a general way as follows:

$S + h\nu \rightarrow S^*$	absorption
$S^* \rightarrow S$	emission, internal conversion, etc.
$S^* + X \rightarrow S + R\cdot$	sensitization

Here S is the absorbant, called the sensitizer, X is either a suitable electron acceptor or donor which can react with the excited sensitizer S^* to generate a radical $R\cdot$ through an electron transfer reaction. Two types of electron transfer sensitizer can be identified.[105] In one case the excited sensitizer S^* functions as an electron acceptor. In the presence of a suitable electron donor, D, reduction of S^* produces the donor cation $D^{+\cdot}$, which may be transformed into a species capable of initiation of polymerization. In the other case, the excited sensitizer functions as an electron donor for a suitable ground state electron acceptor A, and the reduced acceptor $A^{-\cdot}$ can produce radical initiators on further reaction. The first kind of sensitization is called photoreducible sensitization and the process can be expressed as:

$$S^* + D \rightarrow S^{-\cdot} + D^{+\cdot}$$

$$D^{+\cdot} \rightarrow R\cdot + M^+$$

An example is aryl sulphonites:

$$S^* + ArSO_2^- \rightarrow S^{-\cdot} + ArSO_2\cdot$$

$ArSO_2\cdot$ is an initiator capable of initiating radical polymerization.

The second kind of sensitization is called photooxidizable sensitization and the process can be expressed as:

$$S^* + A \rightarrow S^{+\cdot} + A^{-\cdot}$$

$$A^{-\cdot} \rightarrow R\cdot + M^-$$

An example is:

$$S^* + ArN_2^+ \rightarrow S^{+\cdot} + ArN_2\cdot$$

$$ArN_2\cdot \rightarrow Ar\cdot + N_2$$

The radical $Ar\cdot$ is capable of initiating polymerization. This type of reaction is also called reductive photofragmentation.

The general mechanism of the radical-initiated polymerization can be expressed as scheme 4.2.

initiation	$R^\bullet + M \xrightarrow{k_i} M_1^\bullet$	R_i
propagation	$M_1^\bullet + M \xrightarrow{k_1} M_2^\bullet$,	R_P
	$M_2^\bullet + M \xrightarrow{k_2} M_3^\bullet$	
	. . . . .	
	$M_i + M \xrightarrow{k_i} M_{i+1}$	
termination	$M_i^\bullet + M_i^\bullet \xrightarrow{k_t} (M_i)_2$	R_t

Scheme 4.2 Kinetics of Radical Polymerization

Termination may occur by combination of any two radicals to give a stable molecule. Assuming that the rate constant for combination of radicals is the same for any of the radicals M_i present in the system the rate of termination may be expressed in terms of the total radical concentration in the system:

$$R_t = k_t [\sum_{i=1}^{n} (M_i^\bullet)]^2 = k_t (M^\bullet)^2$$

where $M^\bullet$ is the total radical concentration. Under steady-state conditions the rate of the radical initiation should equal the rate of radical termination, $R_i=R_t$. Therefore the total radical concentration may be expressed as :

$$[M^\bullet] = (\frac{R_i}{k_t})^{1/2}$$

By further assuming that in the propagation the rate constants for each chain extending reaction are the same, that is: $k_1=k_2= k_3...= k_i =k_p$, then the expression for the rate of polymerization is:

$$R_p = \frac{-d\,[M]}{dt} = k_1[M_1^\bullet]\,[M] + k_2\,[M_2^\bullet]\,[M] + \cdots k_n\,[M_n^\bullet]\,[M]$$

$$= k_p \sum_{i=1}^{n} M_i^\bullet\,[M] = k_p\,[(M^\bullet)]\,[M]$$

$$= k_p\,(\frac{R_i}{k_t})^{1/2}\,[M]$$

where k_p and k_t are rate constants for chain propagation and termination, respectively, [M] is the concentration of monomer. In photochemically initiated polymerization, $R_i=2\phi I_a$, where ϕ is the quantum yield for radical production and I_a is the number of quanta of light absorbed per unit volume and time. The rate of polymerization can be expressed as:

$$\frac{-d[M]}{dt} = k_p \left(\frac{\phi I_a}{k_t}\right)^{1/2} [M]$$

This expression shows that the rate of polymerization in this case is proportional to the first power of the concentration of monomer and proportional to the square root of the absorbed light intensity.

The results described in Chapters two and three showed that in aqueous solution in the presence of various acceptor molecules the initial reaction of the excited dianion of rhodizonic and croconic acids was electron transfer to the proper acceptors. Because of their strong absorbing properties and the potential efficiency of the photochemical reactions, particularly of croconate dianion, these dianions appear to be promising initiators for photochemical polymerization. In order to test the efficiency of photopolymerization initiated by photolysis of oxocarbon dianions, we studied the process and mechanism of photopolymerization of acrylamide using the dianions as initiators. Acrylamide can be polymerized in aqueous solution via radical chain reaction processes and is widely used as a model monomer in polymerization studies.[108-112]

4. 2 Experimental

4. 2. 1 Photolysis and Measurement of Quantum Yield

A monomer (acrylamide) concentration of 1.0 M in aqueous solution was used in most photopolymerization experiments. The light source used in the experiments was either the tungsten lamp or the medium-pressure mercury lamp which was described in chapter 2 and chapter 3, respectively, according to which dianion was used in the photopolymerization. Solutions containing monomer and electron acceptors and solutions

containing croconate dianion or rhodizonate dianion were separately degassed by freeze-pump-thaw cycles five times and then mixed under vacuum in the photolysis cell. The absorbance at 363 nm (with croconate dianion) or 483 nm (with rhodizonate dianion) of the solution in the cell was monitored during the course of photolysis to give the concentration of croconate dianion or rhodizonate dianion. The photolysed solution containing the polymer product and other unreacted chemicals was poured into a beaker containing 200 mL methanol, thus precipitating the acrylamide polymer. After a few hours in the dark, the polymer was filtered using Whatmen glass microfiber filter paper and was washed with methanol three times. Finally, the polymer was dried at 60^0 C until constant weight. Solutions containing monomer were protected from visible light during the preparation and photolysis processes.

The percentage polymerization was based on the initial input of monomer to the photolysis cell and the final yield of polymer formed during the photolysis. A small polymerization observed on photolysis under the same condition except without oxocarbon dianion was subtracted from the polymerization yield.

The quantum yield of the photopolymerization was calculated according to the following equation:

$$\phi = \frac{N_0}{I_0\, t\, (1 - 10^{-A})}$$

N_0: number of molecules of monomer reacted during the polymerization process.

I_0: light intensity reaching the photolysis cell, (photon sec^{-1})

t: photolysis time (sec.)

A: average absorbance of oxocarbon dianion during the photolysis process. Because the decay in absorbance was not liear with time, th average absorbance was obtained from severl redings taken on the cause of the reaction.

Number of molecules reacted (N_0) can be calculated as:

$$N_0 = \frac{\text{Weight of polymer}}{\text{Molecular weight of monomer (71.08)}} \times N$$

N: Avogadro's number 6.02×10^{23}

In the study of hotopolymerization using croconate dianon as sensitizer, the dependence of quantum yield on light intensity was investigated. The incident light intensity was attenuated using a cell filled with the required concentration of aerated croconate dianion. The oxygn acted as an efficient quencher o the excited dianion and prevented consumption of the croconate dianion.

4. 2. 2 Measurement of Average Molecular Weight of Polymer

The molecular weight of the polymer was obtained by measuring the viscosity of the aqueous polymer solution. The viscosity was measured by a Cannon-Fenske Routine Viscometer (also called Ostwald vicometer) supplied by Cannon Instrument Company. The viscometer was cleaned thorughly until the measurement for water reached a constant time. Similar cleaning was also made between the measurementsof samples. Since the quantity of polymer was limited, the viscosity of the aqueous polymer solution with the highest polymer concetration was measured first, followed by successive dilution ntil measurements of viscosity of the aqueous polymer solution with five different polymer concentrations were obtained. In each measurement of the viscosity for a particlar polymer concentration, measurements were repated until good agreement was obtained. All the viscosity measurements were made at 25^0 C.

The relation between the viscosity and the time of the flow as measured in an Ostwald Viscometer is given as:[113]

$$\eta = \rho B t$$

where ρ is the density of the solution and B is a constant for a particular viscometer tube. Assuming that the density of the polymer solutions are not significantly different from pure water, then the ratio of the viscosities of the water and polymer solutions is:

$$\eta/\eta_0 = t/t_0$$

where η and η_0 are the viscosities of the polymer solutions and solvent respectively, t and t_0 are times (second) required for a fixed volume of diluted polymer solution and solvent to run through the capillary tube of the viscometer, respectively.

In the determination of the molecular weight of polymer by viscosity measurement the following equation can be derived:[113]

$$\lim_{C \to 0} \frac{(\eta / \eta_o) - 1}{C} = [\eta]$$

C is the concentration of the polymer in solution (g/100mL). The quantity (η/η_0-1) is called the specific viscosity η_{sp}. The value of η_{sp}/C at C=0 is obtained by extrapolation of the linear portion of the plot of η_{sp}/C as a function of [C] and this value is called the intrinsic viscosity or limiting viscosity number of the polymer solution $[\eta]$. The empirical relationship between $[\eta]$ and the molecular weight of polymer is expressed as:

$$[\eta] = k \times (\bar{M})^{\alpha}$$

where k and α are constants. The values of k and α are different for different polymers and they also vary with the solvent used and the temperature at which the viscosities were measured. From the viscosity measurement an averaged molecular weight of polymer can be obtained. Although the viscosity of a polymer solution does depend in part on the size of the polymer molecules, the molecular weight obtained by measurement of the viscosity of polymer solutions often does not conform to either the simple number or weight-average quantity, and is called "viscosity average". In general, it is much closer to the weight-average

molecular weight than to the number-average quantity.

4. 2. 3 Materials

The additives used as electron acceptors with rhodizonate dianion were tetracyanoethylene, 4-nitrobenzylbromide, 4-nitrobenzylchloride, and with croconate dianion were biacetyl, 4-nitrobenzylbromide, 4-nitrobenzylchloride, methyl viologen, potassium ferricyanide and 4-aminodiphenylamine diazonium sulfate (4DS). Potassium ferricyanide was recrystallized from warm water-ethanol solution and 4-nitrobenzylbromide was recrystallized twice from warm water-methanol solution. Other reagents were used without further purification. The additives which caused polymerization with both rhodizonate dianion and croconate dianion absorbed less than 1% of the irradiating light at the highest concentrations used.

4. 3 Results

4. 3. 1 Initiation by Photolysis of Rhodizonate Dianion

Polymerization of acrylamide by initiation of rhodizonate dianion was attempted because of the potential value of an initiator which absorbs visible light. As described in Chapter 2, the maximum quantum yield for disappearance of rhodizonate dianion was about 10^{-2} with the acceptors hydrogen peroxide and ferricyanide and was 4×10^{-2} with tetracyanoethylene and it was concluded that irreversible conversion of the monoanion radical did not compete effectively with the back electron transfer to form ground state reactants. Because of this efficient reverse transfer, the rate of polymerization in the presence of acrylamide was not efficient. A maximum quantum yield for polymerization of 44 was obtained in the presence of 4-nitrobenzylbromide. Although the acceptor TCNE gave the highest quantum yield in the photolysis of rhodizonate dianion the quantum yield

for polymerization was lower than with 4-nitrobenzylbromide. The results of the polymerization with rhodizonate dianion are summarized in Table 4.1. The lower limits for the rate of polymerization and for the quantum yield are based on a lower limit of about 1 mg for recovery of polymer with the present technique. The low quantum yield for polymerization indicates that the yield of radicals which escape the cage recombination is small and is therefore consistent with the quantum yield measurements described in Chapter 2. Further studies of the kinetics of polymerization using rhodizonate dianion as initiator were therefore not pursued.

4. 3. 2 Initiation by Croconate Dianion

Photolysis of croconate dianion in the presence of monomer but in the absence of acceptors led to small yields of polymerization barely greater than the limit of detection. In the presence of the acceptors 4-nitrobenzylbromide, 4-nitrobenzylchloride and biacetyl the rate of polymerization of acrylamide was greatly increased and a maximum quantum yield for polymerization of 2×10^3 was observed with the additive 4-nitrobenzylchloride in neutral solution. The additive 4DS also led to polymerization[114-116] with rates comparable to those observed with biacetyl. Polymerization was not observed in the presence of ferricyanide or methyl viologen, although both these additives had increased the quantum yield for disappearance of croconate dianion on irradiation in neutral and basic solution.

The rate of polymerization of acrylamide was measured using an initial concentration of croconate dianion of 2.3×10^{-5} M, corresponding to an absorbance of 0.90. An average rate of polymerization was calculated as the total weight of polymer recovered divided by the irradiation time. Significant loss of croconate dianion occurred during the time necessary to produce sufficient polymer for accurate measurement and an average value for the light absorbed by croconate dianion was therefore used for the calculation of

Table 4.1

Rates and Quantum Yields of Polymerization Initiated by Photolysis of Rhodizonate Dianion

$[C_6O_6^{2-}] = 2.5\times10^{-5}$ M, pH = 7, [Monomer] = 1.0 M

Additive	[Additive] (M)	Rate (Ms^{-1})	ϕ
No Additive	0	ND	ND
TCNE	2.0×10^{-4}	2.0×10^{-6}	8
$BrCH_2C_6H_4NO_2$	3.2×10^{-4}	1.0×10^{-5}	44
$ClCH_2C_6H_4NO_2$	1.0×10^{-4}	$\leq5\times10^{-7}$	≤2

the quantum yield for polymerization. The quantum yield of polymerization using 4-nitrobenzylhalides as acceptor as a function of pH is shown in Table 4.2. Some results with biacetyl or 4DS as additive are summarized in Table 4.3. Irradiation of solutions of acrylamide alone at 366 nm did not cause measurable polymerization but a small measurable rate was observed in the presence of 4-nitrobenzylbromide, 4-nitrobenzylchloride and biacetyl. In the case of 4-nitrobenzylchloride, this rate was less than 1% of the rate in the presence of croconate dianion under all conditions. With 4-nitrobenzylbromide the rate was about 20% of the rate in the presence of croconate dianion at pH 7--8 and somewhat less (12%) at pH 12, while with biacetyl the rate without croconate dianion was about 30% of that measured in the presence of croconate dianion. In calculating the quantum yield of polymerization initiated by the photolysis of croconate dianion, the rate of polymerization was corrected for the rate measured in the presence of additive but in the absence of croconate dianion. For example, in the photolysis of croconate dianion at pH 8 using 4-nitrobenzylbromide as electron acceptor with a concentration of 6.45×10^{-4} M, the concentration of acrylamide was 1.0 M, the photolysis period was 3 minutes and the volume of the solution photolysed was 3.0 mL. The initial amount of monomer was :

$0.0030\times1.0\times71.08 = 0.213$ g

The polymer recovered after photolysis was 0.062 g. The fraction of monomer converted to polymer in this case therefore is:

$0.062/0.213 = 29\%$

The rate of polymerization is:

$$\frac{0.062/71.08}{60\times3}\ \frac{1000}{3} = 1.6\times10^{-3}\ \text{M s}^{-1}$$

By a similar measurement the rate of polymerization of acrylamide in the presence

Table 4. 2

Quantum Yield of Photopolymerisation with the Additives 4-nitrobenzylhalides

$[C_5O_5^{2-}] = 2.3\times10^{-5}$ M, $[BrCH_2C_6H_4NO_2] = 6.4\times10^{-4}$ M, $[ClCH_2C_6H_4NO_2] = 1.6\times10^{-4}$ M

Photolysis Period: 3 minutes

pH	$ClCH_2C_6H_4NO_2$	$BrCH_2C_6H_4NO_2$
4	1400	1000
5		1400
6	2000	1600
7	2500	1700
8	2200	1700
9		1700
10	1800	1600
11		1600
12	1700	1500

Table 4. 3

Quantum Yield of Polymerisation with the Additives Biacetyl and 4DS

$[C_5O_5^{2-}] = 2.3\times10^{-5}$, Photolysis period: 30 minutes

[BA] (M)	ϕ
3.2×10^{-4}	19
6.4×10^{-4}	93
9.4×10^{-4}	100
1.25×10^{-3}	130
1.61×10^{-3}	140
[4DS] (M)	
3.2×10^{-4}	86
6.4×10^{-4}	130
9.4×10^{-4}	130

of 4-nitrobenzylbromide in the absence of croconate dianion is 3.15×10^{-4} M s^{-1}. The corrected rate of polymerization therefore is:

$1.6\times10^{-3} - 0.32\times10^{-3} = 1.3\times10^{-3}$ Ms^{-1}

The average absorbance of croconate dianion during the photolysis was 0.60, so that the quantum yield for polymerization of acrylamide is

$$\phi = \frac{1.3\times10^{-3} \times 0.0030 \times 6.02\times10^{23}}{2.28\times10^{15}\,(1-10^{0.60})}$$

$$=1400$$

The rates of polymerization of acrylamide as a function of the concentration of additives 4-nitrobenzylbromide and biacetyl in aqueous solution are shown in Figures 4.1 and 4.2 respectively. The rates expressed in these figures were corrected for polymerization in the absence of croconate dianion. With each additive the rate approached a plateau value, indicating a limiting efficiency in the photoproduction of radicals. The maximum concentration of 4-nitrobenzylbromide was limited by its solubility in water. The dependence of the polymerization rate on the concentration of 4-nitrobenzylchloride was not studied because the solubility of this additive in water is very small. The rate of photopolymerization measured at a concentration corresponding to the plateau value for 4-nitrobenzylbromide (within the limitation of the solubility) and for 4-nitrobenzylchloride near the limit of its solubility (1.6×10^{-4} M) is shown as a function of the pH of the solution in Figure 4.3. Figure 4.4 shows the rate of polymerization as a function of pH for the additive biacetyl.

According to the mechanism described in the introduction the rate of polymerization

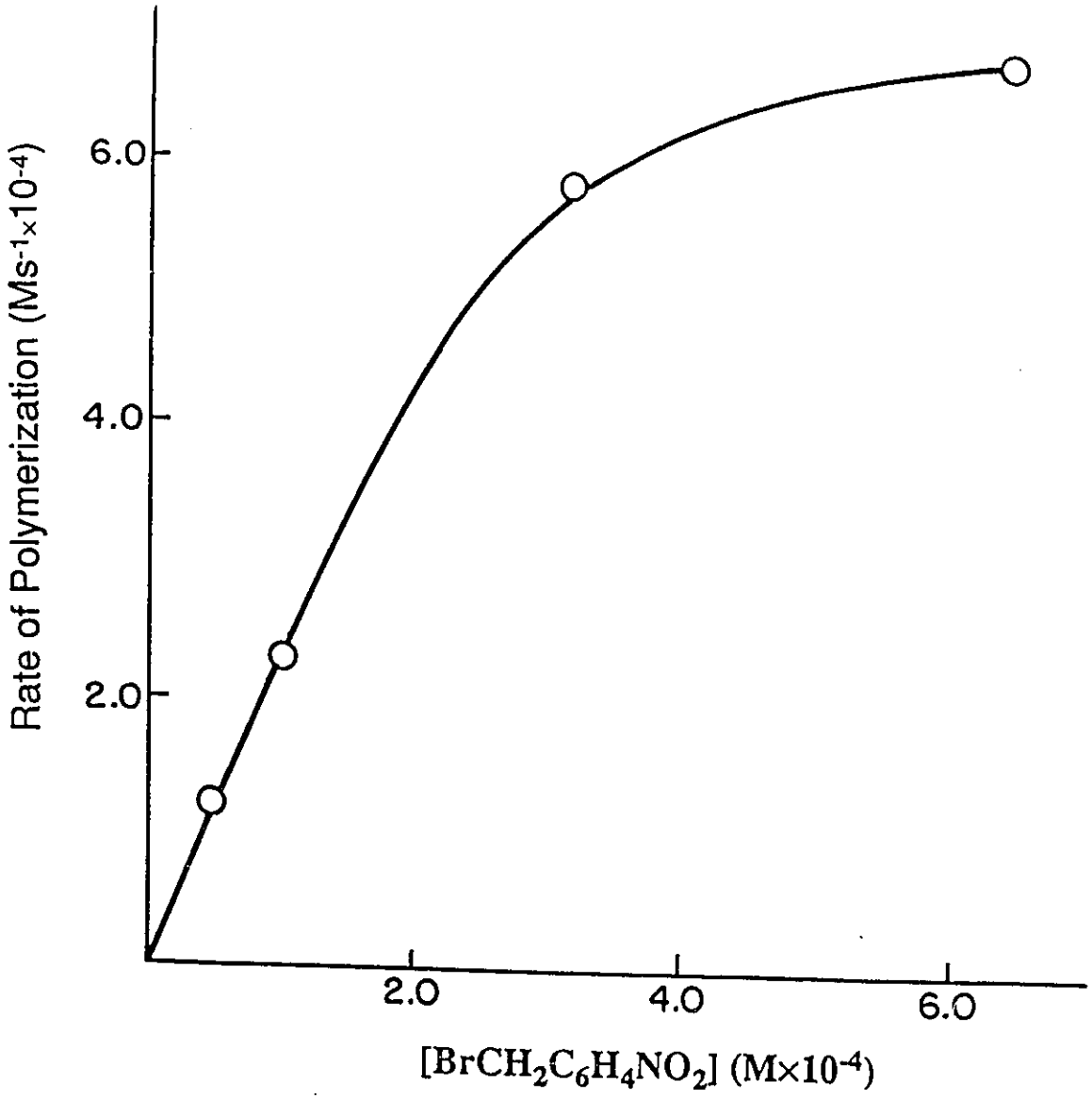

Figure 4.1 The rate of polymerization as a function of the concentration of 4-nitrobenzylbromide.

[Monomer]=1.0 M; $[C_5O_5^{2-}]=2.3\times10^{-5}$ M; aqueous solution.

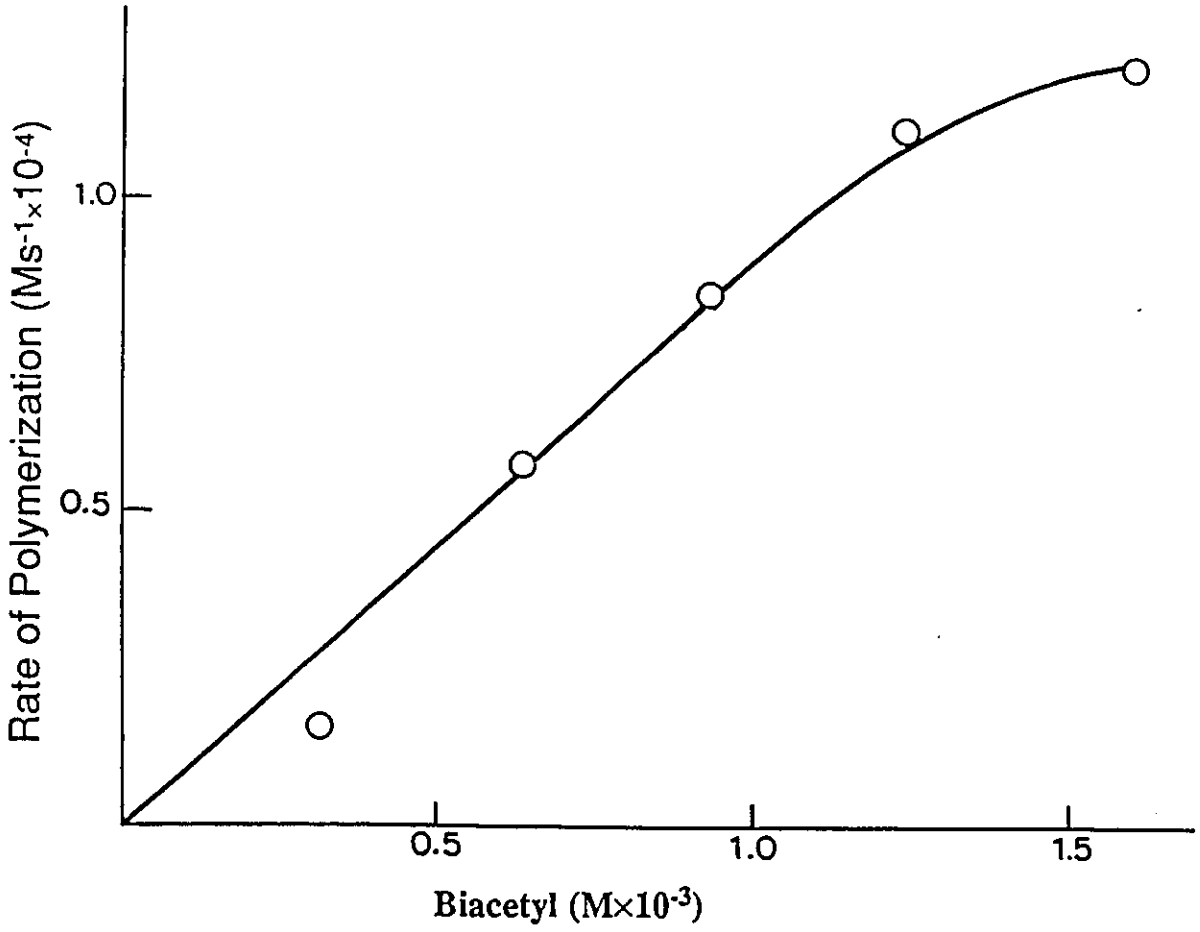

Figure 4.2 The rate of polymerization as a function of the concentration of biacetyl

[Monomer] = 1.0 M; $[C_5O_5^{2-}] = 2.3\times10^{-5}$ M; aqueous solution.

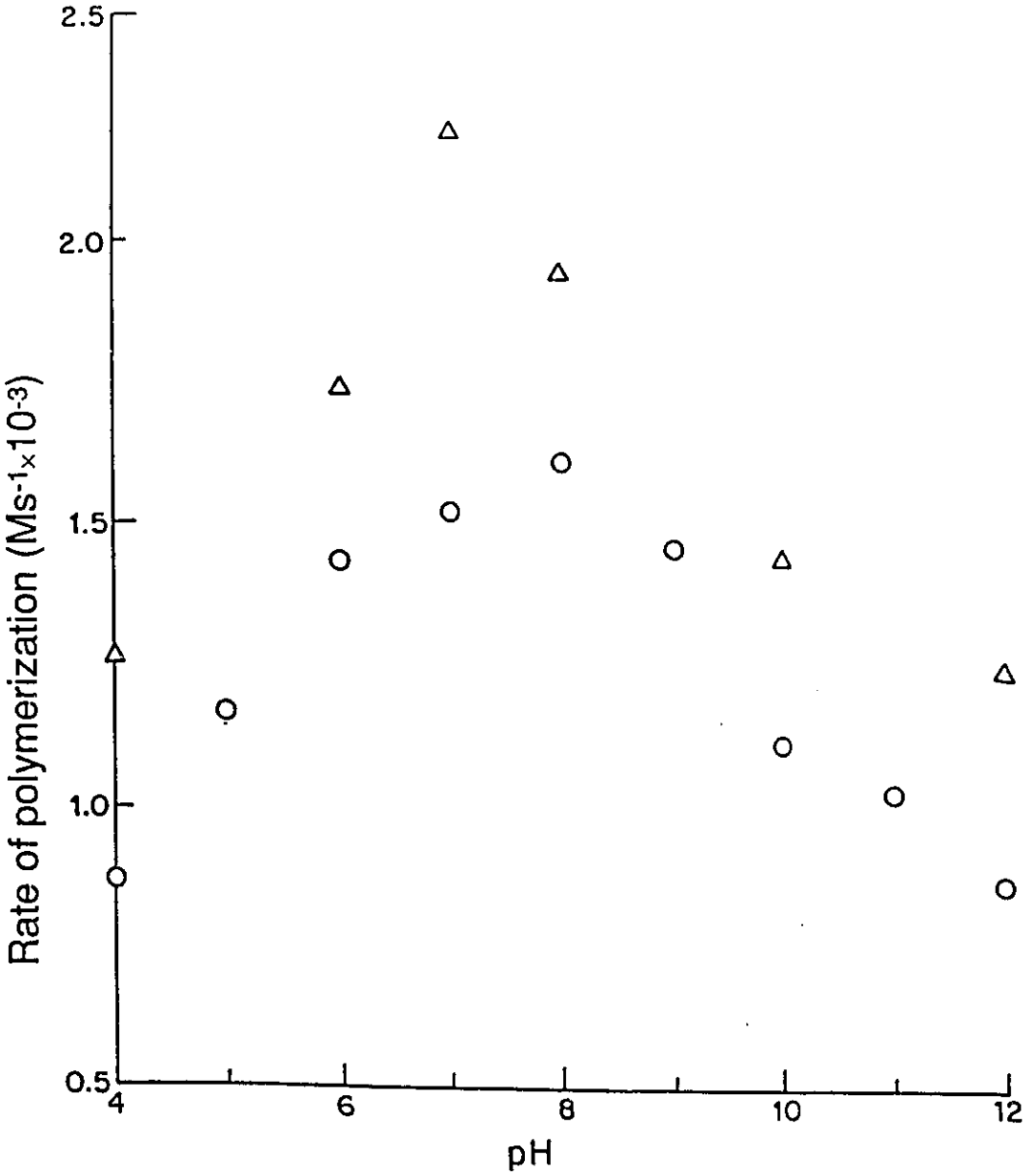

Figure 4.3 The rate of polymerization as a function of the pH of the solution for the additives 4-nitrobenzylhalides. [Monomer] = 1.0 M; $[C_5O_5^{2-}] = 2.3\times10^{-5}$ M.

Δ: [4-nitrobenzylchloride] = 1.6×10^{-4} M; o: [4-nitrobenzylbromide] = 6.4×10^{-4} M

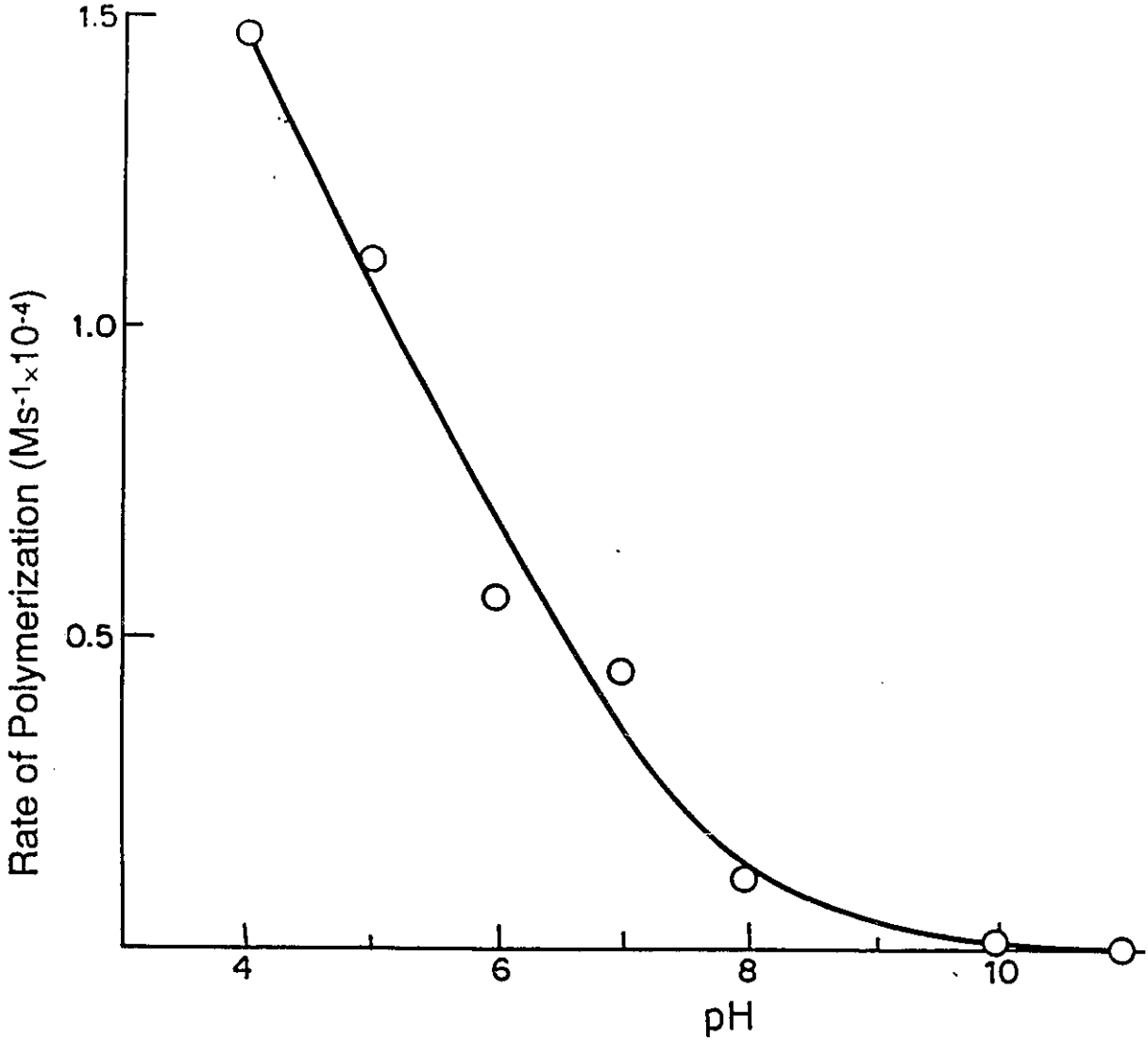

Figure 4.4 Rate of polymerization as a function of the pH of the solution for the additive biacetyl

[Monomer] = 1.0 M; $[C_5O_5^{2-}]$ 2.3×10^{-5} M; [Biacetyl] = 6.4×10^{-4} M

may be expressed as:

$$R_p = k_p\left(\frac{\phi_R I_{abs}}{k_t}\right)^{1/2}[M]$$

The quantum yield for polymerization is

$$\phi = \frac{R_p}{I_{abs}}$$

and thus may be expressed as:

$$\phi = k_p\left(\frac{\phi_R}{I_{abs}\, k_t}\right)^{1/2}[M]$$

The rate of polymerization using 4-nitrobenzylbromide as a function of the square root of the light intensity absorbed by croconate dianion at two monomer concentrations is shown in Figure 4.5. The results show that the rate of polymerization is proportional to the square root of light intensity absorbed by the croconate dianion when the concentrations of additive and monomer are fixed.

The quantum yield of polymerization is shown as a function of the concentration of monomer in Figure 4.6 using 4-nitrobenzylbromide as additive. In the range of pH 6--8, where the rate is a maximum, the quantum yield is a linear function of the concentration of monomer. The rates of polymerization presented in both Figures 4.5 and 4.6 were corrected for the rate of polymerization measured in the absence of croconate dianion. It was observed that the rate of polymerization in the absence of croconate dianion was a linear function of the relative incident light intensity, with constant concentration of reactants. The mechanism for this polymerization is not known and was not further investigated since the correction was small.

The average molecular weight of the polymers formed using the additives

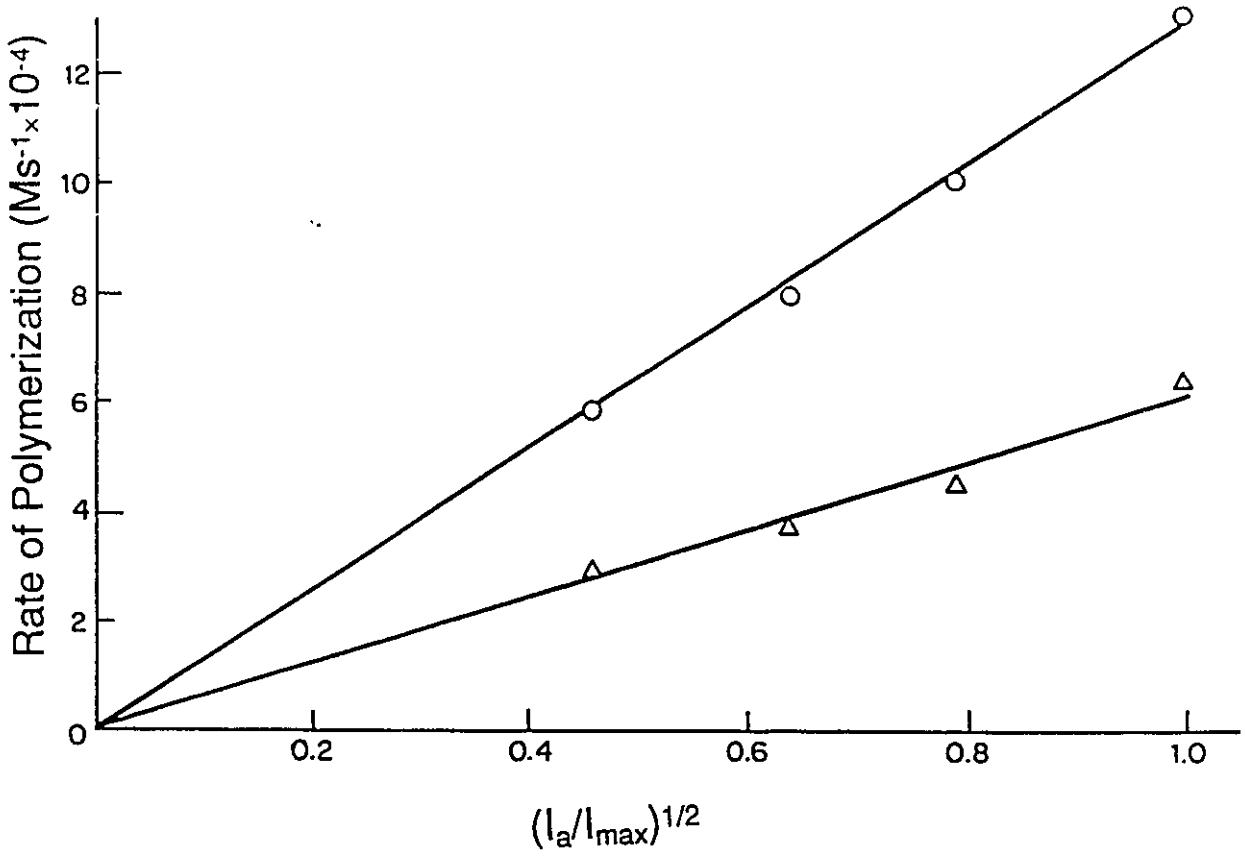

Figure 4.5 The rate of polymerization as a function of the square root of the relative rate of light absorption by the croconate dianion.

[4-nitrobenzylbromide] = 6.4×10^{-4} M; $[C_5O_5^{2-}] = 2.3 \times 10^{-5}$ M; pH = 8

0: [Monomer] = 1.0 M; Δ: [Monomer] = 0.5 M

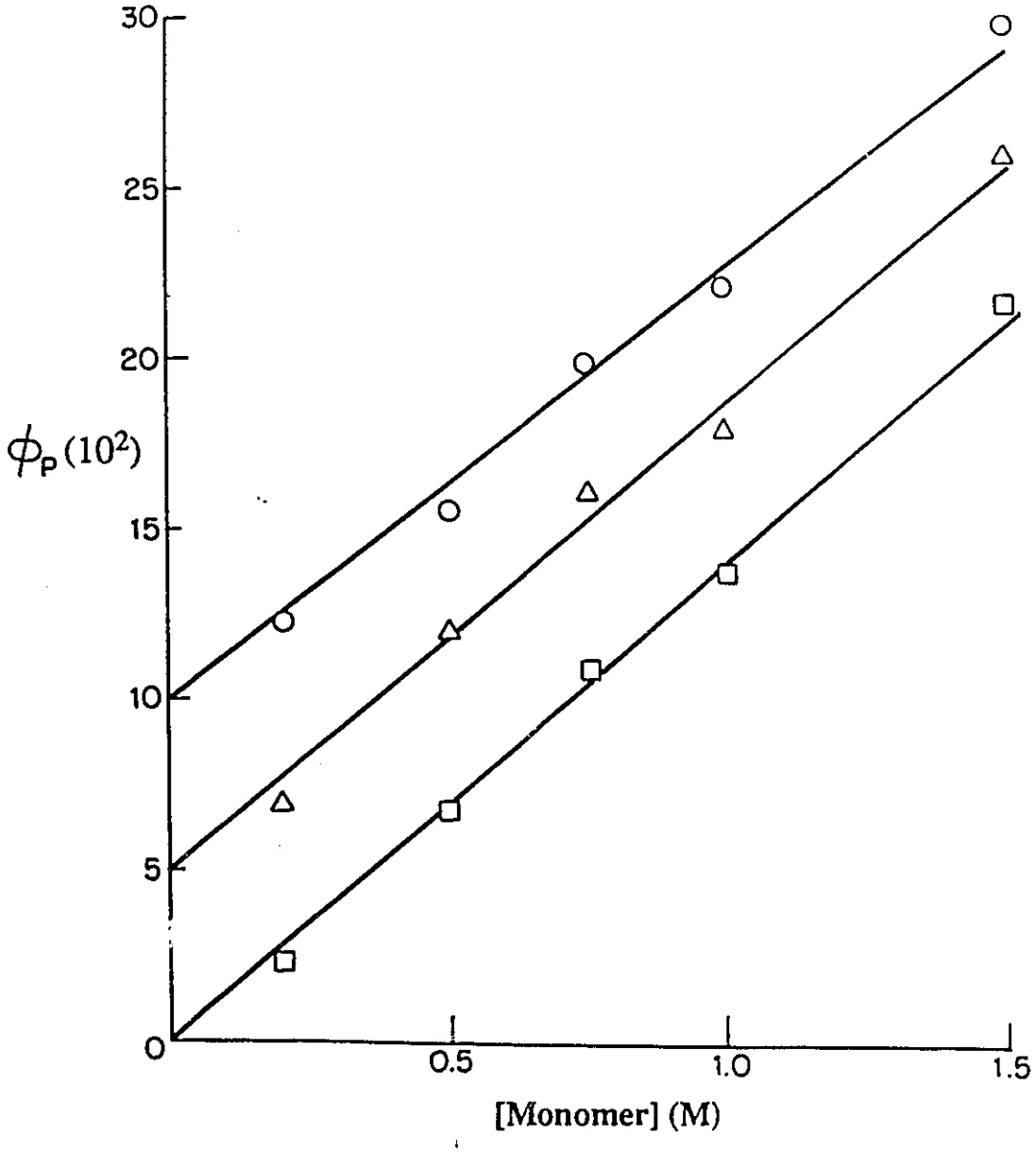

Figure 4.6 The quantum yield for polymerization as a function of the concentration of monomer

For clarity the x-axis has been displaced upwards by 500 units for pH 7

and by 1000 units for pH 6. o: pH 6; Δ: pH 7; □: pH 8

4-nitrobenzylbromide, 4-nitrobenzylchloride and biacetyl under the conditions of maximum rate was obtained from the viscosity measurements using the parameters measured by Collinson, Dainton and McNaughton as follows:[117]

$$[\eta] = 6.8\times10^{-4}\,(\bar{M})^{0.66}$$

where $[\eta]$ is the intrinsic viscosity. The experimental results of the viscosities for the three polymers at different concentrations as well as their intrinsic viscosities are presented in Table 4.4. The plots of specific viscosities η_{sp} as a function of polymer concentration (g/100mL) for three polymers are shown in Figure 4.7. The calculation of the molecular weight of the polymer obtained in the presence of the additive 4-nitrobenzylbromide is shown below as an example. The intrinsic viscosity of the polymer solution is 3.03, therefore

$$3.03=6.8\times10^{-4}(\bar{M})^{0.66}$$

$$0.66\log\bar{M}=\log\frac{3.03}{6.8\times10^{-4}}$$

$$\bar{M}=3.4\times10^{5} \qquad g\ mol^{-1}$$

The molecular weights of polymers obtained by viscosity measurement are presented in Table 4.5.

4.4 Discussion

The kinetics of the polymerization of acrylamide initiated by the photolysis of croconate dianion in the presence of electron acceptors provides good evidence that polymerization proceeds by the general mechanism for radical polymerization with photoinitiation, where the rate of generation of radicals is proportional to the light absorbed and termination occurs by bimolecular combination of radicals. As an example, the initial reactions in the presence of 4-nitrobenzylbromide may be expressed as:

Table 4.4 Measurement of Viscosity of Polymers

t_0 =233.0 Sec.

C (g/100mL)	t (Sec.)	t/t_0	$[\eta_{sp}]$	$[\eta]$
$BrCH_2C_6H_4NO_2$				3.03
0.512	911.0	3.91	5.68	
0.410	721.5	3.10	5.11	
0.308	563.0	2.42	4.60	
0.206	429.0	1.84	4.08	
0.104	320.0	1.37	3.59	
0.052	273.0	1.17	3.30	
$ClCH_2C_6H_4NO_2$				3.70
0.407	796.5	3.42	5.95	
0.305	613.0	2.63	5.37	
0.208	467.0	2.00	4.85	
0.104	335.5	1.44	4.27	
0.052	281.0	1.21	3.96	
Biacetyl				3.10
0.440	759.5	3.26	5.49	
0.330	609.0	2.61	4.89	
0.224	558.0	2.39	4.31	
0.112	330.0	1.42	3.72	
0.056	278.0	1.19	3.45	

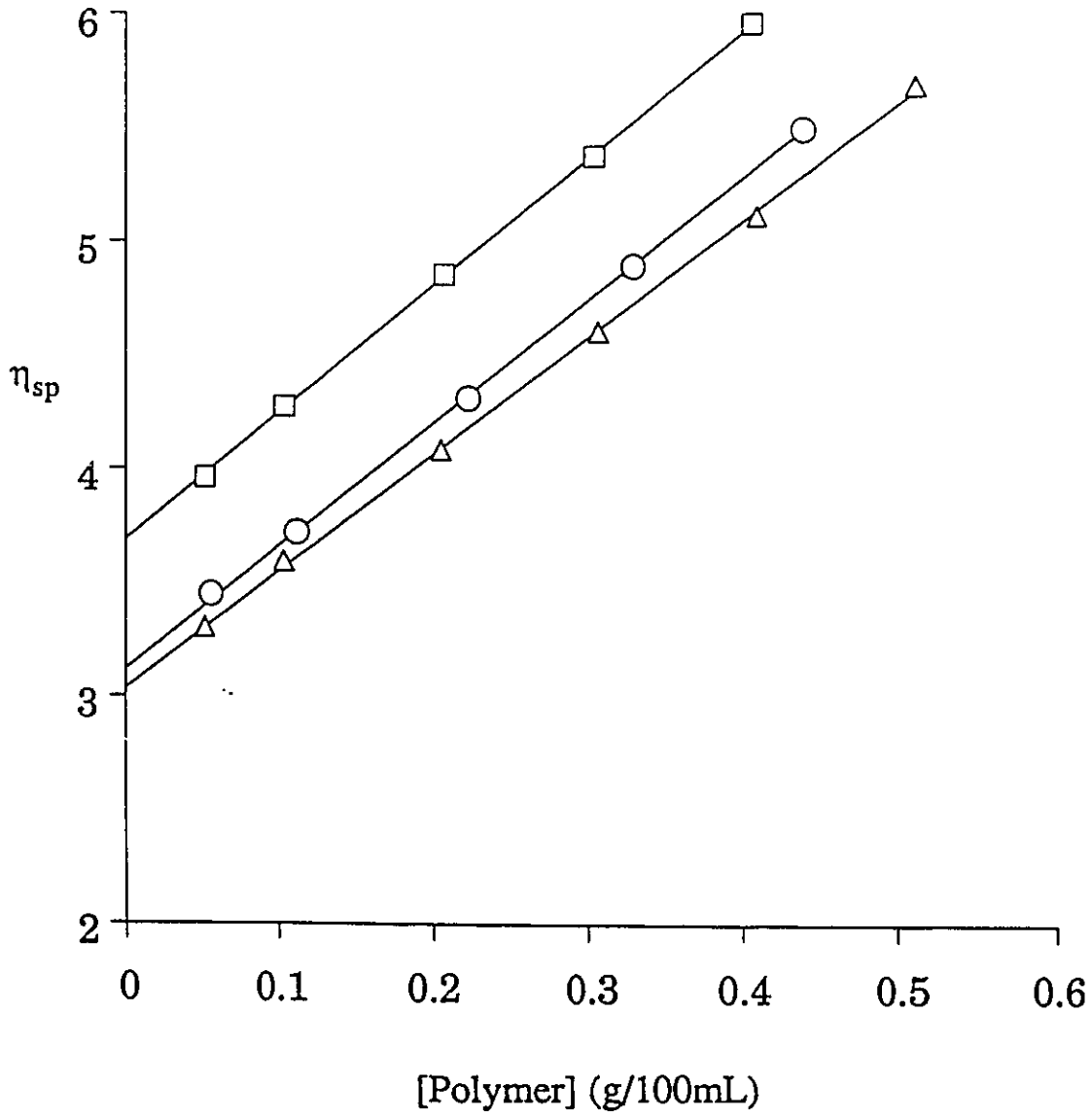

Figure 4.7 Specific viscosity as a function of concentration of polymer

Additives: □: $ClCH_2C_6H_4NO_2$; o: Biacetyl; △: $BrCH_2C_6H_4NO_2$.

Table 4. 5

Molecular Weight of Polymers Obtained Using Different Additives

$[ClCH_2C_6H_4NO_2] = 3.2\times10^{-4}$ M

$[BrCH_2C_6H_4NO_2] = 6.4\times10^{-4}$ M

[Biacetyl] = 6.4×10^{-4} M

Additive	R_P (Ms^{-1})	R_i (Ms^{-1})	ϕ_R	Molecular Weight of Polymer (g/mol.) $71.08\times R_p/R_i$	Viscosity Measurem.
$ClCH_2C_6H_4NO_2$	2.2×10^{-3}	4.2×10^{-7}	0.350	3.7×10^5	4.6×10^5
$BrCH_2C_6H_4NO_2$	1.52×10^{-3}	2.00×10^{-7}	0.167	5.4×10^5	3.4×10^5
Biacetyl	1.47×10^{-4}	4.2×10^{-9}	3.5×10^{-3}	2.5×10^6	3.5×10^5

Reaction condition: For 4-nitrobenzylhalides, at pH 7; for biacetyl, at pH 4.

$$C_5O_5^{2-} + h\nu \rightarrow C_5O_5^{2-*}$$

$$C_5O_5^{2-*} + BrCH_2\text{-}C_6H_4\text{-}NO_2 \rightarrow C_5O_5^{-} + {}^{\cdot}BrCH_2\text{-}C_6H_4\text{-}NO_2$$

$${}^{\cdot}BrCH_2\text{-}C_6H_4\text{-}NO_2 \rightarrow {}^{\cdot}CH_2\text{-}C_6H_4NO_2 + Br^-$$

The radical ${}^{\cdot}CH_2\text{-}C_6H_4\text{-}NO_2$ is capable of initiating polymerization of acrylamide through chain reactions.

The results in Figure 4.5 show that the rate of polymerization of acrylamide initiated by the photolysis of croconate dianion is a linear function of $[I_a]^{1/2}$ demonstrating that the termination of radical chain growth is through a biradical combination process. The absorbed intensity in Figure 4.5 is expressed as a relative value I_a/I_{max}, where I_{max} is the absorbed intensity by croconate dianion at the maximum intensity of the lamp. The intensity dependence was measured at two concentrations of acrylamide, 1.0 M and 0.5 M respectively. The slope of the plots in Figure 4.5 is

$$k_p\left\{\frac{\phi_R\, I_a}{k_t}\right\}^{1/2}[M]$$

The values of the slope at a monomer concentration of 0.5 M is 6.04×10^{-4} Ms^{-1} and is 1.29×10^{-3} Ms^{-1} at a monomer concentration of 1.0 M. The fact that the values of the two slopes are different by a factor of two is evidence that the rate of the polymerization of acrylamide is linearly dependent on the concentration of monomer.

Figure 4.6 provides further results to show that the quantum yield of polymerization of acrylamide is linearly dependent on the concentration of monomer. Linear regression analysis of the results in Figure 4.6 (correlation coefficient > 0.997) indicates that the slopes,

$$k_P\left\{\frac{\phi_R}{I_a k_t}\right\}^{1/2}$$

increase from 1300 M^{-1} at pH 6 to 1400 M^{-1} at pH 7 and 1450 M^{-1} at pH 8. The results of Currie, Dainton and Watt[118] showed that the ratio $(k_p/k_t^{1/2})$ increased about 5% between pH 6 and pH 8. Although this is somewhat less than the 12% increase observed in the slope from pH 6 to 8, the combined uncertainty in both the present and previous results suggests that the variation in $(k_p/k_t^{1/2})$ is sufficient to account for the present trend, noting that I_a was constant in these experiments.

If no chain transfer occurs with either the croconate monoanion or additive radicals then the ratio of the rate of polymerization (R_p) to the rate of radical formation (R_i), $R_p(gL^{-1}s^{-1})/R_i(Ms^{-1})$, gives directly the average molecular weight ($gmol^{-1}$) of the polymer. The rate of initiation of polymerization is:

$$R_i = \left\{\frac{R_P}{(k_p/k_t^{1/2})\,M}\right\}^2$$

Using the values for $(k_p/k_t^{1/2})$ at 25^0 C measured by Currie, Dainton and Watt of 3.5 $M^{-1/2}s^{-1/2}$ at pH 4 and 3.4 $M^{-1/2}s^{-1/2}$ at pH 7, the value of R_i can be calculated once the rate of polymerization and the reaction conditions are known. For example, the rate of polymerization with 4-nitrobenzylbromide concentration of 6.4×10^{-4} M and at pH 7 is 1.52×10^{-3} Ms^{-1}. Therefore the rate of initiation under these conditions can be calculated as:

$$R_i = \left\{\frac{1.52\times10^{-3}}{3.4\times1.0}\right\}^2$$

$$= 2.00\times10^{-7}\ Ms^{-1}$$

Some results of R_i for three polymerization reactions are presented in Table 4.5.

The molecular weight of the polymer obtained with 4-nitrobenzylbromide under the same conditions is therefore

$$M_w = \frac{R_P}{R_i} \times 71.08$$

$$= \frac{1.52\times10^{-3}}{2.00\times10^{-7}} \times 71.08$$

$$= 5.4\times10^{5}\ gM^{-1}$$

where the value of 71.08 is the molecular weight of acrylamide. Values of the calculated molecular weight of three polymers based on the rate of polymerization are given in Table 4.5.

For the 4-nitrobenzylhalides the calculated average molecular weight is in reasonable agreement with the measured molecular weight and for these additives chain transfer is not an important reaction in the polymerization process. With biacetyl the calculated average molecular weight is 7 times higher than the measured value. With this additive therefore chain transfer makes an appreciable contribution at a concentration of biacetyl of 6.4×10^{-4} M. Table 4.5 shows that even though the average molecular weight obtained with biacetyl from viscosity measurement is similar to those with the 4-nitrobenzylhalides the rate of initiation in the presence of biacetyl is much slower, leading to a higher value for the ratio of R_p/R_i. This low rate of initiation is in accordance with the results of the photolysis of croconate dianion in the presence of biacetyl.

The quantum yield for the production of radicals can be obtained from the equation $R_i=\phi_R I_a$, and therefore is:

$$\phi_R = \frac{R_i}{I_{abs}}$$

The calculated quantum yields, ϕ_R, for the three polymers in the presence of additives 4-nitrobenzylchloride, 4-nitrobenzylbromide and biacetyl are presented in Table 4.5. For example, from the rate of initiation of polymerization in the presence of biacetyl at pH 4, the quantum yield for the production of radicals is:

$$\phi_R = \frac{R_i}{I_a} = \frac{4.2\times10^{-9}}{1.2\times10^{-6}} = 3.5\times10^{-3}$$

The quantum yield for the loss of croconate dianion in the photolysis experiment in aqueous solution should not exceed this value. In acid solution the quantum yield for loss of croconate dianion in the presence of biacetyl was too small to be detected. For the 4-nitrobenzylhalides, ϕ_R is larger than the quantum yield for disappearance of croconate dianion in neutral solution. This indicates that without monomer present, loss of radicals by recombination must be important.

There was no indication that the acrylamide quenched the excited croconate dianion. Although the energy level of the triplet state of the croconate dianion is not known, the difference in energy between the first absorption bands of croconate dianion and of acrylamide (<270 nm) suggests that quenching of the triplet excited state of croconate dianion by acrylamide is energetically very unfavorable.

The quantum yield for loss of croconate dianion increased with increasing pH and at pH 12 approached a value of one with the additive 4-nitrobenzylbromide and biacetyl and somewhat lower values with other additives. In contrast, the quantum yield for polymerization with the additives 4-nitrobenzylbromide and 4-nitrobenzylchloride reached a maximum at pH 7--8 and declined in more basic solution (Figure 4.3). With biacetyl the quantum yield declined steadily with increasing pH. It should be pointed out that these effects of pH on the rate of polymerization are much greater than the small change in the

ratio($k_p/k_t^{1/2}$) for acrylamide over the pH range 4--12 observed by Currie, Dainton and Watt. It appears that the reactions leading to loss of croconate dianion, indicated by the reactions [4], [5], [8] and [9] in chapter 3 are not all preceded by the formation of radicals free to diffuse throughout the solution. As the pH value is increased, reaction with hydroxyl ion, reaction [6], becomes dominant, leading to the formation of the exciplex $(C_5O_5^{2-}...OH^-)^*$ as the major primary reaction product. Thus at higher pH the reaction with hydroxyl ion becomes the main process for the loss of croconate dianion instead of reaction with the additive leading to the formation of radicals. As well, increasing the pH can also inhibit the formation of radicals through reaction [4].

The rate of initiation of radicals in the presence of additive may be equated to the rate of reaction [3]. A steady-state treatment of the mechanism in chapter 3 led to the following expression for the quantum yield for the generation of radicals:

$$\phi_3 = 2\left[\frac{k_1[A]}{k_D + k_1[A] + k_6[OH^-]}\right]\left[\frac{k_3}{k_2 + k_3 + k_4[OH^-]}\right]$$

This expression reflects the rate of radicals produced from the electron transfer reaction, both the croconate monoanion radical and the radical formed from the additive by accepting one electron from the excited croconate dianion. Using the values of the rate constants for 4-nitrobenzylbromide in Table 3.7, the quantum yields for the production of radicals (ϕ_3) at pH 6--10 are summarized in Table 4.6. These values may be compared to the quantum yields for production of radicals, ϕ_R, obtained from the rate of polymerization, as described earlier. Values for ϕ_R with the additive 4-nitrobenzylbromide at different pH values are also given in Table 4.6. Quantum yields calculated from the equation above for ϕ_3 are roughly a factor of two larger than the corresponding quantum yields calculated from the rate of polymerization, ϕ_R. This suggests that only one radical formed from the electron

Table 4. 6

Rate of Initiation and Quanum Yield for Production of Radicals

$[BrCH_2C_6H_4NO_2] = 6.4\times10^{-4}$ M

pH	R_P (Ms^{-1})	R_i (Ms^{-1})	ϕ_R	ϕ_3
6	1.43×10^{-3}	1.77×10^{-7}	0.148	0.348
7	1.52×10^{-3}	2.00×10^{-7}	0.167	0.346
8	1.61×10^{-3}	2.24×10^{-7}	0.187	0.338
9	1.46×10^{-3}	1.84×10^{-7}	0.153	0.264
10	1.11×10^{-3}	1.07×10^{-7}	0.089	0.080

transfer reaction functions as an initiator for polymerization.

In the initial electron transfer from the excited croconate dianion, two radicals are formed, the croconate monoanion radical and the radical formed by the acceptance of the additive. If the croconate monoanion radicals were effective in polymerization of acrylamide, then we would expect the polymerization reaction would take place with each additive. This, however, was not the case. Polymerization occurred only in the presence of the additives biacetyl and 4-nitrobenzylhalides. It must be concluded that the croconate monoanion radical is not effective in polymerization. It follows that the anion radical formed through the electron transfer to the acceptor is the radical which induces polymerization. The 4-nitrobenzylbromide is a typical example of an anion radical which releases a neutral radical following electron transfer:

$$BrCH_2C_6H_4NO_2^{\cdot-} \rightarrow Br^- + \cdot CH_2C_6H_4NO_2$$

The efficiency of biacetyl in promoting polymerization seems surprising unless the biacetyl anion has sufficient energy to undergo dissociation,[119]

$$CH_3COCOCH_3^{\cdot-} \rightarrow CH_3CO^- + CH_3CO\cdot$$

and release a radical to the solution, so that the polymerization reaction may take place.

On the other hand, the results show that the monocation of methyl viologen, $MV^{+\cdot}$ does not initiate polymerization of acrylamide. This observation was also reported by Iwai, Uesugi and Takemura in their study of the photopolymerization of acrylamide using tris(2,2'-bipyridine)rhuthenium as sensitizer[110].

The reason for the lack of reactivity of the croconate monoanion is not readily apparent but might suggest that the monoanion retains a high degree of delocalization, making a less reactive radical center.

Chapter 5

Laser Flash Photolysis

5.1 Introduction

The quenching of an excited state by energy transfer or by electron transfer are two most important processes for photoinduced chemical reactions:

$$M^* + Q \rightarrow M + Q^*$$

$$M^* + Q \rightarrow M^{\mp} + Q^{\pm}$$

These two processes are conceptually related.[120-123] In both cases, spatial overlap of donor and acceptor orbitals is required, no bond-making or breaking process takes place, and Franck-Condon restrictions must be obeyed because electronic rearrangement (energy transfer) or the net transfer of an electron occurs in a time that is short compared to that required for nuclear motion. When both processes are thermodynamically allowed, which one will dominate? This is a question that has been difficult to answer in most cases. There is not enough experimental data to derive a concrete criterion to determine which one will dominate. Nevertheless some general considerations have been suggested.[124] When both energy transfer and electron transfer are thermodynamically allowed, it seems electron transfer process will predominate. This may be because for an energy transfer process, favorable and simultaneous overlap of orbital pairs HOMO-HOMO and LUMO-LUMO of the donor and acceptor couple is required, whereas such a criterion is less stringent for electron transfer process where only one such overlap is required. It should be noted that the formation of an excited quencher or of a quenching product is not a proof of an energy-transfer quenching, because the primary electron transfer quenching product M^- and Q^+(or M^+ and Q^-) could undergo subsequent reaction to yield M and Q^*.[61]

Photoinduced electron transfer to form radical ions is now well established as an important mechanism for product formation in photochemistry.[125] The overall quantum yields for these radicals vary over a wide range. The determination of intermediates in electron transfer reactions and measurement of the kinetics of the reactions of these intermediates are very important in understanding reaction mechanisms. Some experimental techniques commonly used in detecting electron transfer intermediates are described in the following sections.[126-129]

5. 1. 1 Flash Photolysis

In many cases, short-lived transients formed during a photochemical reaction can be detected spectroscopically by flash photolysis.[128-129] A conventional low-speed flash photolysis using a high energy xenon flash lamp is suitable only for detecting relatively long-lived transients, such as free radicals, with a time scale of milli or microsecond. Use of lasers with narrow pulse width as flash sources enables one to expand the detection of transient intermediates into the nanosecond range. Measurement of the lifetime of short-lived radicals and triplet excited states becomes possible. Using the picosecond time domain laser flash photolysis enables the measurement of the kinetics of very fast chemical or physical reactions, such as fluorescence, or isomerization reactions.

Measurement of spectra using flash photolysis techniques is divided into two categories: transient spectroscopy and kinetic spectroscopy. Transient spectroscopy is concerned with the absorption spectrum of the intermediate. Usually the absorbance of the transient is recorded at a number of wavelengths using a fixed time window. Since the region of absorption of the transient and the precursor frequently overlap the measurement of the transient absorbance is recorded as a difference between the total absorbance and the absorbance of the precursor.

Kinetic spectroscopy refers to the measurement of the kinetics of the transient following the laser flash, either decay or growth. If the transient formed during the laser pulse produces a detectable change in a physical property and this change is proportional to the transient concentration, then the kinetics of the transient can be obtained by monitoring this physical property as a function of time. If the primary photolysis product does not exhibit a conveniently-measurable absorbance, but one of its reaction products does, the growth kinetics of the signal-producing transient can be used to provide information about the kinetics leading to its formation, as well as other modes of decay of its precursor. Both decay and growth kinetics have been studied in the present experiment. The rate expressions for both decay and growth kinetics will be derived later.

Radicals formed through the electron transfer reaction following the laser pulse may be detected by absorption, fluorescence, resonance Raman spectroscopy, or conductivity measurements.[126, 130] Among these techniques, detection by absorption is the most widely used. In the present study, because the radical formed has a fairly strong absorption in the visible region, all measurements were obtained using detection by absorption.

5.1.2 ESR

Electron Spin Resonance (ESR) can be used to detect the presence of ion radicals resulting from electron transfer. Radicals can be defined as species capable of independent existence that contain one or more unpaired electrons, so that the species is paramagnetic, is attracted slightly to a magnetic field and thus can be detected by ESR. These species sometimes are highly reactive. Radicals can easily be formed when a covalent bond is broken if one electron from each of the shared pair remains with each atom (homolytic fission). The energy required by dissociation of the covalent bond may be provided by heat, or by electromagnetic radiation.[126]

ESR can detect radicals at concentration as low as 10^{-10} mol L^{-1} but the radicals must have a lifetime sufficiently long to be measured. For measurement of short lived radicals, several approaches can be employed to make the radical detectable.

a) Use of a flow system, whereby the radicals are continuously generated in the spectrometer so as to maintain a steady-state concentration.

b) Generation of radicals in a frozen transparent solid matrix which prevent them from colliding with other species and undergoing reaction. By allowing the matrix to warm up, reactions of the radicals can be observed.

c) Trapping a highly reactive radical, which is difficult to observe by normal ESR, by reaction with a compound to produce a long-lived radical which can be detected by normal ESR.

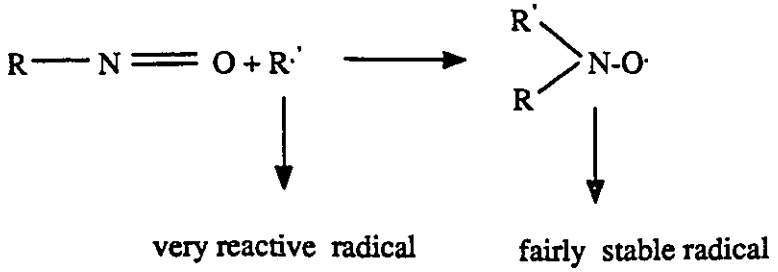

Nitroso compounds (-R-N=O) and nitrones ($R=N^{+}-O^{-}$) are two types of the most widely used spin trapping materials

5. 1. 3 Radical trap

In some cases, certain reactants can be added to the reaction system to capture the newly generated radicals.[77] By observing changes in chemical or physical properties of the reactant information on the generation of radicals in the reaction system may be obtained. Use of this technique was described in Chapter 3, where the radical trap DPPH

was added to the solution of croconate dianion. The change in the concentration of DPPH was measured and used to estimate the formation of croconate monoanion radical qualitatively.

The results described in Chapter 2 and 3 established that the first step of the reactions between the excited dianions and suitable electron acceptors was an electron transfer process. Studies on the kinetics of the steady state photolysis experiments, use of DPPH as a radical trap and polymerization of acrylamide initiated by the photolysis of the dianions have shown that radicals were generated during the photochemical reaction. In order to detect directly the presence of the intermediate monoanion radicals and to study the kinetics of the reactions of the radicals in solution, laser flash photolysis experiments were performed. Absorption of the croconate monoanion radical was detected and its lifetime was measured. The lifetimes of excited states of both dianions were determined by measuring the rate of recovery of the ground state of each dianion.

5.2 Experimental

5.2.1 Flash Photolysis Apparatus

Most of the laser flash photolysis experiments were performed at the Sussex Drive Laboratories of the National Research Council of Canada. A description of the laser flash photolysis system employed in the present study is given.[131-133] A diagram of the arrangement of the photolysis apparatus is shown in Fig. 5.1

(1) Excitation source

Samples were excited with a single laser pulse from either a Molectron UV-24 nitrogen laser (8--10 ns, 337.1 nm, ~10 mJ/pulse), or a Candela 500 M dye laser which with

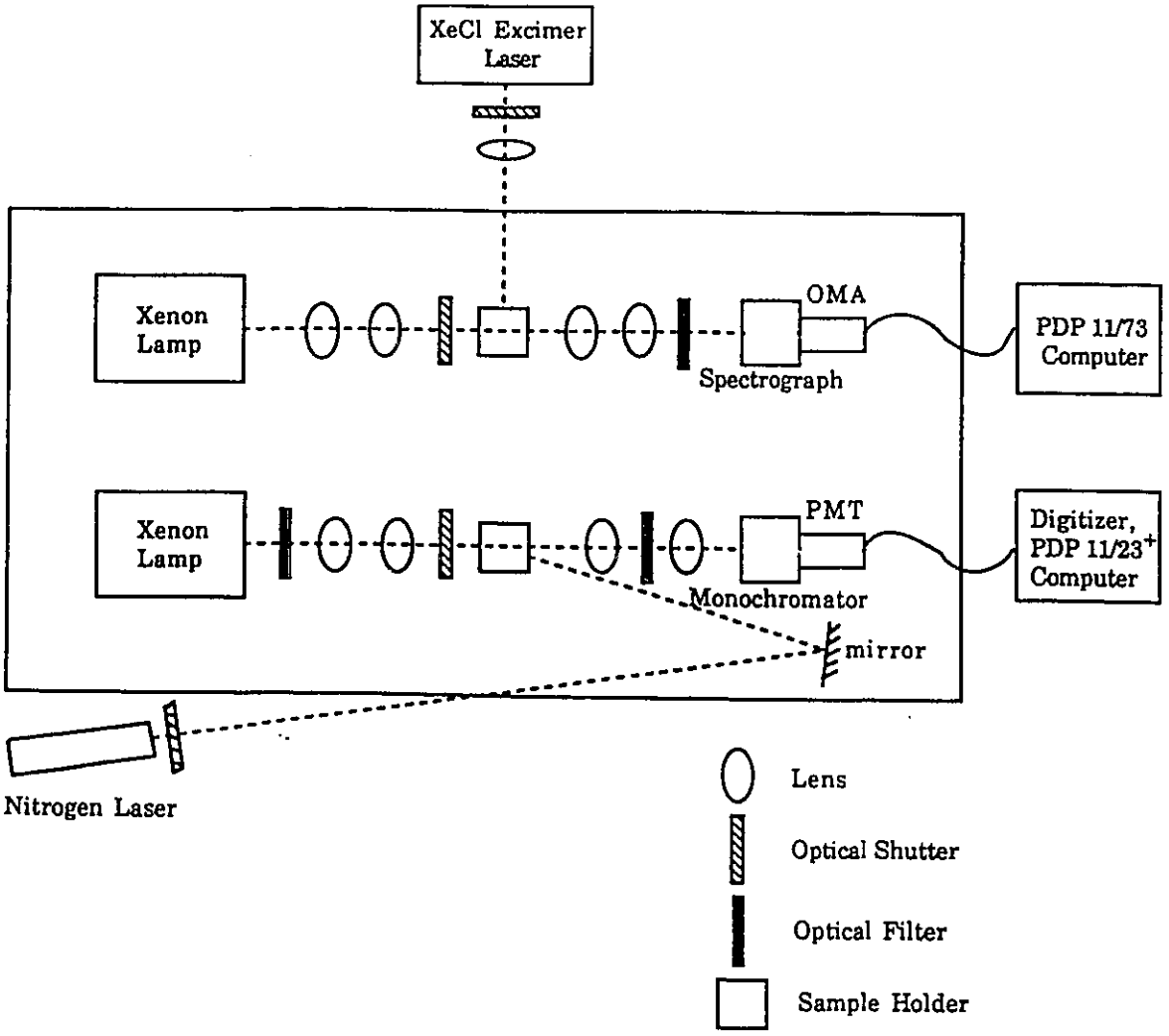

Figure 5.1 Arrangement of the Laser Flash Photolysis Apparatus

Rhodamine 6G has 200--250 ns duration and up to 2.5 J/pulse. Appropriate frequency doubling crystals make wavelengths in the 265--310 nm range available, and a pulse slicer (Model 51016 from laser Metrics) allows the time duration to be adjusted down to 10--20 ns. The excitation dose can be adjusted by using suitable neutral density filters. The pulses were concentrated (but not focussed) on the samples by a combination of spherical and cylindrical lenses. The laser beam from a nitrogen laser entered the sample at 19^0 to the monitoring beam whereas the dye laser beam is used at 80^0 with respect to the monitoring beam. The use of the small-angle approach for the nitrogen laser beam allowed a minimized sample volume to be irradiated and gave a high signal to noise ratio. The pulsed lasers were operated at a frequency of 1 Hz continuously. This regular pulsing leads to a very reproducible pulse energy. Shutters were placed before the lasers and were controlled by computer to allow the selection of one laser pulse for the experiment.

(2) Detection System

Under the irradiation of a reproducible laser pulse, transients are generated from the light-induced reaction in the cell and the concentration of the transients is proportional to their intensity of absorption or emission. The detection system at NRC was conveniently divided into two different systems based on how the signal was detected and treated.

a. Kinetic System

In this detection system, the intensity of the UV-visible absorbance of the transients at a particular wavelength (usually at one of the maxima of absorption) was measured as a function of time. The absorption of the transient changes in intensity according to its growth or decay in concentration. The monitoring system consists of a pulsed 200 watt xenon lamp as light source, a PRA-B204 monochromator, and an RCA-4840

photomultiplier tube as detector. When the sample is flashed by the laser beam, a shutter opens simultaneously to allow the monitoring beam to reach the analyzing monochromator; another command from the computer activates the xenon lamp pulser. This particular unit can also be activated when the computer is ready to gather the information. This kind of approach makes it possible to correct the traces for background and fluorescence. For example, in order to correct for the background, one activates all units except the shutter controlling the laser pulse. To correct for the fluorescence, the shutter for the monitoring beam was closed and the xenon lamp was not activated. The information gathered during these trials could be used to correct for the background and for the fluorescence. The monitoring beam was focussed on to the sample and the transmitted light from the sample cell was passed onto the monochromator; the photomultiplier transforms the light signal from the monochromator into a voltage signal which is proportional to the light intensity. The output from the photomultiplier was captured by a R7912-Tektronix transient digitizer. A tektronix 607 storage oscilloscope displays each trace stored by the digitizer and the digitizer memory was read by a PDP $11/23^{+}$ computer. This computer converted the voltage signal to a change of absorbance (Δ O.D.); finally, a decay or a growth trace of the absorption as function of time was obtained.

b. OMA System

Detection of transient signals using the Optical Multichannel Analyzer (OMA, EG. & G. 1420-1024) allows the absorbance to be measured over a range of wavelengths. As well, a luminescence emission spectrum could be obtained. The light source for detection in this system is a 150 W xenon lamp, which could be operated in a pulsed mode if needed. The optics, shutters and sample holder were the same as those used in the kinetic system, but the way of treating the data obtained from the sample was different from that of the

kinetic system. In the OMA system, the transmitted monitoring radiation was focused onto a Jarrel-Ash MonSpec27 spectrograph with a 600 grooves/inch grating blazed at 500 nm. The light was passed on to the OMA giving a set of voltage signals as a function of array channel (proportional to wavelength); these voltage signals were fed into the detector controller (EG. & G. Model 1463) and the output from the controller was transmitted to an EG. & G. Model 1461 interface. Finally, these data were read and processed by the PDP 11/73 computer and displayed as the transient absorption over the measured wavelength. The time duration for the OMA gate to be open to collect the light signal was typically 20 nanoseconds. This gate can be delayed in time from the end of the laser pulse up to 1 ms after the laser pulse in steps of 10 ns. This allows collection of transient spectra at different times after the laser fires.

Transient absorption spectra can also be obtained with the kinetic system by acquiring a transient kinetic trace at several different wavelengths and plotting the ΔO.D. for each as a function of monitoring wavelength. Since ΔO.D. is measured, the transient spectrum measures the difference between the absorption spectrum of the substrate and that of the transient. Usually ten flashes per decay were required to generate transient spectra using the kinetic system. In the present experiments this method of data acquisition provided better signal/noise because of the averaging effect. All the transient absorption spectra in the present study were obtained using the kinetic system. Fig. 5.2 is one example of the transient absorption spectrum for croconate monoanion radical obtained using this technique.

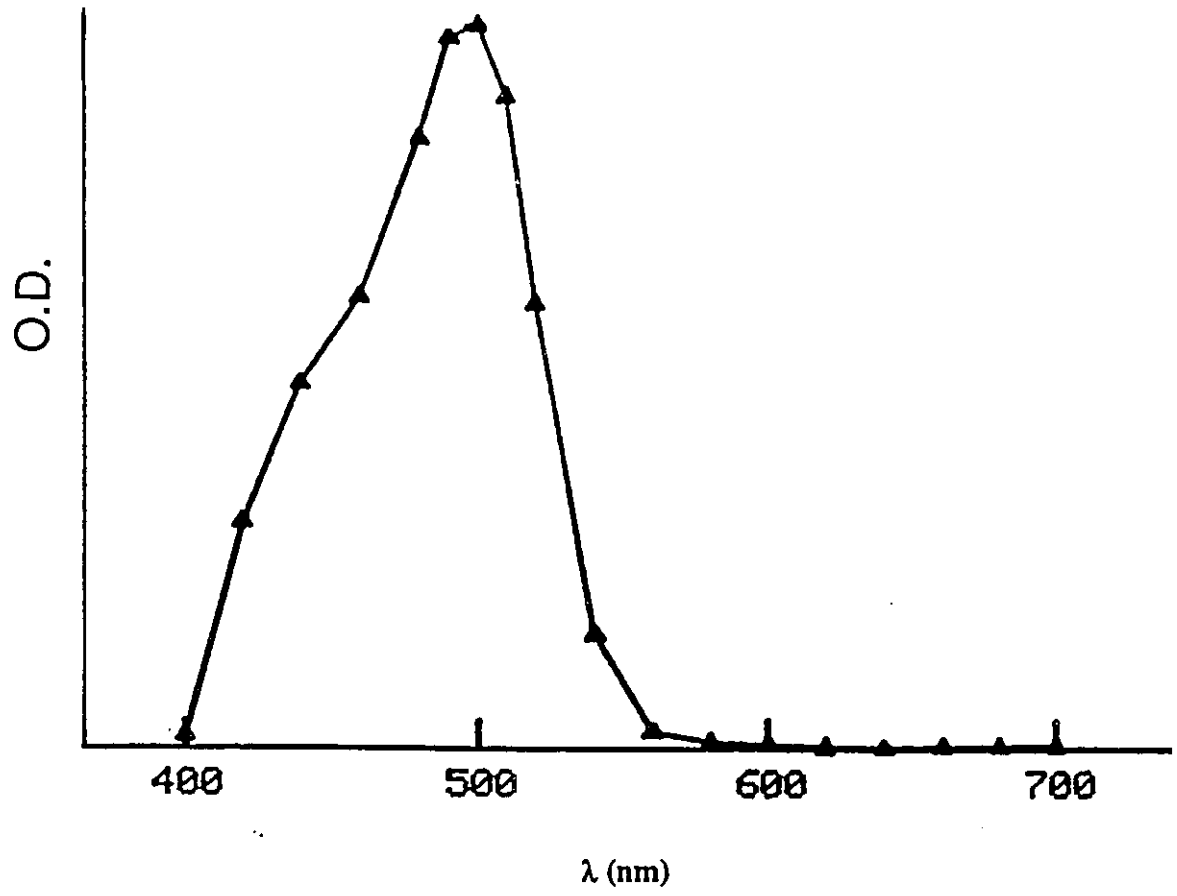

Figure 5.2 Transient Absorption of Croconate Monoanion Radical in the Presence of Biacetyl

[Biacetyl]=1.46×10^{-3} M, pH = 6.2, $\lambda_{exc.}$=337 nm, Top O. D.=0.04

5. 2. 2 Reaction System

The flash photolysis cell used in the experiments was a 7×7 mm^2 quartz flow cell connected to a 100 mL reservoir. The solutions were saturated with nitrogen gas. Buffer solutions were used for pH values other than neutral. A concentration of croconate dianion of 3.7×10^{-5} M was used for the flash photolysis experiments with excitation wavelength of 337.7 nm. In the experiments with the excitation wavelength of 335 nm, a concentration of croconate dianion of 2.7×10^{-5} M was used. These concentrations gave an absorbance of the croconate dianion at the respective excitation wavelengths of 0.70 with the 7 mm path length. The concentration of additives was increased gradually by adding concentrated additive solution to the reservoir stepwise. After each addition of the concentrated additive solution, the reaction solution in the reservoir was degassed with nitrogen for another ten minutes before the next flash photolysis measurement was performed. At each concentration of additive, the measurement of the transient kinetics was repeated to ensure that the concentration of reactants in the cell was uniform. For each additive at a particular condition, measurements were performed for at least five additive concentrations.

5.3 Results

5.3.1 Rhodizonate Dianion

No transient absorption was observed over the wavelength range 460-700 nm following flash photolysis of the rhodizonate dianion, using either the Xenon flash lamp or the dye laser. The rate of recovery of the ground state was obtained by monitoring the rhodizonate absorption at 480 nm after the flash from a dye laser. The rate of recovery was first order and recovery of the dianion was complete in neutral solution. An example is shown in Figure 5.3. Under the condition of these experiments (pH 7, no additive), reactions of the excited dianion are negligible and the only loss process for the excited state

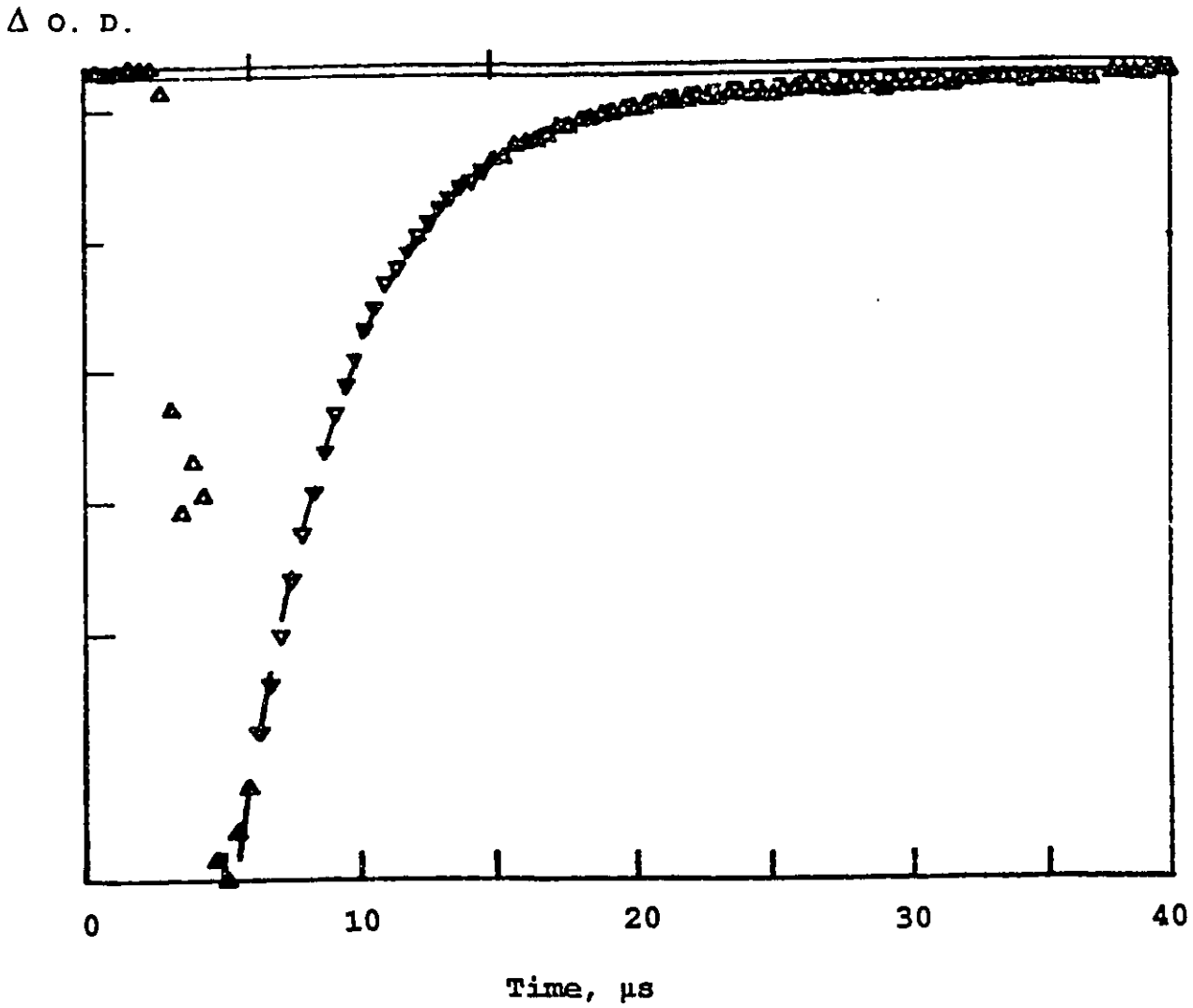

Figure 5.3 Recovery of Ground State of Rhodizonate Dianion

pH=7.0, Top O. D.=0.033

is deactivation to the ground state.

$$C_6O_6^{2-*} \rightarrow C_6O_6^{2-} \qquad (D)$$

From the experiment, the value of k_D of 2.4×10^5 s^{-1} was obtained and with the assumption that no other loss processes of the excited dianion occurs the life time of the excited state of the dianion is 4.2 μsec. The presence of oxygen decreased the lifetime and resulted in incomplete recovery of the ground state. The thermal reaction of oxygen with rhodizonate dianion was significant at room temperature, particularly in basic solution. Reaction with the excited state may also occur along with the quenching of the excited state. The effect of oxygen was therefore complex and measurements of the quenching constant was not practical.

5. 3. 2 Croconate Dianion

As with rhodizonate dianion, no transient absorption was observed over the wavelength range 400-700 nm following flash photolysis of the neutral solution of croconate dianion by itself. In neutral solution the quantum yield for disappearance of croconate dianion was less than 10^{-3} and it may be assumed that the only significant loss process of the excited dianion is deactivation to the ground state:

$$C_5O_5^{2-} + h\nu \rightarrow C_5O_5^{2-*} \qquad [I_{abs}]$$

$$C_5O_5^{2-*} \rightarrow C_5O_5^{2-} \qquad [D]$$

The recovery of the ground state was monitored at 360 nm and a typical trace, showing the fit of the date to a first order equation, is shown in Figure 5.4. Measurements were made at both pH 7 and pH 9 and the first order rate constants for recovery of the ground state are given in Table 5.1.

Oxygen was an efficient quencher of the excited state of croconate dianion. The rate of recovery of the ground state of croconate dianion was measured as a function of the

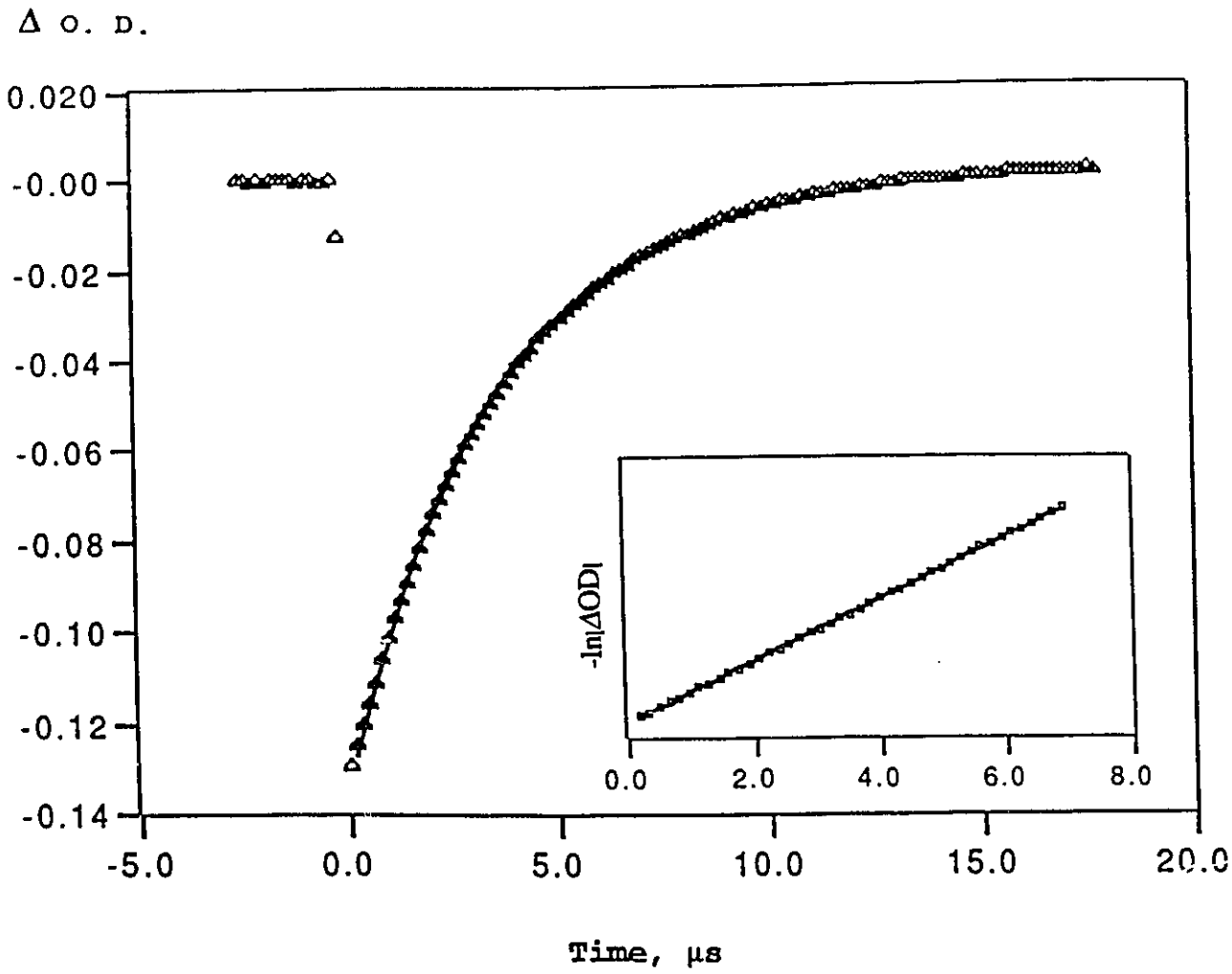

Figure 5.4 Recovery of Ground State of Croconate Dianion

pH=7.0

Table 5.1

Rate Constants for Reactions of Transients in the Photolysis of Rhodizonate and Croconate Dianions

Reactants	pH	k_D (s^{-1})	k_T ($M^{-1}s^{-1}$)	k_5 (s^{-1})	k_Q ($M^{-1}s^{-1}$)
$C_6O_6^{2-}$	7.0	2.4×10^5			
$C_5O_5^{2-}$	7.0	2.8×10^5			
	9.0	2.9×10^5			
Biacetyl + $C_5O_5^{2-}$	6.2	2.3×10^5	2.0×10^8		
MV^{2+}+ $C_5O_5^{2-}$	7.2	3.0×10^5	3.7×10^{10}		
$BrCH_2C_6H_4NO_2$+ $C_5O_5^{2-}$	7.0	3.2×10^5	2.8×10^9	5.3×10^3	
	9.0	2.7×10^5	2.6×10^9	2.4×10^4	
O_2 + $C_5O_5^{2-}$	7.4				4.5×10^9

concentration of oxygen. Aqueous solutions (pH 7.4) were prepared with a range of concentrations of oxygen by saturation with a suitable mixture of nitrogen and oxygen gases. Unlike the system containing rhodizonate dianion, oxygen does not react chemically with the ground state croconate dianion, nor with the excited state croconate dianion, and in the presence of oxygen, a complete recovery of ground state croconate dianion occurred following the laser flash photolysis. The only additional reaction occurring in the presence of oxygen is therefore the quenching of the excited state:

$$C_5O_5^{2-*} + {}^3O_2 \rightarrow C_5O_5^{2-} + O_2^* \qquad [Q]$$

This reaction may be very efficient if the singlet state of O_2 is formed. For a particular concentration of oxygen and because oxygen is in large excess, the observed rate of recovery was first-order and may be expressed as:

$$k_{obs} = k_D + k_Q[O_2]$$

Figure 5.5 shows the relation between the concentration of oxygen and the observed first order rate constant for recovery of the ground state. The data in Figure 5.5 show some scatter, probably due to the inaccuracy in measuring the concentration of oxygen in the solution. The value of k_Q obtained from the results in Figure 5.5 is 4.5×10^9 $M^{-1}s^{-1}$.

In the presence of the electron acceptors, methyl viologen, biacetyl and 4-nitrobenzylbromide, a new transient absorption spectrum was observed with a maximum at 500 nm following the flash photolysis of croconate dianion at 337 nm (or 355 nm). Using the kinetic system the absorption was measured as a function of wavelength for four fixed time intervals following the flash. The spectra at the time delay giving the maximum absorption are shown in Figures 5.2, 5.6 and 5.7 for each additive. In the presence of methyl viologen, the transient absorption spectrum has two peaks at 393 nm and 603 nm, which are due to the absorption from the methyl viologen monocation radical $MV^{+\cdot}$. Because the absorption at 500 nm was observed with all three additives it may be concluded

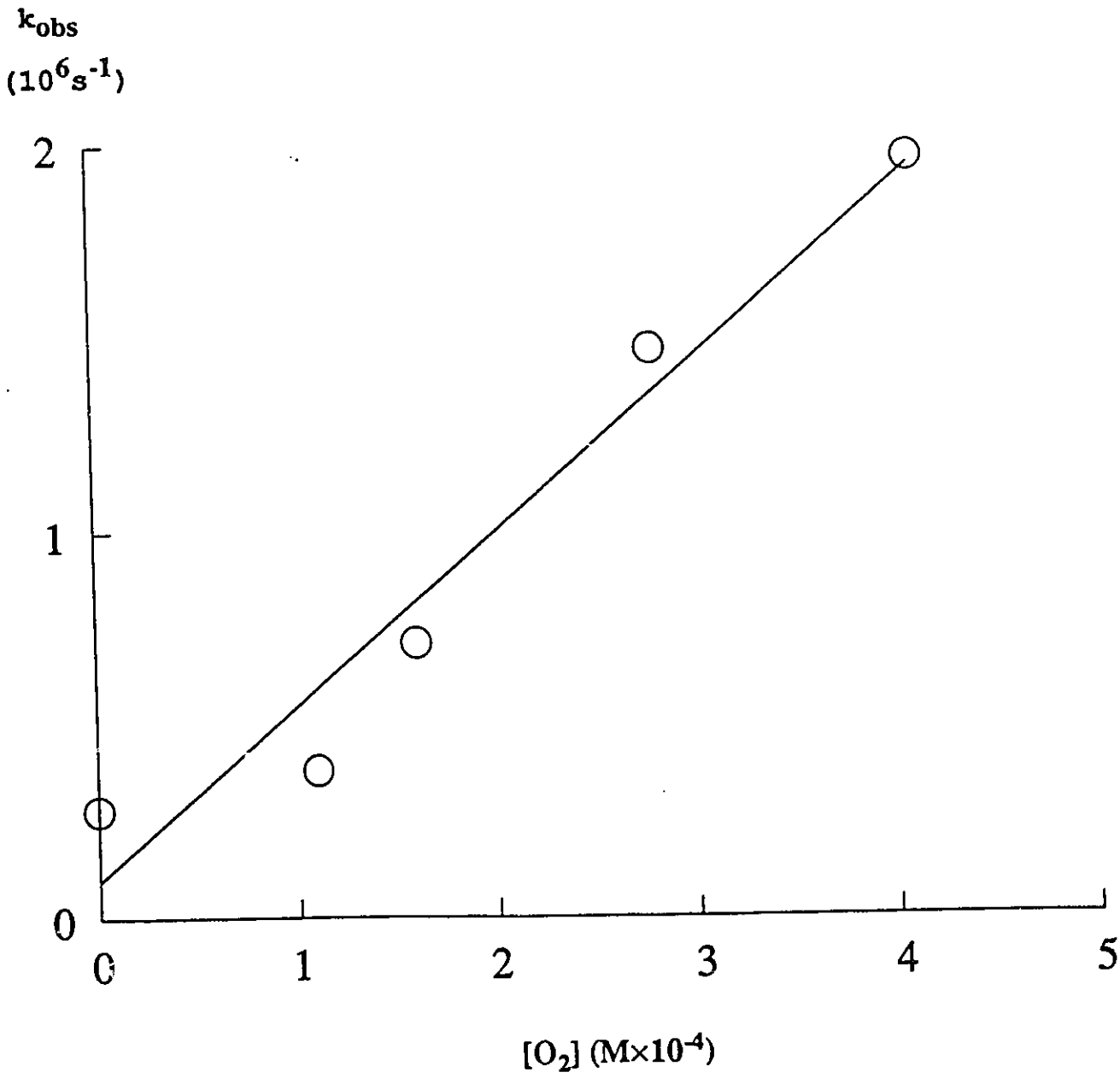

Figure 5.5 Observed Rate Constant for the Recovery of Ground State of Croconate Dianion as a Function of Concentration of Oxygen, pH=7.4

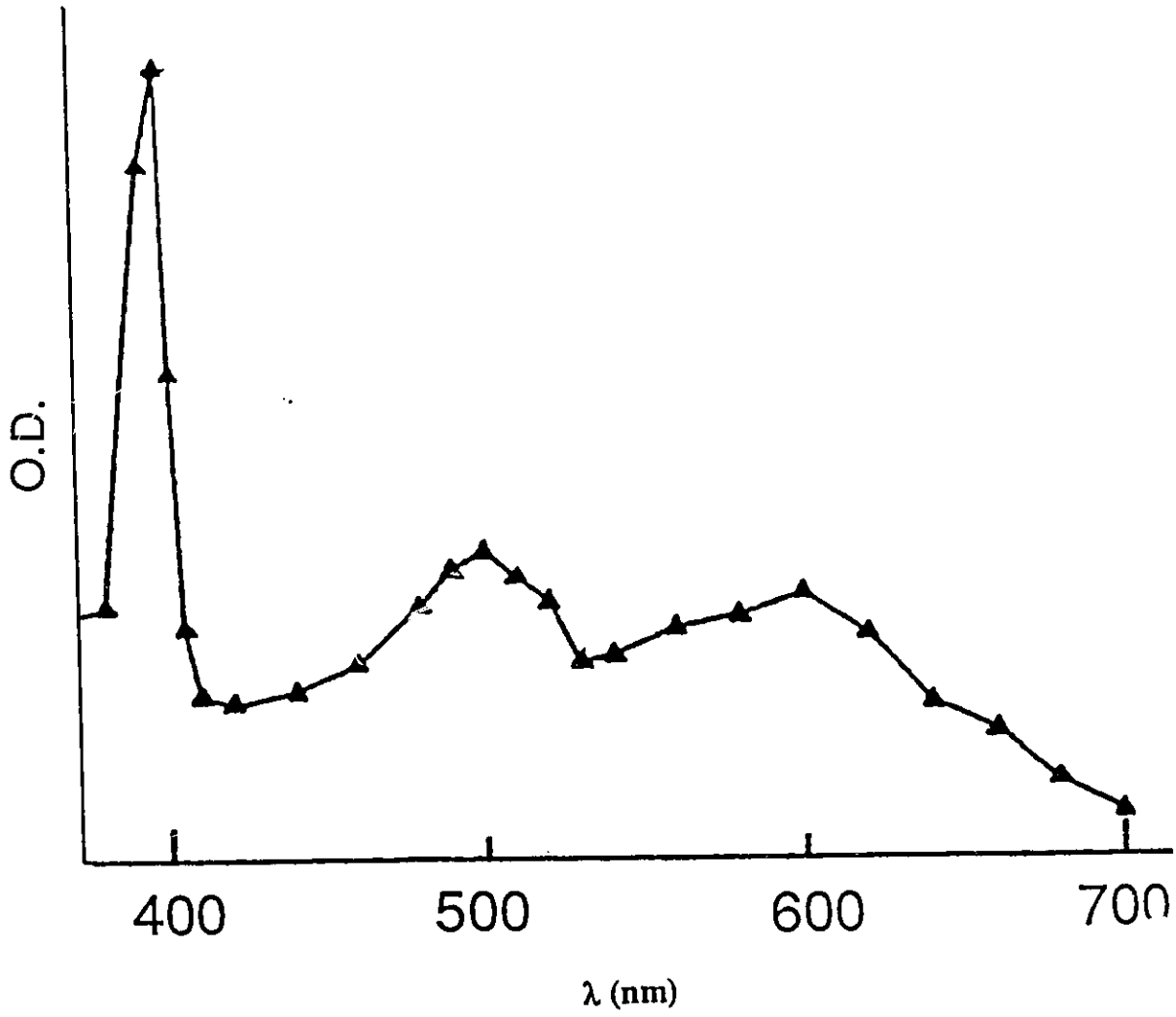

Figure 5.6 Transient Absorption of Croconate Monoanion Radical and Methyl Viologen Monocation Radical

$[MV^{2+}]=1.48\times10^{-4}$ M, pH=7.2, $\lambda_{exc.}$=337 nm, Top OD=0.05

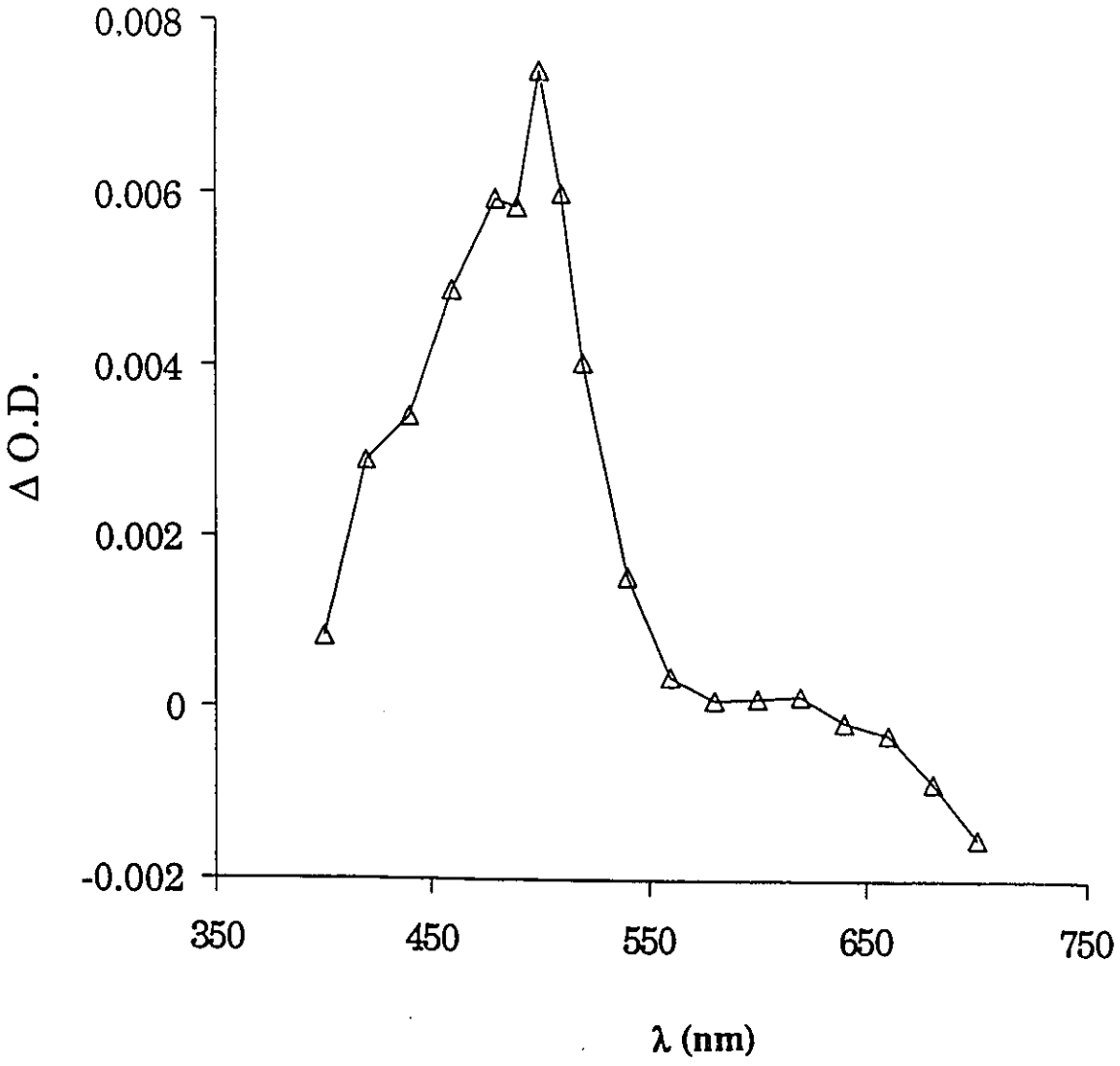

Figure 5.7 Transient Absorption of Croconate Monoanion Radical in the Presence of 4-Nitrobenzylbromide

$[BrCH_2C_6H_4NO_2]=1.18\times10^{-4}$ M, pH=7.0, $\lambda_{exc.}$=355 nm.

that this absorption is due to the presence of the croconate monoanion radical formed following electron transfer from the excited dianion to the acceptors. Although the transient absorption spectra were not very well resolved, in the presence of biacetyl and 4-nitrobenzylbromide some indications of a double maximum in the absorption band between 460-500 nm is evident, especially in the case of 4-nitrobenzylbromide. This double maximum characteristic is consistent with the absorption pattern of the parent croconate dianion, showing that the transient monoanion may still have a highly symmetrical structure and the Jahn-Teller effect is significant.

The transient absorption spectra were obtained at the early stage of the reactions where there is no measurable decay of the radical absorption. These measurements will be described later. In neutral solution, the growth kinetics were the same for both methyl viologen cation radical and croconate monoanion radical. The rate constants measured by monitoring the absorption either at 500 nm or at 603 nm were identical. It may also be assumed that at the early stages of the reaction, the radicals of methyl viologen and croconate are formed in equal amounts, so that the extinction coefficient for the croconate monoanion radical at 500 nm may be derived from the transient absorption spectrum. The extinction coefficient for the methyl viologen monocation radical absorption at 603 nm is 1.2×10^4 $M^{-1}cm^{-1}$.[135] Thus the extinction coefficient for the croconate monoanion radical absorption at 500nm may be estimated from Figure 5.6 as 0.7×10^4 $M^{-1}cm^{-1}$.

Figure 5.8 shows a typical trace of growth of the absorbance at 500 nm with 4-nitrobenzylbromide in neutral solution. The formation of croconate monoanion through the electron transfer between the excited croconate dianion and acceptor following flash photolysis can be expressed as:

$$C_5O_5^{2-*} + A \rightarrow C_5O_5^{\cdot-} + A^- \qquad [T]$$

Referring to the mechanism for the reaction of croconate dianion in the presence of

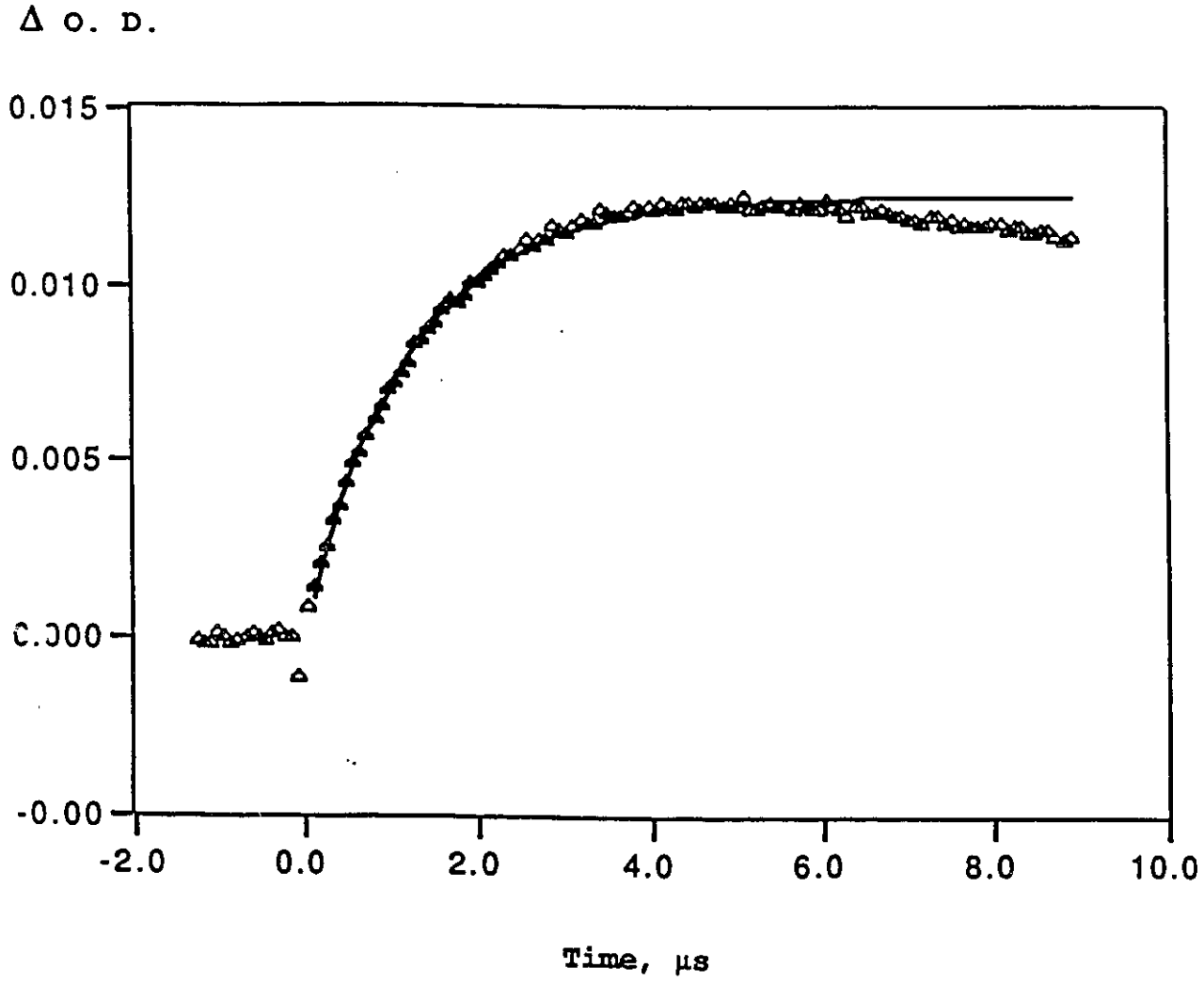

Figure 5.8 Growth of $C_5O_5^{-\cdot}$ Absorbance at 500 nm, in the Presence of 4-Nitrobenzylbromide.

[4-Nitrobenzylbromide] = 1.74×10^{-4} M; pH = 7.0

additive derived in Chapter 3 (page 93), the rate constant for the electron transfer can be expressed as:

$$k_T = k_1 \frac{k_3}{k_2 + k_3}$$

In the absence of oxygen, the simple mechanism of reactions [I_{abs}], [D] and [T] describes the formation of the monoanion radical, and if the loss of the monoanion radical can be expressed by a single order process, the whole process can be expressed as follows:

$C_5O_5^{2-} + h\nu \rightarrow C_5O_5^{2-*}$ [I_{abs}]

$C_5O_5^{2-*} \rightarrow C_5O_5^{2-}$ [D]

$C_5O_5^{2-*} + A \rightarrow C_5O_5^{\cdot-} + A^-$ [T]

$C_5O_5^{\cdot-} \rightarrow$ product [P]

Assuming that the duration of the laser pulse (8-10 nsec.) and the lifetime of the triplet croconate dianion are short compared with the monoanion radical lifetime, the following relation should hold:

$$\frac{-d\,[C_5O_5^{2-*}]}{dt} = (k_D + k_T\,[A])\,[C_5O_5^{2-*}] \qquad (5\text{-}1)$$

$$\frac{d\,[C_5O_5^{\cdot-}]}{dt} = k_T\,[\,C_5O_5^{2-*}]\,[A] - k_P\,[C_5O_5^{\cdot-}] \qquad (5\text{-}2)$$

In the early stages of the reaction, $k_T[C_5O_5^{2-*}][A] >> k_P[C_5O_5^{\cdot-}]$. This can be verified by viewing the trace of the absorption at 500 nm as a function of time (Figure 5.8). The first order growth of the absorption at 500 nm of the monoanion radical was not distorted in the first few microseconds. Therefore equation (5-2) can be written as:

$$\frac{d\,[C_5O_5^{\cdot-}]}{dt} = k_T\,[\,C_5O_5^{2-*}]\,[A] \qquad (5\text{-}3)$$

Therefore, the rate of formation of the monoanion radical is related to the rate of loss of the excited croconate dianion as follows:

$$d[C_5O_5^{\cdot-}] = -\,\frac{k_T\,[A]}{k_D + k_T[A]}\,d[C_5O_5^{2-*}] \qquad (5\text{-}4)$$

Equation (5-4) can be integrated from a concentration of $C_5O_5^{\cdot-}$ at any time, t, to a time, t_{max}, where $C_5O_5^{\cdot-}$ reaches its maximum concentration, $(C_5O_5^{\cdot-})_{max}$ (see Figure 5.8). At this point the concentration of $C_5O_5^{2-*}$ is practically zero. Therefore:

$$\int_{[C_5O_5^{\cdot-}]_t}^{[C_5O_5^{\cdot-}]_{max}} d[C_5O_5^{\cdot-}] = -\int_{[C_5O_5^{2-*}]_t}^{0} \frac{k_T[A]}{k_D + k_T[A]}\,d[C_5O_5^{2-*}]$$

$$[C_5O_5^{\cdot-}]_{max} - [C_5O_5^{\cdot-}]_t = \frac{k_T[A]}{k_D + k_T[A]}\,[C_5O_5^{2-*}]_t \qquad (5\text{-}5)$$

The term $[C_5O_5^{2-*}]$ in equation (5-5) can be substituted by the relation in equation (5-3), and we have:

$$[C_5O_5^{\cdot-}]_{max} - [C_5O_5^{\cdot-}]_t = \frac{1}{k_D + k_T[A]}\,\frac{d[C_5O_5^{\cdot-}]}{dt}$$

$$\frac{d[C_5O_5^{\cdot-}]}{[C_5O_5^{\cdot-}]_{max} - [C_5O_5^{\cdot-}]_t} = (k_D + k_T[A])dt \qquad (5\text{-}6)$$

We integrate (5-6) from 0 to t, $t<T_{max}$,

$$-\ln ([C_5O_5^{-\cdot}]_{max} - [C_5O_5^{-\cdot}]_t) \Big]_0^{[C_5O_5^{-\cdot}]_t} = (k_D + k_T[A])\, t$$

$$\ln \frac{[C_5O_5^{-\cdot}]_{max}}{[C_5O_5^{-\cdot}]_{max} - [C_5O_5^{-\cdot}]_t} = (k_D + k_T[A])\, t \qquad (5\text{-}7)$$

Because the concentration of $C_5O_5^{-\cdot}$ is proportional to its absorbance at 500 nm, the concentration of $C_5O_5^{-\cdot}$ in equation (5-7) can be substituted by the transient absorbance at 500 nm

$$\ln \frac{[A_{500}]_{max}}{[A_{500}]_{max} - [A_{500}]_t} = (k_D + k_T[A])\, t \qquad (5\text{-}8)$$

The value of $[A_{500}]_{max}$ and $[A_{500}]_t$ can be obtained from the transient absorption growth trace, and a plot of $\ln\{[A_{500}]_{max}/([A_{500}]_{max} - [A_{500}]_t)\}$ against time t for a particular additive concentration should give a linear relation in the early stages of the reaction. Figure 5.9 shows the data plotted according to equation (5-8), at five different 4-nitrobenzylbromide concentrations. The slopes of these lines represent the observed first order rate constants expressed as:[136-137]

$$k_{obs} = k_D + k_T [A] \qquad (5\text{-}9)$$

Plots of the experimental results with additives methyl viologen and biacetyl in aqueous solution are shown in Figures 5.10 and 5.11 and with additive 4-nitrobenzylbromide at pH 7 and pH 9 are shown in Figures 5.12 and 5.13, respectively. All plots showed a linear relationship between k_{obs} and [A]. The first order decay constant k_D, and the second order electron transfer rate constant k_T for each additive are summarized

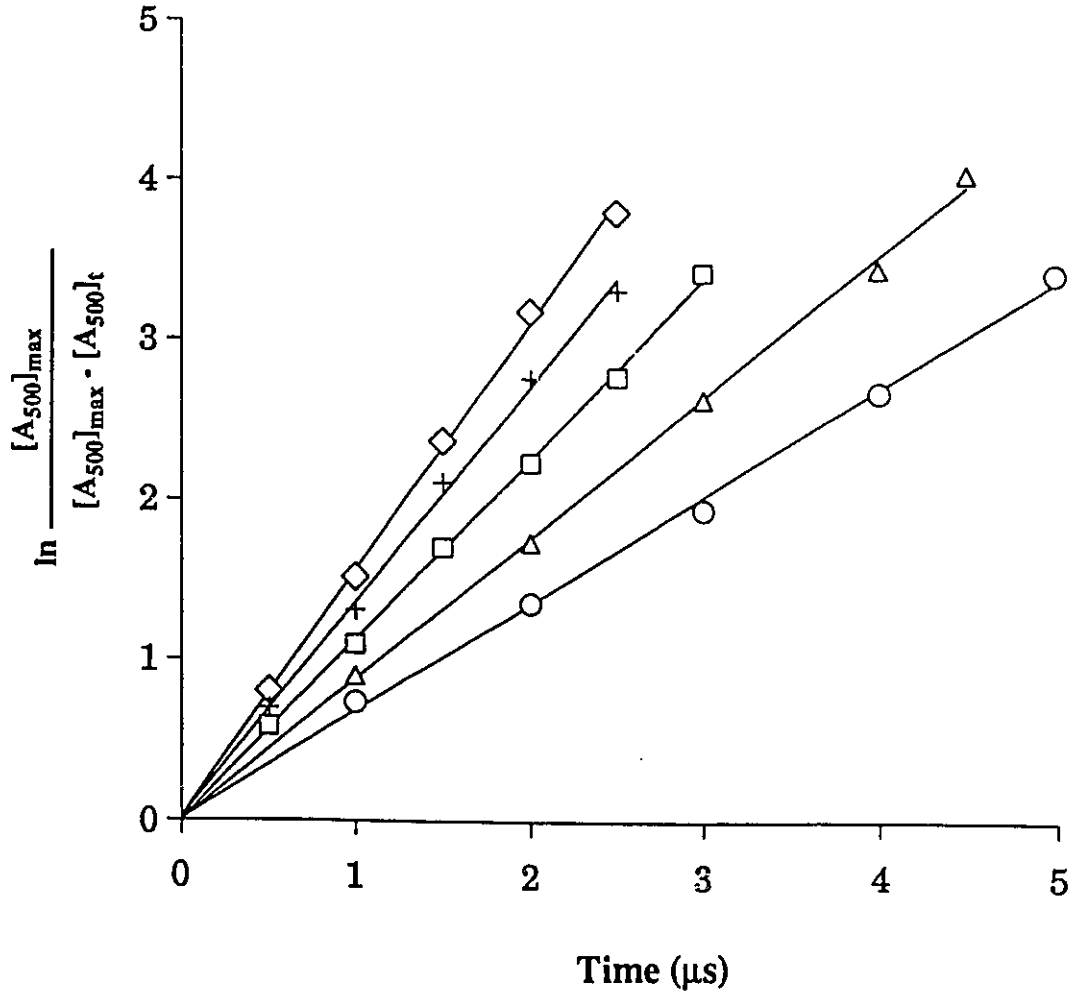

Figure 5.9 Semilogarithm Plot of the absorption of $C_5O_5^{-\cdot}$ at 500 nm as a Function of Time in the Presence of 4-nitrobenzylbromide; pH=7.0.

$[BrCH_2C_6H_4NO_2]$: o: 1.18×10^{-4} M; Δ: 1.74×10^{-4} M;

□: 2.45×10^{-4} M; x: 3.25×10^{-4} M; ◊: 4.05×10^{-4} M.

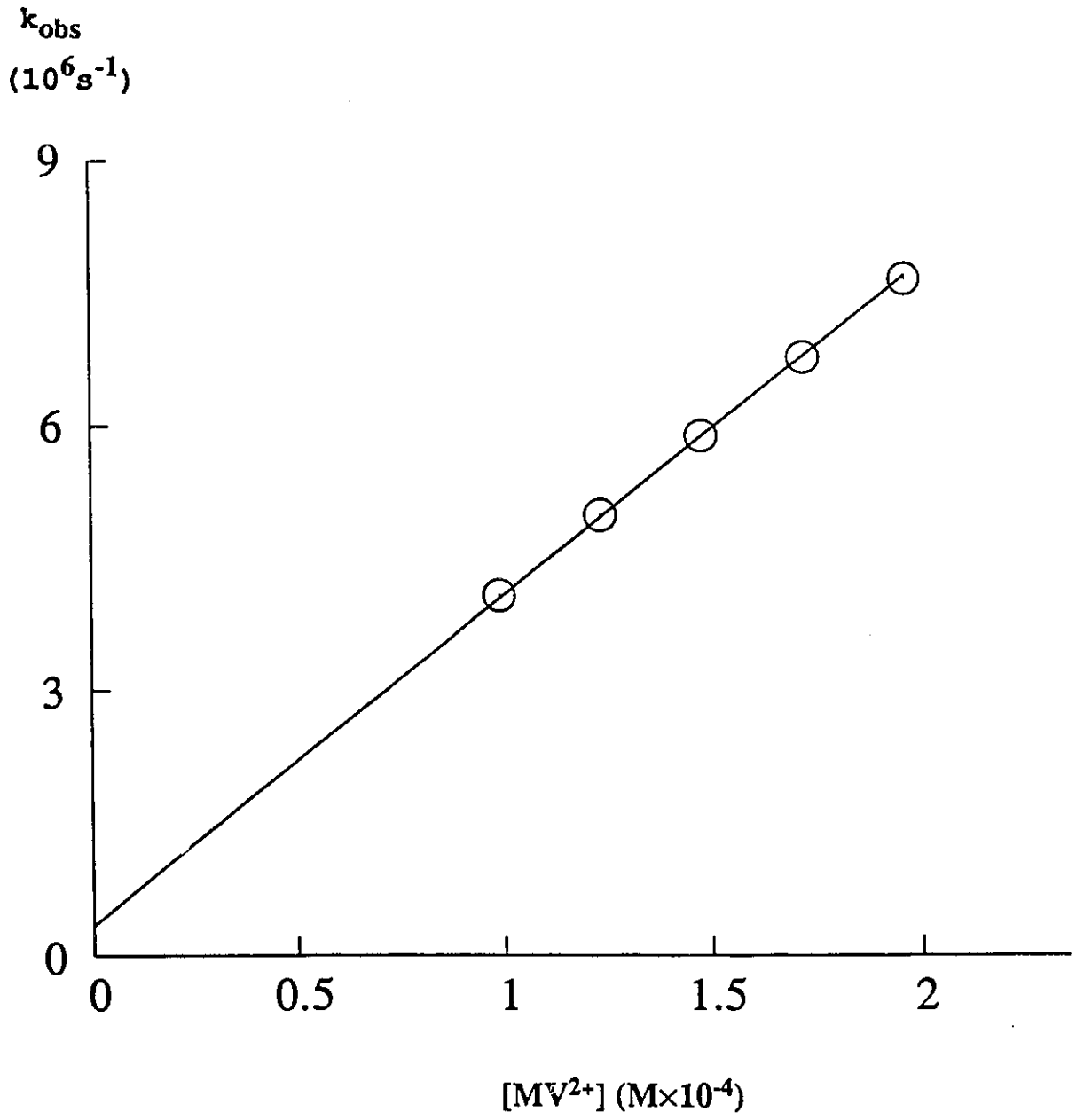

Figure 5.10 Observed Rate Constant of the Formation of $C_5O_5^{-\cdot}$ as a Function of Concentration of Methyl Viologen. pH = 7.2

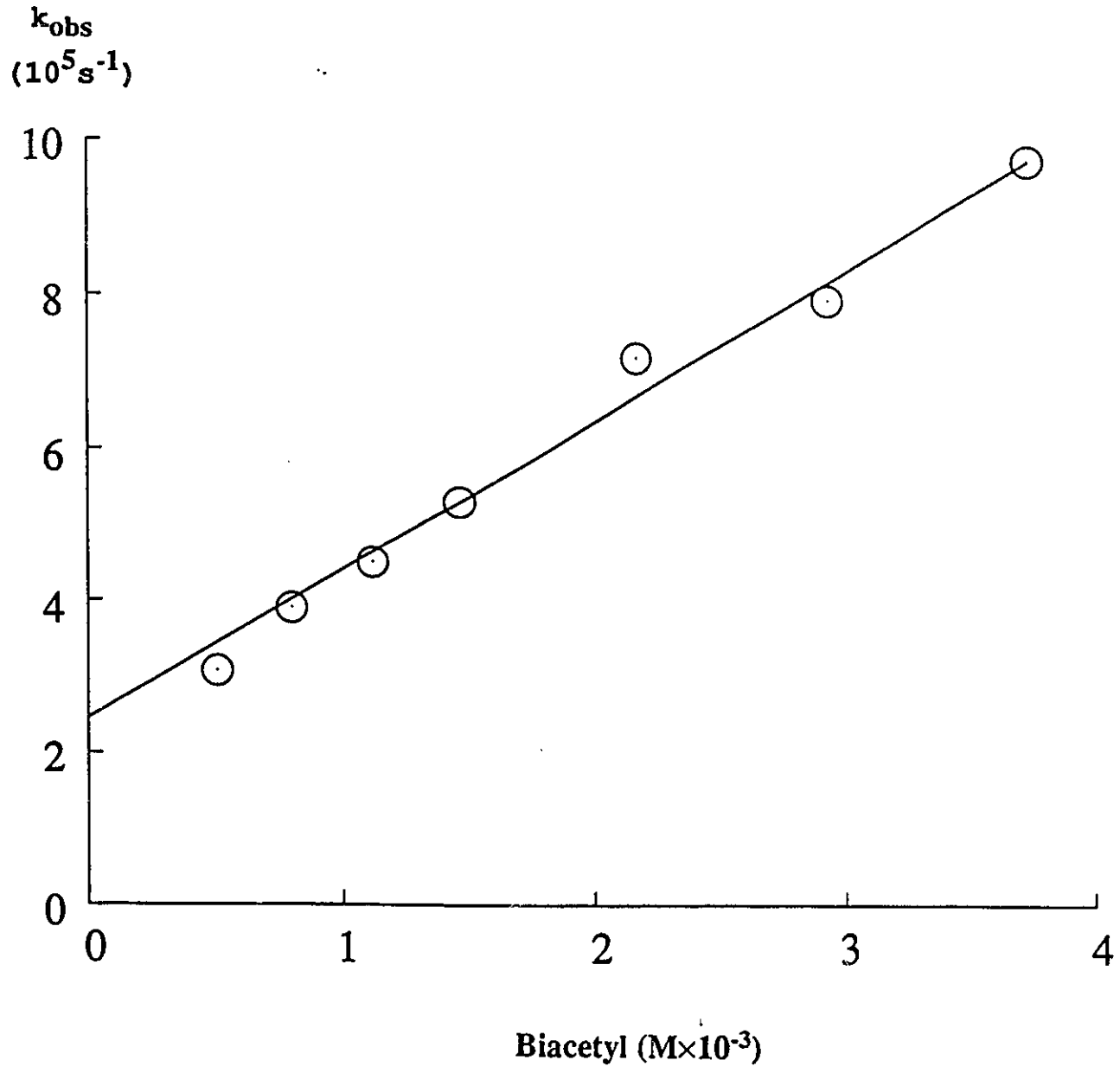

Figure 5.11 Observed Rate Constant of the Formation of $C_5O_5^{\cdot-}$ as a Function of Concentration of Biacetyl. pH = 6.2

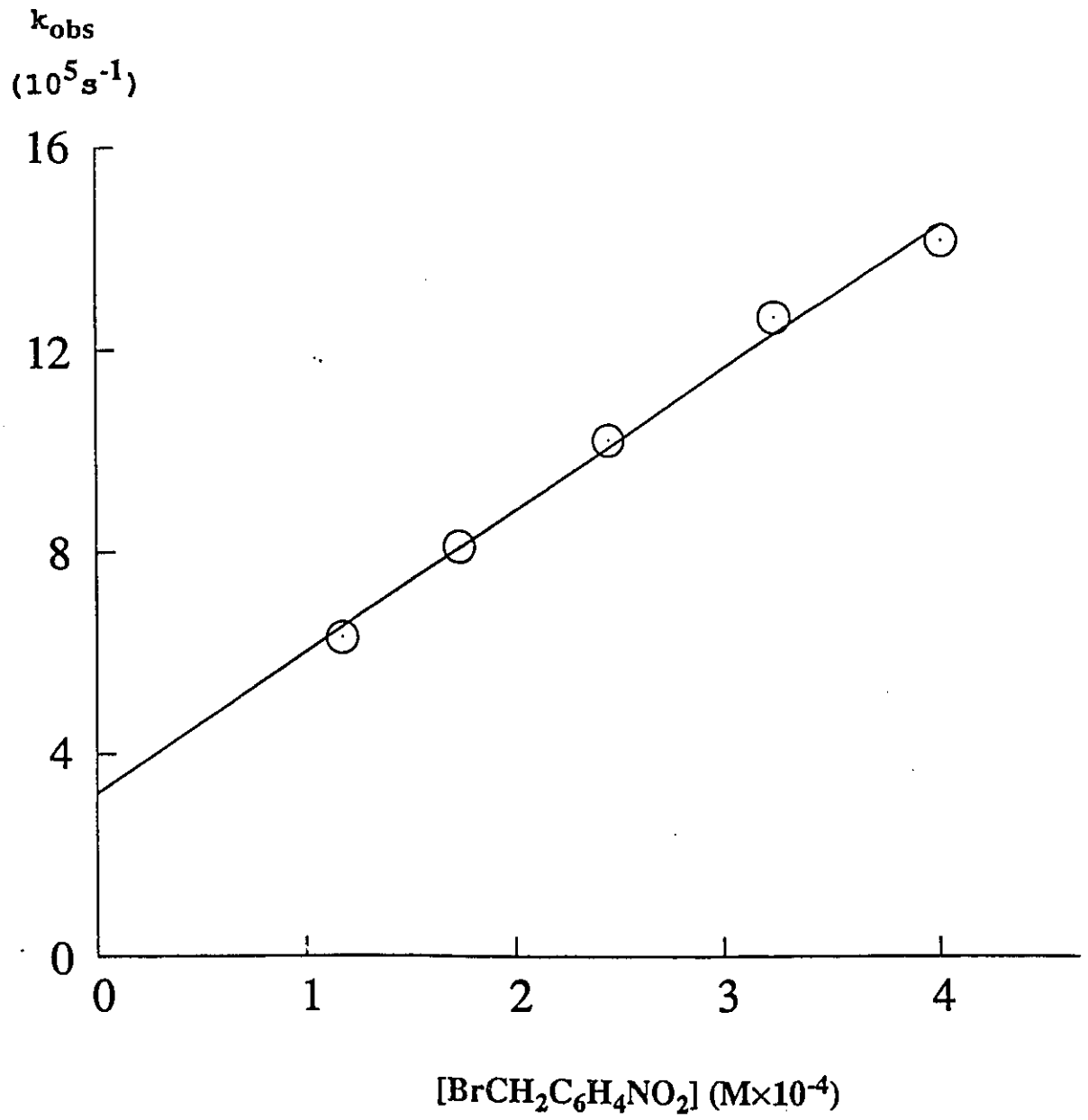

Figure 5.12 Observed Rate Constant of the Formation of $C_5O_5^{-\cdot}$ as a Function of Concentration of 4-Nitrobenzylbromide. pH = 7.0

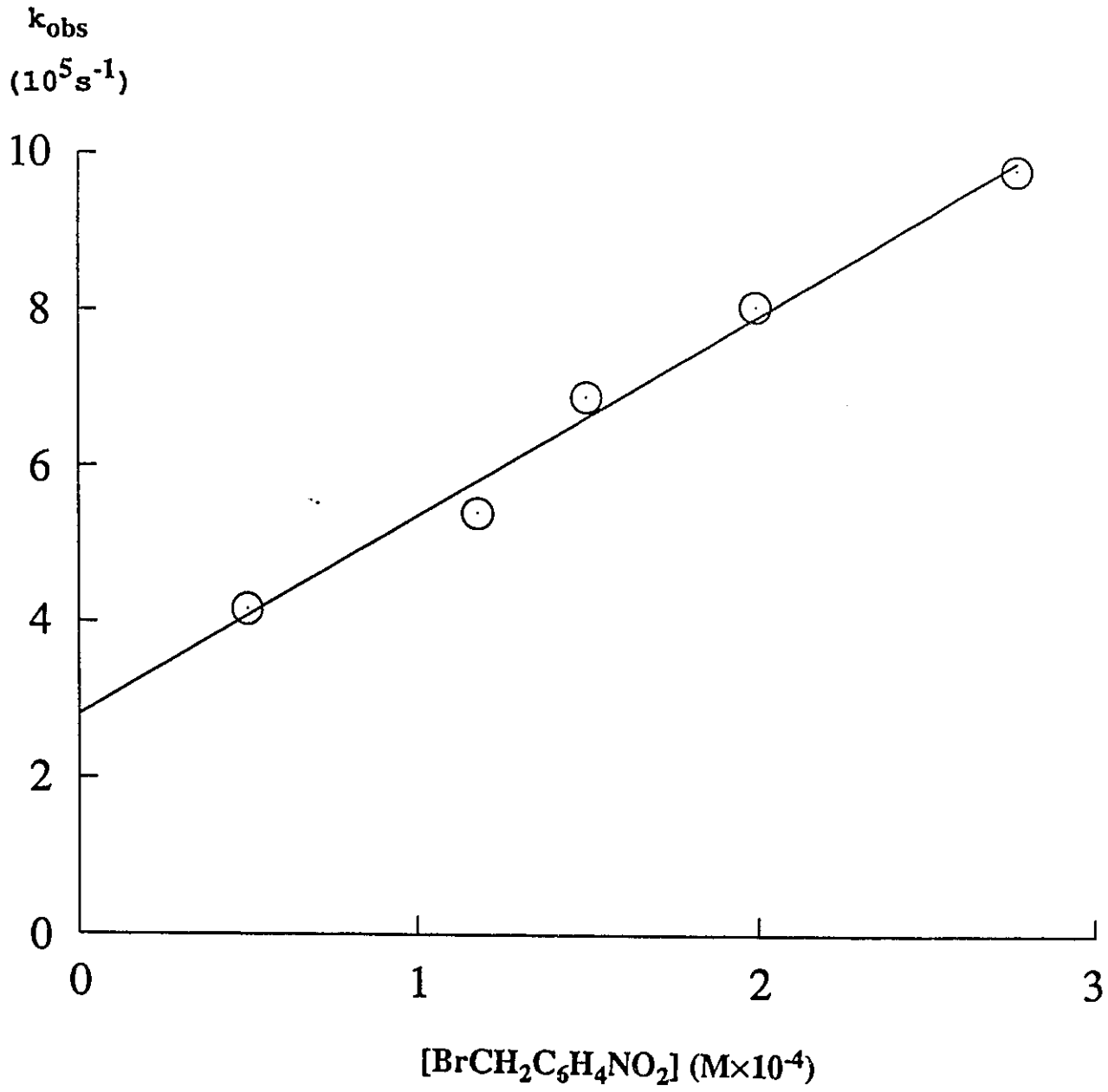

Figure 5.13 Observed Rate Constant of the Formation of $C_5O_5^{\cdot-}$ as a Function of Concentration of 4-Nitrobenzylbromide. pH = 9.0

in Table 5.1. The decay trace of the croconate monoanion absorption at 500 nm is shown in Figure 5.14. The first-order rate constant for the decay at two different pH values are given in Table 5.1. The rate of decay is clearly too slow to interfere with the measurement of the first order rate of growth.

5.4 Discussion

According to the reaction mechanism derived in Chapter 3, in the absence of additive, the recovery of ground state croconate dianion from the excited state is through the deactivation reaction [D], and through the sequence of reactions [6] and [7]. The rate of recovery can be expressed as:

$$\frac{d[C_5O_5^{2-}]}{dt} = \left(k_D + \frac{k_7}{k_7 + k_8} k_6 [OH^-] \right) [C_5O_5^{2-*}]$$

Using the rate constants given in Table 3.7, in neutral solution the second term on the right hand side calculated is negligible and the recovery rate is equal to the rate of decay of the excited state. At pH 9, recovery through the sequences of reaction of [6], [7] and [8] is about 3% of the recovery through deactivation. This correction to the measured decay rate constant was made for both measurements at pH 9. The magnitude of the correction is however within the error of the measurement. The effect will, however, be important at higher pH values.

The values obtained for k_D, the rate constant for deactivation of the excited state to the ground state, are in reasonable agreement from all the experiments, both with and without additives. The average value, 2.9±0.4 μsec., clearly indicates the excited state is triplet. This conclusion is substantiated by the measurement of the lifetime of the singlet state of croconate dianion as ~ 2 nsec. The highest concentration of the reactants, either

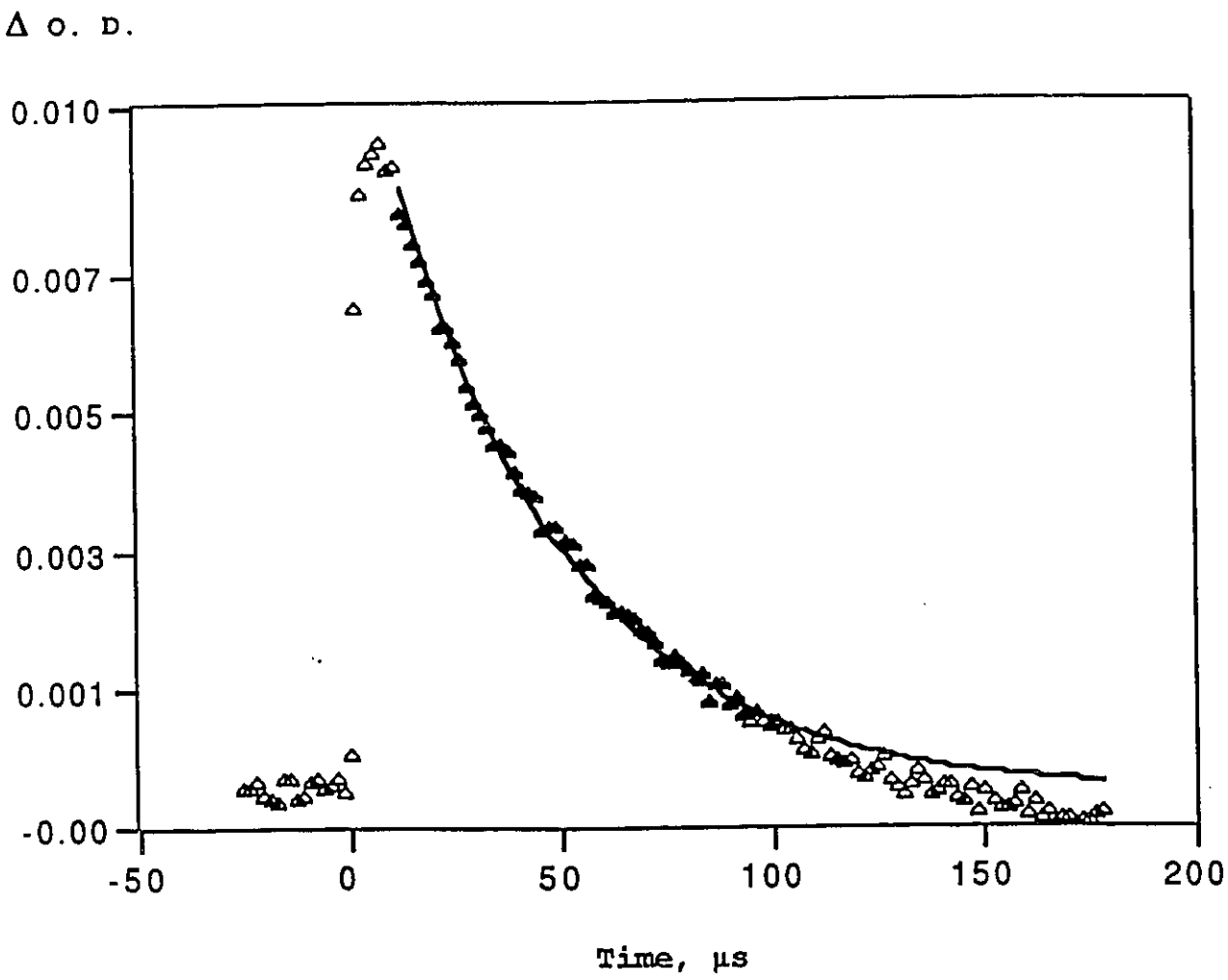

Figure 5.14 Decay of $C_5O_5^{\cdot-}$ Absorbance at 500 nm,

in the Presence of 4-Nitrobenzylbromide

[4-Nitrobenzylbromide] = 1.18×10^{-4} M; pH = 9.0

OH^-, 0.01 M, or the electron acceptor, 10^{-3} M, are not sufficient to react with an excited singlet state with this short lifetime. In Table 5.2 are shown for comparison, some triplet lifetimes for various types of carbonyl and olefin compounds.[138-143]

It was shown in Chapter 3 that quantum yields of one for loss of croconate dianion were observed in the presence of some additives, also, only a very weak fluorescence ($\phi_F<10^{-3}$) was observed from the first singlet state of the croconate dianion. It may be concluded that the intersystem crossing must be 100% efficient. Such efficient intersystem crossing is common with carbonyl compounds where excitation usually involves an n--π^* transition but in the oxocarbon dianions the allowed lowest excitation is a π--π^* transition.

Plots of the experimental observed rate constants k_{obs} against the concentration of additives methyl viologen, biacetyl and 4-nitrobenzylbromide shown in the Figures 5.11, 5.12, 5.13 and 5.14, all exhibit a very good linear relation between the two variables. This is a clear indication that the reactions of croconate dianion with all the additives follow the mechanism represented by the reactions of $[I_{abs}]$, [D], [T] and [P] shown on page 167. With the three additives used a 180-fold variation was observed in the value of k_T. The fastest rate, which even exceeds a diffusion-controlled rate, occurs with the positive ion methyl viologen. This is higher than all the rate constants of the electron transfer reactions of methyl viologen with the excited triplet neutral donors reported in the literature.[144-149] In our case, coulombic attraction must be important. Possibly a loose ground-state complex of methyl viologen cation and croconate dianion may form prior to the photoexcitation. Coulombic attraction would not be a factor with the molecules 4-nitrobenzylbromide and biacetyl and with the former, k_T has a value close to a diffusion-controlled rate constant. The lower value for k_T observed with biacetyl may reflect a lower electron affinity, or reduction potential for the redox process. This characteristic will influence the value of k_1 in the scheme for the reactions of the excited croconate dianion derived in Chapter 3. This

Table 5.2

Triplet Lifetime of Some Selected Compounds

Compounds	Solvent	τ(μsec.)	Reference
1,4-Diphenyl-1,3-butadiene	Benzene	2.6	17
Tetraphenylethylene	Benzene	0.13	6
1,3-Cyclohexadiene	Benzene	1.3	11
Butanone	Water	0.18	32
2,3-Hexenedione	Benzene	3.7	36
1-Phenyl-1,2-butanedione	Benzene	5.9	72
Croconate Dianion	Water	3.4	This work

lower value of k_T also reflects a lower ratio of $k_3/(k_3+k_2)$, as k_T is the product of k_1 and this ratio. Taking the values of k_1, k_2 and k_3 from Table 3.7, the product of k_1 and the ratio $[k_3/(k_2+k_3)]$ is 2.5×10^8 $M^{-1}s^{-1}$ for biacetyl, compared with the experimentally measured rate constant k_T of $2.0\times10^8 M^{-1}s^{-1}$. These two values are in very good agreement, showing that the values of the rate constants in Table 3.7 obtained by fitting the results of steady state photolysis experiments to the reaction scheme are in reasonable agreement with the results obtained from flash photolysis experiments. In the case of 4-nitrobenzylbromide, the product of k_1 and the ratio $[k_3/(k_2+k_3)]$ is 0.43×10^9 $M^{-1}s^{-1}$, using the values of rate constants in Table 3.7, and the rate constant for k_T obtained from the experiment is 2.8×10^9 $M^{-1}s^{-1}$. This discrepancy seems outside the errors in the measurements and the estimation of the rate constants, and suggests that a change in the mechanism occurs in the flash photolysis experiments. One possibility is a more efficient separation of the ion radicals in the cage complex under the conditions of the flash photolysis experiments. Thus the ratio $k_3/(k_2+k_3)$ could increase and bring the value of k_T estimated from the rate constants in Table 3.7 closer to the measured value of k_T.

Claim to Original Research

1. This study has shown that rhodizonate dianion reacts with hydrogen peroxide, ferricyanide and tetracyanoethylene both thermally and photochemically, with the first step being an electron transfer from rhodizonate dianion to acceptors with sufficiently strong oxidizing potential (>0.1 v). The mechanism of the reaction with hydrogen peroxide and ferricyanide is different from that with tetracyanoethylene, but for a particular acceptor the mechanism is the same under both thermal and photochemical conditions. The main reaction product is croconate dianion and the rate of conversion from rhodizonate dianion to croconate dianion varies with the acceptors present.

2. The quantum yield for disappearance of rhodizonate dianion was low under all conditions studied. The highest value for the quantum yield was 0.04 in the presence of tetracyanoethylene. The low quantum yield for the disappearance of rhodizonate dianion demonstrates that for the reactions of rhodizonate dianion and acceptors

$$(C_6O_6^{\cdot-} \ldots A^-) \underset{k_{-2}}{\overset{k_2}{\rightleftharpoons}} C_6O_6^{\cdot-} + A^-$$

$$(C_6O_6^{\cdot-} \ldots A^-) \xrightarrow{k_{-4}} C_6O_6^{2-} + A$$

$k_{-4} >> k_2$. Most of the caged complex ($C_6O_6^{\cdot-}...A^-$) reforms the reactants instead of separating into the oxidized and reduced products.

3. Croconate dianion reacts with electron acceptors photochemically only. The

quantum yield for the disappearance of croconate dianion increased with increasing pH and concentration of additive. In the presence of 4-nitrobenzylbromide and biacetyl the quantum yield reached a value of one at pH 12. The main reaction product was squarate dianion.

4. The mechanism of the photochemical reaction of croconate dianion in the presence of electron acceptors was proposed. The rate constants for each reaction were estimated by analysis of the relation between the quantum yield and the concentration of hydroxyl ion and acceptors. The quantum yields calculated according to these rate constants were in good agreement with those obtained from experiments under a range of conditions.

5. This study has shown that croconate dianion is a promising initiator for photopolymerization. In the presence of 4-nitrobenzylchloride, a quantum yield of 2500 for the polymerization of acrylamide was obtained in neutral solution.

6. The lifetimes of the excited states of rhodizonate and croconate dianion were obtained using flash photolysis techniques, by measurement of the rate of recovery of the ground state from the excited state. Transient absorption spectra of the croconate monoanion radical were detected in the presence of 4-nitrobenzylbromide, biacetyl and methyl viologen. Rate constants for the initial electron transfer reactions between the excited croconate dianion and acceptors (k_T) were measured, showing that these were diffusion-controlled processes. In the case of methyl viologen, a coulombic effect is responsible for the large value of k_T measured with this acceptor.

REFERENCE

1 Robert West, in "Oxocarbons", (Robert West ed.), P.1, Academic Prese, New York, (1980).

2 Robert West, and David L. Powell, J. Amer. Chem. Soc., 85 2577 (1963).

3 L. Gmelin, Ann Physik. Chem. 4 31 (1825).

4 J. F. Heller, Justus Liebig's Ann. Chem., 24 1 (1937)

5 Sidney Cohen, John R. Lacher, and Joseph D. Park, J. Amer. Chem. Soc., 81 3480 (1959)

6 Kiyoyoki Yamada, and Yoshimasa Hirata, Bull. Chem. Soc. Jpn., 31(5) 550 (1958).

7 N. C. Baenziger and J. J. Hegenbarth, J. Amer. Chem Soc., 86 3250 (1964).

8 Jun-ichi Aihara, J. Amer. Chem. Soc., 101 1633 (1981).

9 Claudio Puebla and Tae-Kya Ha, J. Mol. Struct. (Theochem.), 137 171 (1986).

10 Robert West, Israel J. Chem., 20 300 (1980).

11 Lowell M. Schwartz, Robert I. Gelb and Daniel A. Laufer, in "Oxocarbons", (Robert West ed.), P. 43, Academic Press, New York, (1980).

12 Mitsuo Ito, Koji Kaya and Machiko Takahashi, in "Oxocarbons", (Robert West ed.), P. 121, Academic Press, New York, (1980).

13 R. T. Bailey, J. Chem. Soc., (B) 627 (1971).

14 Claude Leibovici, J. Mol. Strut., 13(2) 185 (1972).

15 Robert West and Joseph Niu, in "Non-Benzenoid Aromatics", (J. P. Snyder ed.), Academic Press, New York, Vol.1, 311 (1969).

16 Josef Michl and Robert West, in "Oxocarbons" (Robert West ed.), P. 79, Academic

Press, New York, (1980).

17 Jun-ichi Aihara, Bull. Chem. Soc. Jpn., 47(1), 2899 (1974).

18 Elizabeth Patton and Robert West, J. Phys. Chem., 74(12) 2512 (1970).

19 Elizabeth Patton and Robert West, J. Amer. Chem Soc., 95(26) 8703 (1973).

20 Lowell M. Schwartz, Robert I. Gelb and Janet O. Yardley, J. Phys. Chem., 79(21) 2246 (1975).

21 P. H. Tedesco and H. F. Walton, Inorg. Chem., 8 973 (1969).

22 A. Banerjee, S. Mandal, T. Singh and A. Dey, India J. Chem., 7 733 (1969).

23 M. B. Fleury, G. Molle, Electrochimica Acta, 20 951 (1975).

24 J. Moiroux, J. C. Dufresne aand m. B. Fleury, Electrochimica Acta, 25 1095 (1980).

25 J. Moiroux, D. Escourrou and M. B. Fleury, J. Eletroanal. Chem., 116 333 (1980).

26 R. S. Bottei and D. L. Greene, J. Inorg. Nucl. Chem., 30 1469 (1968).

27 J. M. carpentier, M. B. Fleury and J. F. Vercher, Bull Soc. Chim. Fr., 4 1293 (1972).

28 Robert I. Gelb, Lowell M. Schwartz, Daniel A. Laufer and Janet O. Yardkey, J. Phys. Chem., 81(13) 1268 (1977).

29 Werner Städeli, Roger Hollenstein and Wolfgang von Philipsborn, Helvetica Chimica Acta 60 948 (1977).

30 R. I. Gelb, L. M. Schwartz and D. A. Laufer, J. Phys. Chem., 82(18) 1985 (1978).

31 A. J. Chaplin and E. L. T. Turner, Histochemistry, 79 111 (1983).

32 Theodore S. Prokopov, Mikrochimica Acta, 429 (1973).

33 Robert A. Chalmers and Geoffrey M. Telling, Mikrochim. Acta, 1126 (1967).

34 Fritz Feigl and Hans A. Suter, Industrial and Engineering Chem., 14(10) 840 (1942).

35 Tuulikki T. Terho and K. Hartiala, Analytical Biochem., 41 471 (1971).

36 Loui J. Silvestri, Robert E. Hurst, Leigh Simpson and Juanita M. Settine, Analytical Biochem., 123 303 (1982).

37 Ervin Jungreis and Magda Nechama, Microchemical J., 34 219 (1986).

38 James R. Preer and George B. Murchison, Jr. Environ. Pollut., Ser. B. 1 (1986).

39 Yash Paul Grover, Analytical Chimica Acta, 101 225 (1978).

40 E. Ya.Marchenko, V. P. Shcherbakov, V. I. Vasenko, ***U. S. S. R. SU 917, 077*** (Cl. Go1N31/22), 30Mar. 1982.

41 Spikumar Mukherjee, Narendra S. Rawat, J. Indian Chem. Soc., 56(4) 413 (1979).

42 Srikuumar Mukherjee, N. S. Rawart, Chem. Era., 12(4) 155 (1976).

43 Sen Li, Jinhong Cao, Fenxi Huaxue, 80 (1985).

44 O. C. Saxena, Microchemical J., 17 68 (1972).

45 N. K. Patel, K. S. Shah, J. Franco, Chem. Era., 13(2) 36 (1977).

46 Ricardo Schrebler, Raquel Araya, Adriana Arratia, Denise B. Ciampi, Maria E. Hoffmann, Nelson Duran, Bioelectrochem. and Bioenergetics, 17 523 (1987)

47 M. M. M. Saleem, M. T. Wilson, Inorg. Chim. Acta 137(3) 139 (1987).

48 S. Ray, M. Ray, J. Biosci., 12(4) 405 (1987).

49 E. C. Slater, Trends Biochem. Sci., 8 234 (1983).

50 A. R. Siedle, L. H. Pignolet, Inorg. Chem., 21(8) 3090 (1982).

51 G. R. Choppin, E. Orebaugh, Inorg. Chem., 17(8) 2300 (1978).

52 R. S. Bottei, H. S. Chang, D. A. Lusardi, J. Therm. Anal., 16(2) 389 (1979).

53 Robert West and Hsien Ying Niu, J. Amer. Chem. Soc., 85 2586 (1963).

54 Robert West and Hsien Ying Niu, J Amer. Chem. Soc., 85 2589 (1963).

55 Milton D. Glick, Gene L. Downs and Lawrence F. Dahl, Inorg. Chem., 3(12) 1712 (1964); 5(2) 289 (1966).

56 K. K. Canon, ***Jpn. Kokai Yokkyo Koho*** JP 59 14, 150 [84 14, 150] (Cl, G 11B7/24), 25Jan. 1984; JP 59 60, 443 [84 60 443] (Cl, G03G5/06), 06Apr. 1984; JP60,118, 786 [85, 118, 786] (Cl, C09K19/54), 26Jun. 1985.

57 Konoe Miura, Tettsuo Ozawa, Junko Iwanami, ***Jpn. Kokai Tokkyo Koho*** JP 61 31, 490 [86 31, 490] (Cl, C09K19/54), 13Feb 1986.

58 Juergen Hambrecht, Rudi Wilhelm Reffert, Adolf Echte, Johann Swoboda, (BASF A-G) ***Ger. Offen. DE3, 234, 034*** (Cl.Co8G65/44), 15Mar 1984.

59 Chemical Abstract CA 66:88153y.

60 Anna Bou, Miquel A. Perias, Felix Serratosa, Josep Claret, Joan Miquel Feliu and Carlos Muller, J. Chem Soc., Chem. Commun., 1305 (1982).

61 N. J. Turro," Modern Molecuular Photochemistry", The Benjamin/Cummings Publishing Company Inc. (1978).

62 Geoge J. Kavarnos and Nicholas J. Turro, Chemical Reviews, 60(2) 401 (1986).

63 Luca Moggi, in "Photoelectrochemistry, Photocatalysis and Photoreactions" (M. Schiavello ed.), P. 197, D. Reidel Publishing Company, (1985).

64 a) H. D. Roth, M. L. M. Schilling, G. Jones, II, J. Amer. Chem. Soc., 103 1246 (1981).

b) H. D. Roth, M. L. M. Schilling, J. Amer. Chem. Soc., 103 7210 (1981).

65 G. Jones, II, S. H. Chiang, W. G. Becker, J. A. Welch, J. Phys. Chem., 86 2805 (1985).

66 G. Jones, II, W. G. Becker, Chem Phys. Lett., 85 271 (1982).

67 P. K. Das, A. J. Muller, G. W. Griffin, I. R. Gould, C. H. Tung, N. J. Turro, Photochem. Photobiol., 39 281 (1984)

68 Vincenzo Balzani, Nanda Sabbatini and Franco Scandola, Chemical Reviews, 86(2) 319 (1986).

69 J. F. Rabek, "Experimental Methods in Photochemistry and Photophysics", John Wiley & Sons, 1982.

70 J. G. Calvert,"Photochemistry", Willey, New York 1966.

71 J. H. Baxendale, N. K. Bridge, J. Phys. Chem., 59 783 (1955).

72 Horace S. Isbell, Carbohydrate Research 39 C4--C7 (1975).

73 Wesley Glick Leighton and George Shannon Forbes, J. Amer. Chem. Soc., 52 3193 (1930).

74 Günther Von Bünau and Thomas Wolff, in "Adv. in Photochem.", (D. H. Volman ed.), 14 273, John Wiley & Sons, Inc. (1988).

75 Ralph S. Becher, Kenn Freedman, and Christan Lenoble, J. Phys. Chem., 90 4334 (1986).

76 Pierre-Alain Brugger, Michael Grätzel, J. Amer. Chem. Soc., 102 2461 (1980).

77 Steven Holdcroft, Kenneth H. Yuan, and James E. Guillet, J. Polym. Sci., Part A: Polym. Chem. 28 1495 (1990).

78 David F. Eaton, Pure & Appl. Chem., 60(7) 1107 (1988).

79 Sadakatsu Nishikawa and Yasuyuki Ozono, J. Phys. Chem., 92 6685 (1988).

80 Nader Berenjian, Paul De Mayo, Mary-Ellen Sturgeon, Leiv K. Sydnes, and Alan C. Weedon, Can. J. Chem., 60 425 (1982).

81 Nicholas J. Turro; G. C. Weed, J. Amer. Chem. Soc., 105 1861 (1983).

82 C. Tanford, "The Hydrophobic Efect" 2nd ed., P.63, Wiley-Interscience, New York, (1980).

83 B. Lindman and H. Wennerström, Top. Curr. Chem., 87 1 (1980).

84 Gabriella Caminati, Nicholas J. Turro, Donald A. Tomalia, J. Amer. Chem. Soc., 112 8515 (1990).

85 Robert Bittl; Klaus Schulten; Nicholas J. Turro, J. Chem. Phys., 93(11) 8260

(1990).

86 Yoshikiyo Moroi; Pierre P. Infelta and Michael Grätzel, J. Amer. Chem. Soc., 101 573 (1979).

87 Antonio I. Carbone; F. Paolo Cavasino; Carmelo Sbriolo, J. Phys. Chem., 89 3578 (1985).

88 João B. S. Bonilha; H. Chaimovich; V. G. Toscano; and Frank Quina, J. Phys. Chem., 83(19) 2463 (1979).

89 Claudio Minero; Edmondo Pramauro; and Ezio Pelizzetti, J. Phys. Chem., 92 4670 (1988).

90 J. Kiwi and M. Grätzel, J. Amer. Chem. Soc., 100 6314 (1978).

91 J. Kerry Thomas, Acc. Chemical Res., 10 133 (1977).

92 C. Bohne; M. S. Alnajjar; D. Griller; J. C. Scaiano, J. Amer. Chem. Soc., 113 1444 (1991).

93 Christopher H. Evans and J. C. Scaiano, J. Amer. Chem. Soc., 112 2694 (1990).

94 M. Corrin and D. W. Harkins, J. Amer. Chem. Soc., 69 683 (1947).

95 E. J. Fendler and J. H. Fendler, Adv. Phys. Org. Chem., 8 271 (1970).

96 R. C. Mast and L. V. Hynes, J. Colloid Interface Sci., 53 35 (1975).

97 G. Iraci and M. H. Back, Can. J. Chem., 66 1293 (1988).

98 B. Zhao and M. H. Back, Can. J. Chem., 69 528 (1991).

99 B. Zhao and M. H. Back, Can. J. Chem., 70 135 (1992).

100 James Guillet, "Polymer Photophysics and Photochemistry", Cambridge University Press, (1985).

101 Raymond B. Seymour and Charles E. Carraher, Jr. "Polymer Chemistry", Marcel Dekker, Inc. (1981).

102 Roy W. Tess and Gary W. Poehlein, "Applied Polymer Science", ACS Symposium

Series P. 285, American Chemical Soc., (1985).

103 Masahiro Irie; Yukio Yamamoto and Koichiro Hayashi, Pure and Appl. Chem., 49 455 (1977).

104 H-J. Timpe, in "Topics in Current Chemistry" (J. Mattary ed.), Springer-Verlag, 156 167 (1990).

105 David F. Eaton, Pure and Appl. Chem., 56 1191 (1984).

106 David F. Eaton, Adv. Photochem., 13 427 (1986).

107 G. A. Delzenne; H. K. Peeters and U. L. Laridon, The J. Photographic Sci., 22 23 (1974).

108 A. R. Shultz, J. Polym. Sci.: Polym. Phys. Edi., 22 1753 (1984).

109 T. Balakririshnan and S. Subbu, J. Polym. Sci.: Part A: Polym. Chem., 24 2271 (1986).

110 Kaoru Iwai; Maki Uesugi and Fukuo Takemura, Polymer Journal 17(9) 1005 (1985).

111 C. Namasivayam and P. Natarajam, J. Polym. Sci.: Part A: Polym. Chem., 21 1385 (1983).

112 G. Muralidharan; Q. Anwaruddin and L. U. Natarajan, J. Macromol. Sci-Chem. A19(4) 501 (1983).

113 Arthour W. Adamson, "A Textbook of Phys. Chem.", third ed., Academic Press, Inc. (1986).

114 Toshihiro Yamase and Tsuneo kawa, Photographic Sci. and Eng., 17(1) 28 (1973).

115 Toshihiro Yamase and Tsuneo Ikawa, ibid, 17(3) 268 (1973).

116 Toshihiro Yamase; Takashi sumi; Ysuneo Ikawa; Hiroshi Kokado and Eiichi Inoue, ibid, 18(1) 25 (1974).

117 E. Collinson; F. S. Dainton and G. S. McNaughton, Trans. Faraday Soc., 53 489

(1957).

118 (a) F. S. Dainton and M. Tordoff, ibid, 53 499 (1957).

(b) D. J. Currie; F. S. Dainton; W. S. Watt, Polymer, 6(9) 451 (1965).

119 Fukuo Takemura; Kaoru Iwai; Minako Ikesu; Kimi Itoh and Atsuko Matoike, Polymer Journal, 20(7) 565 (1988).

120 M. Julliard and M. Chanon, Chem. Rev., 83 425 (1983).

121 V. Balzani; F. Bolletta; M. T. Gandofi; and M. Maestri, Top. Curr. Chem., 75 1 (1978).

122 (a) V. Balzani; F. Bolletta; F. Scandola; and R. Ballardini, Pure & Appl. Chem., 51 299 (1979).

(b) V. Balzani; F. Bolletta; and F. Scandola, J. Amer. Chem. Soc., 102 2153 (1980).

123 D. Manzerall; S. G. Ballard, Annu. Rev. Phys. Chem., 33 377 (1982).

124 K. Nakimi; M. Nakashima; K. J. Yoshihara, J. Chem. Phys., 71 925 (1979).

125 J. A. Howard, in "Free Radicals", (Jay K. Kochi ed.), Vol II, John Wiley & Son, (1973).

126 Warren V. Sherman, in "Adv. in Free Radical Chemistry", (G. H. Williams ed.), Vol. III, P.1, Logos Press, (1969).

127 Barry Halliwell and John M. C. Gutteridge, "Free Radicals in Biology and Medicine", Oxford, (1985).

128 Linda M. Hadel,in "Handbook of Organic Photochemistry", (J. C. Scaiano ed.), Vol. I, P. 279, CRC Press, Inc., (1989).

129 J. N. Demas, "Excited State Lifetime Measurements", Academic Press, New York, (1983).

130 J. C. Scaiano and Ji-Liang Shi, Chem. Phys. Lett., 173(4) 271 (1990).

131 J. C. Scaiano, J. Amer. Chem. Soc., 102 7747 (1980).

132 J. C. Scaiano; M. Tanner; D. Weir, ibid, 107 4396 (1985).

133 Christopher H. Evans, Ph. D. thesis, Univ. Ottawa, (1989).

134 Robert H. Young; David Brewer; and Richard A. Keller, J. Amer. Chem. Soc., 92 375 (1973).

135 Phillip Hyde and Anthony Ledwith, J. Chem. Soc. Pekin Trans. II, 1768 (1974).

136 Richard D. Small, and J. C. Scaiano, J. Amer. Chem Soc., (a), 81 826 (1977); (b), 81 2126 (1977); (c), 82 2662 (1978).

137 Richard A. Caldwell and Chi Van Cao, J. Amer. Chem. Soc., 103 3594 (1981).

138 S. K. Chattopadhyay; C. V. Kumar and P. K. Das, J. Photochem., 26 39 (1984).

139 H. Görner, J. Phys. Chem., 86 2028 (1982).

140 C. V. Kumar; S. K. Chattopadhyay; and P. K. Das, Chem. Phys. Lett., 106 431 (1984).

141 M. V. Encinas; E. A. Lissi; and J. C. Scaiano, J. Phys. Chem., 84 948 (1980).

142 N. J. Turro and T.-J. Lee, J. Amer. Chem. Soc., 91 5651 (1969).

143 P. J. Wagner; R. G. Zepp; K. C. Liu; M. Thomas; T. J. Lee and N. J. Turro, ibid, 98 8125 (1976).

144 Richard A. Caldwell and Chi Van Cao, J. Amer. Chem. Soc., 104 6174 (1982).

145 S. Baral-Tosh; S. K. Chattopadhyay and P. K. Das, J. Phys. Chem., 88 1404 (1984).

146 P. K. Das, (a) Tetrahedron Letter, 22 1307 (1981); (b) J. Chem. Soc. Faraday Trans. I, 1135 (1983).

147 T. Wismontski-Knittel and T. Kilp, J. Phys. Chem., 88 110 (1984).

148 O. Johansen; A. W. H. Mau and W. H. F. Sasse, Chem. Phys. Lett., 94 107 (1983).

149 R. A. Caldwell and M. Singh, J. Amer. Chem. Soc., 104 6121 (1982).